SISSA
Scuola
Internazionale
Superiore di
Studi Avanzati

Physics Area - PhD course in
Astroparticle Physics

Spontaneously Broken Symmetries: Positivity Bounds beyond Lorentz Invariance and Cosmological solutions of dRGT Massive Gravity

Candidate:
Alessandro Longo

Advisor:
Paolo Creminelli

Academic Year 2024-2025

Acknowledgements

Although this PhD journey has been marked by a multitude of emotions and events, I will try to be as concise as possible.

First of all, I would like to thank my supervisor, Paolo Creminelli, for his patience, support, and guidance throughout these years of research. His critical spirit and physical intuition strongly motivated me and encouraged me both to step out of my comfort zone and to embrace the challenges of research. I will always be indebted to him for allowing me to enter the world of research by working alongside him.

During my PhD, I had the privilege of collaborating with brilliant researchers, including Leonardo Senatore, Luca Santoni, Borna Salehian, Ahmadullah Zahed, Oliver Janssen, Miguel Zumalacárregui, Giovanni Tambalo, and Lavinia Heisenberg. Interacting with them gave me the opportunity to exchange ideas and grow both scientifically and personally.

I am also grateful to my fellow PhD colleagues, particularly Matteo, Clemente, Giulio, Lodovico, and Vincenzo, together with Marina, Beniamino, Shreyansh, Vincenzo, Meriem, Cecilia, Francesco, Kendall, and Mina, for bringing the right amount of fun and serenity into this adventure.

A special "thank you" goes to my parents, Sandra e Francesco, who have always supported me unconditionally. I will never stop telling you how much I love you.

And "thank you" to Roberta, my friend, partner, and (recently) wife. Without your love and support, I don't think I would have managed to complete this part of the journey. Thank you for brightening my path every day with your smile and affection. I love you.

A heartfelt thanks is also reserved for my friends, in particular Bucci, Antonio, Urlink, Audrien, Sauron, Eugenio, Elio and Dall'Acqua. Your presence is a constant in my life, and one I could never give up.

Finally, a personal dedication goes to Trieste. For ten years you have been a quiet yet ever-present companion, one that I have learned to appreciate over time. You were the

cradle of invaluable friendships, and you witnessed my growth as both a physicist and a person. You witnessed the start of the journey of Roberta and me together. Only recently have I realized what it means to move away from here, and I admit that I have felt, in a certain sense, disoriented (a bit like Luffy after the Buster Call at Sabaody Archipelago). I do not know what the future will bring. My only wish is that, one day, I may return here. Thank you for everything you have given me.

Abstract

Effective Field Theories (EFTs) offer a systematic framework for describing low-energy phenomena without requiring full knowledge of the underlying ultraviolet (UV) completion. In Lorentz-invariant settings, general principles such as causality, unitarity, and locality ensure that scattering amplitudes are analytic functions of the Mandelstam invariants, enabling dispersion relations that link infrared EFT coefficients to ultraviolet physics. This connection leads to powerful *positivity bounds* that sharply constrain the space of consistent low-energy theories.

While this approach has been extensively developed for Lorentz-invariant systems, many physical contexts of interest, ranging from relativistic field theories at finite density to cosmological backgrounds, feature spontaneous breaking of boosts. In such cases, the standard S-matrix framework faces conceptual challenges: the altered analytic structure of amplitudes may obstruct direct application of positivity arguments, and the link between UV and IR physics becomes more subtle.

In this thesis, we address these challenges by pursuing two complementary strategies. First, we investigate the fate of the S-matrix in a simple, fully UV-complete Lorentz-violating model: the complex $\lambda|\Phi|^4$ theory at finite charge density. This model allows explicit computation of Goldstone scattering amplitudes, revealing new non-analytic features tied to boost breaking and highlighting the limitations of standard positivity methods in such settings.

Second, motivated by these limitations, we turn to observables whose analyticity properties are still clearly readable without Lorentz invariance: retarded correlation functions. We analyze their analytic structure and derive multidimensional dispersion relations for their Fourier transform $G(\omega, k)$ and for the function $F(\omega, k) = \omega G(\omega, k)$. Combining causality, unitarity, and passivity, we prove strict positivity of $\operatorname{Im} F$ in its domain of analyticity, both with and without rotational invariance. These properties lead to new constraints

on response functions in passive systems and imply, in particular, that $\operatorname{Im} G$ cannot have compact support in frequency–momentum space.

Finally, as a complementary application, we extend symmetry-based classification methods to identify admissible flat FLRW cosmologies in dRGT massive gravity, imposing background symmetries directly on the theory's building blocks. This approach yields novel perspectives on self-accelerating and fluid-like branches, as well as insights into their perturbative stability.

Together, these results provide new conceptual and technical tools for constraining Lorentz-violating EFTs, bridging S-matrix and correlator-based approaches, and applying them to modified gravity scenarios of cosmological relevance.

Publications

The present thesis is based on the following works:

- P. Creminelli, M. Delladio, O. Janssen, A. Longo, L. Senatore, "Non analyticity of the S-Matrix with spontaneously broken Lorentz invariance", JHEP 06 (2024) 201, 2312.08441
- L. Heisenberg, A. Longo, G. Tambalo, M. Zumalacarreguì, "To the problem of cosmic expansion in massive gravity", JCAP 08 (2025) 026, 2411.19873

The discussion of chapter 4 is built on the material of an upcoming paper

- P. Creminelli, A. Longo, B. Salehian, A. Zahed, "Analyticity and positivity properties of Green functions", to appear

1 Introduction **1**

2 Setting the stage **5**

2.1 Dispersion Relations and Positivity Bounds 5

2.1.1 Locality 6

2.1.2 Poincarè Invariance 6

2.1.3 Causality and Analyticity 7

2.1.4 Unitarity 10

2.1.5 Positivity at work: the Goldstone toy-model 12

2.1.6 An EFT Argument for Positivity 15

2.2 dRGT Massive Gravity 18

2.2.1 Massive Fierz-Pauli 18

2.2.2 Full dRGT 21

3 S-Matrix non-analyticity **27**

3.1 The $U(1)$ model 28

3.1.1 Canonical quantization 30

3.2 LSZ reduction formula and lack of analyticity 33

3.3 The S-matrix 38

3.3.1 Interesting limits 40

3.4 Decay rate of the Goldstone 43

3.4.1 $\omega \ll M$ 44

3.4.2 $\omega \gg M$ 44

3.5 Discussion and future directions 46

4 Retarded Green's functions without boosts **49**

4.1 Causality and Analyticity 50

4.1.1 $0+1$ Dimensions 50

4.1.2 $d+1$ Dimensions . . . 53
4.1.3 Rotational Invariance . . . 55
4.2 Multi-variable dispersion relations . . . 56
4.3 Positivity and its implications . . . 59
4.3.1 Implications for Passive Systems . . . 62
4.3.2 Non-compactness . . . 63
4.4 Generalizations . . . 64
4.4.1 Subtractions . . . 65
4.4.2 Breaking rotations . . . 66

5 dRGT Cosmologies **71**
5.1 Single-field $P(X)$ vs multi-field $P(\mathcal{X})$ . . . 72
5.2 Applications to dRGT . . . 74
5.2.1 dRGT: setup . . . 74
5.2.2 dRGT: Minimal Model . . . 76
5.2.3 dRGT: Full Theory . . . 80
5.3 Perturbations in the Unitary Gauge . . . 86
5.3.1 Tensors . . . 88
5.3.2 Vectors . . . 88
5.3.3 Scalars . . . 90
5.4 Discussion and future directions . . . 92

6 Conclusions **95**

A **99**
A.1 Second derivation of LSZ . . . 99
A.2 Feynman rules . . . 101
A.2.1 Scattering amplitudes . . . 104
A.3 S-matrix in the low-energy EFT . . . 107
A.4 Estimate of the decay width . . . 108

B **111**
B.1 A crash course on Tempered Distributions . . . 111
B.1.1 $S(\mathbb{R}^d)$ . . . 111
B.1.2 Distributions in $1+d$ Dimensions . . . 112

B.2 Double dispersion relations with subtractions 119
B.3 Explicit Construction Without Rotations 120

C **125**
C.1 Viable Configurations 125
C.1.1 Λ-Branch 126
C.1.2 Mixed Branch 128
C.2 Perturbations with Matter 129
C.2.1 Λ-Branch 130
C.2.2 Mixed Branch 131

Bibliography **135**

Chapter 1

Introduction

Modern physics extensively uses Effective Field Theories (EFTs) to describe systems across energy scales. In particle physics, the Fermi theory [1] captured weak interactions long before the discovery of electroweak bosons [2–4], while chiral perturbation theory [5] systematically describes pion dynamics in non-perturbative QCD. In condensed matter, EFTs account for collective excitations like phonons [6] and spin waves [7]. Even General Relativity can be viewed as an EFT of a massless spin-2 field [8]. These examples highlight the power of EFTs: they allow low-energy predictions without requiring full knowledge of the ultraviolet (UV) theory.

The central idea is simple: high-energy details decouple at low energies. One can understand atomic energy levels without resolving nucleon structure, or describe planetary motion without quantum gravity. EFTs formalize this intuition by organizing physics around hierarchies of scales.

When such a separation of scales is present, an EFT can be constructed by:

- identifying the low-energy degrees of freedom, typically including modes below the cutoff, like the Goldstone bosons in theories with spontaneous symmetry breaking [9, 10];
- determining the symmetries of the system, both linearly and non-linearly realized;
- writing all allowed operators consistent with these symmetries, ordered by relevance in a derivative or dimensional expansion.

This yields a predictive theory where ignorance of UV dynamics is encoded in a set of Wilson coefficients multiplying higher-dimensional operators.

From a top-down perspective, starting from the full microscopic theory, one can derive the EFT by integrating out the heavy degrees of freedom that cannot be excited below the cutoff. This procedure generates the higher-order operators and fixes their Wilson coefficients in terms of the parameters of the UV theory.

In many relevant cases, however (particularly in gravity and cosmology), the UV completion is unknown, and one must proceed bottom-up. From this perspective, the EFT coefficients are treated as free parameters to be fixed by low-energy data. Remarkably, this viewpoint is not entirely unconstrained: it turns out that general physical principles (such as causality, unitarity and locality) impose inequalities on the EFT coefficients. These constraints must be satisfied for the EFT to admit a healthy UV completion, in the sense of a Lorentz-invariant, causal, local, and unitary QFT (or even a weakly coupled string theory) [11]. In a certain sense, these bounds demonstrate that the UV and IR regimes are not entirely decoupled. While positivity bounds do not rely on any specific assumptions about the ultraviolet (UV) completion, general principles such as causality, unitarity, and Lorentz invariance are sufficient to constrain the low-energy coefficients. Conversely, one may also reverse the logic and use these constraints to extract information about the UV theory itself. In particular, experimental evidence for a violation of these bounds would indicate that at least one of the fundamental assumptions about the UV physics must be reconsidered.

In Lorentz-invariant theories, these constraints are most commonly derived by exploiting the analyticity of the S-matrix. Under mild assumptions about the UV behavior, in particular, causality and locality, the $2 \to 2$ scattering amplitude is analytic in the Mandelstam invariants. Using Cauchy's theorem, one can derive a dispersion relation that relates the low-energy behavior of the amplitude (which depends on the EFT coefficients) to an integral over its imaginary part (a manifestly positive quantity due to unitarity). The resulting positivity bounds then impose inequalities on the Wilson coefficients of the EFT.

The power of these constraints, which are essentially UV-agnostic[1], has motivated an extensive body of work over the past two decades [12–27], applying the positivity program to a wide range of EFTs to chart the space of consistent low-energy theories.

However, most existing applications of positivity bounds assume Lorentz invariance as an exact symmetry of the low-energy theory. While this is well motivated in particle physics, many important systems, especially in cosmology and condensed matter, do not enjoy this symmetry. Instead, Lorentz transformations are spontaneously broken, and

[1] They do not depend on the details of a specific UV completion.

the symmetry is non-linearly realized. This is particularly relevant in cosmology, where the presence of a time-dependent background breaks time translations and boosts, and in condensed matter, where solids or fluids break boost invariance. In these scenarios, the standard S-matrix assumptions may no longer hold, and the positivity logic may require significant modification.

Extending positivity bounds to such cases is both challenging and potentially highly informative. In cosmology, for instance, they could help identify the subset of inflationary or dark energy EFTs (see [28, 29]) that admit a healthy UV completion. Many such models, including Horndeski [30, 31] theories and the de Rham-Gabadadze-Tolley (dRGT) theory of Massive Gravity [32], rely on a delicate balance of higher-derivative operators to avoid ghost instabilities or to preserve second-order equations of motion. Some recent attempts have applied positivity arguments to Galileon [33] or dRGT-like theories expanded around Minkowski space. In the Lorentz-invariant case, however, recent analyses [11, 25] have shown that the forward-limit positivity bounds place extremely restrictive constraints on the allowed parameter space of dRGT massive gravity. In particular, the requirement that all dispersion-relation coefficients remain positive forces the EFT cutoff scale Λ to lie only marginally above the graviton mass m, leaving little room for a parametrically large hierarchy. Moreover, the same set of bounds completely excludes the cubic Galileon as a consistent Lorentz-invariant EFT, ruling out one of the simplest infrared modifications of gravity on fundamental grounds. These constraints are of potential cosmological importance: the well-known no-go theorem forbidding flat FLRW solutions in Lorentz-invariant dRGT already limits its cosmological viability, and the combined effect of these theoretical obstacles further motivates exploring Lorentz-violating generalizations where both the no-go theorem and the positivity bounds may be evaded or substantially modified.

It is not clear, however, how the presence of a time-dependent background affects the shape and strength of these bounds. The spontaneous breaking of Lorentz invariance raises new conceptual issues:

- low-energy excitations (e.g., phonons in solids) do not correspond, in general, to well-defined asymptotic states at high energies, undermining standard S-matrix methods;
- the analytic structure of the amplitude may be altered;
- the link between UV and IR physics, which underpins dispersion relations, becomes more subtle.

These difficulties suggest that amplitudes may not always be the optimal observables for connecting UV and IR in Lorentz-violating settings, as it will be argued in the present thesis work. Alternative approaches, such as using retarded correlators, or studying the stability of cosmological backgrounds in modified gravity theories, can provide complementary tools for extending the positivity logic into these regimes. Both these directions will be explored throughout the discussion.

Outline

The thesis is organized as follows. Chapter 2 provides an introductory background, focusing on two key topics: the derivation of dispersion relations for $2 \to 2$ scattering amplitudes within the framework of positivity bounds, and the construction of the Lagrangian of dRGT Massive Gravity.

Chapter 3 investigates the effects of spontaneous boost breaking in a UV-complete model: a U(1) linear sigma model at finite chemical potential. We analyze how the chemical potential modifies both the dispersion relations of the theory's degrees of freedom and the analyticity properties of the S-matrix. In particular, the tree-level computation of the $2 \to 2$ Goldstone scattering amplitude reveals new non-analyticities that are not governed by unitarity.

Chapter 4 studies the properties of retarded two-point functions in states that spontaneously break boosts. We review the necessary and sufficient conditions linking causality to analyticity of retarded correlators, and derive a new result regarding the absence of zeros within the primitive domain of analyticity. This result is further generalized to cases where rotations are also spontaneously broken.

Chapter 5 focuses on cosmological solutions in dRGT massive gravity. It provides a classification of possible flat FLRW cosmologies and analyzes the stability of linear perturbations around these backgrounds.

Finally, Chapter 6 summarizes the main findings of the thesis, discusses their implications, and outlines potential directions for future research.

A set of appendices will complement the discussion.

Chapter 2

Setting the stage

Given that the aim of this thesis is to understand how to export the positivity machinery to those scenarios which are characterized by a spontaneous breaking of Lorentz invariance, it is important to remind the logic and the steps involved in the formulation of the positivity arguments when Lorentz transformations are linearly realized. In the first part of the present chapter, the technical aspects behind the extraction of Positivity Bounds for Lorentz invariant EFTs are reviewed.

The second part, instead, focuses on the construction of the dRGT Lagrangian, with a particular stress both on the technial difficulties that the inclusion of a mass term for a spin-2 field brings and on to the cosmological applications of the full dRGT theory.

2.1 Dispersion Relations and Positivity Bounds

As mentioned in the introduction, when Lorentz transformations are linearly realized, the S-matrix emerges as the natural and optimal bridge between low-energy EFT data and high-energy UV dynamics. In particular, positivity bounds leverage the analyticity and unitarity of scattering amplitudes to relate low-energy Wilson coefficients to dispersive integrals over physical cross sections at high energies. These powerful constraints rely on minimal UV assumptions and encode deep consequences of quantum field theory. We now review, following [34, 35] how fundamental principles like locality and Poincaré invariance ensure the analytic structure and consistency of scattering amplitudes.

2.1.1 Locality

In quantum field theory, locality is the principle that physical degrees of freedom are encoded in local operators[1] $\mathcal{O}(x)$ that depend on spacetime points x^μ. This means that observables are constructed from operators defined at definite spacetime locations, such as fields $\phi(x)$, currents $j^\mu(x)$, or stress-energy tensors $T^{\mu\nu}(x)$.

This assumption underpins the construction of both free and interacting theories via local Lagrangian densities built from fields and their derivatives. Locality allows one to define local observables, including n-point correlation functions:

$$\langle \mathcal{O}_1(x_1)...\mathcal{O}_n(x_n)\rangle \tag{2.1.1}$$

which encode the dynamical content of the theory.

Importantly, locality (in combination with relativistic causality) ensures that spacelike-separated operators commute:

$$[\mathcal{O}(x), \mathcal{O}(y)] = 0\ ,\ (x-y)^2 < 0. \tag{2.1.2}$$

preserving causal structure and enabling the analytic properties of the S-matrix used in dispersion relations. It is important to emphasize that microcausality holds as an operator identity, independent of the quantum state on which the commutator is evaluated. Consequently, the requirement that operators commute at spacelike separation remains valid even in situations where the state of the theory spontaneously breaks Lorentz invariance. In such cases, certain correlators need not be Lorentz invariant, while still respecting the principle of relativistic causality.

2.1.2 Poincarè Invariance

Poincaré invariance asserts that the underlying spacetime symmetry of the theory is the Poincaré group, which consists of spacetime translations and Lorentz transformations. This means that QFT is formulated on flat Minkowski spacetime, and the theory is invariant under spacetime translations, rotations, and boosts.

This symmetry has distinct implications for fields and for physical states:

- fields transform under finite-dimensional representations of the Lorentz group. These transformation properties determine the tensorial or spinorial nature of the fields, and

[1] More precisely, operator-valued distributions.

how local operators behave under spacetime symmetries. Fields provide the building blocks for constructing Lorentz-invariant observables and Lagrangians.

- states transform under infinite-dimensional unitary irreducible representations of the full Poincaré group. According to Wigner's classification [36], single-particle states are labeled by their mass and spin (or helicity in the massless case). They are denoted $|p, s\rangle$, with momenta p^μ that vary continuously over the on-shell hyperboloid:

$$p^2 = m^2 \ , \ p^0 > 0. \tag{2.1.3}$$

This structure ensures that the Hilbert space of states includes all possible relativistic momenta consistent with the mass-shell condition.

Moreover, invariance under Lorentz boosts ensures that low-energy states are continuously connected to high-energy ones, a key ingredient for the analyticity and dispersion relations of scattering amplitudes.

2.1.3 Causality and Analyticity

In relativistic quantum field theory, causality asserts that no signal can propagate faster than light. Operationally, this means that measurements performed at spacelike separated points must be independent. This condition is formally captured by microcausality, which requires that local operators commute at spacelike separation.

This fundamental principle has powerful consequences for the analytic structure of correlation functions and, ultimately, of scattering amplitudes.

As an illustrative example, consider the retarded two-point function of a scalar field ϕ evaluated in the vacuum:

$$G_R(x, y) = -i\theta(x^0 - y^0)\langle 0|[\phi(x), \phi(y)]|0\rangle \tag{2.1.4}$$

Microcausality implies that the commutator vanishes outside the lightcone. Therefore, $G_R(x, y)$ has support only in the forward lightcone, i.e., when $x - y$ is future timelike or null. Retardedness, in particular, ensures that the response to a perturbation at y can only be felt at later times $x^0 > y^0$.

To analyze this in momentum space, consider the Fourier transform:

$$\tilde{G}_R(p) = \int d^4x \, e^{ip\cdot x} G_R(x) \ . \tag{2.1.5}$$

Because $G_R(x)$ vanishes outside the forward lightcone and is assumed to be a tempered distribution[2] (i.e., it grows at most polynomially), the exponential $e^{ip\cdot x}$ ensures convergence when the imaginary part of p^μ lies inside the forward lightcone. Thus, $\tilde{G}_R(p)$ is analytic in the tube $\mathcal{T}_+ \equiv \mathbb{R}^4 + iV_+$, with $V_+ \equiv \{\mathrm{Im}[p]^2 > 0\ ,\ \mathrm{Im}[p^0] > 0\}$. This analyticity is a direct consequence of microcausality and the support properties of $G_R(x)$.

The analytic structure of correlation functions in QFT can be extended to the study of scattering amplitudes. As an illustrative example, let us focus on the $2 \to 2$ scattering of identical scalar particles of mass m. Lorentz invariance constrains the amplitude to depend only on the Mandelstam invariants s and t[3], enabling us to characterize its analytic properties in terms of these variables.

The connected part of the amplitude can be derived from the LSZ reduction formula as

$$T^{\text{conn.}}_{p_1,q_1\to p_2,q_2} = i\int d^4z, e^{i(q_1+q_2)\cdot z/2}(\Box_{z/2}+m^2)(\Box_{-z/2}+m^2)\langle p_2|T\{\phi^\dagger(z/2)\phi(-z/2)\}|p_1\rangle. \tag{2.1.6}$$

Notice that we are already implementing invariance under spacetime translations. Moreover, we are using a complex field $\phi(x)$ to interpolate for the particles involved in the scattering process.

To investigate the analytic structure, it is more instructive to replace[4] the time-ordered correlator with a retarded one:

$$T^{\text{conn.}}(q) = i\int d^4z, e^{iq\cdot z}(\Box_{z/2}+m^2)(\Box_{-z/2}+m^2)\theta(z^0)\langle p_2|[\phi^\dagger(z/2),\phi(-z/2)]|p_1\rangle, \tag{2.1.7}$$

where $q = (q_1+q_2)/2$ and where we have suppressed the subscripts to avoid proliferation of characters. Because the commutator vanishes outside the light cone (by microcausality), the integrand is supported only in the forward light cone, $z^2 \geq 0$ and $z^0 > 0$. Under the assumption that the commutator grows at most polynomially (as it is a tempered distribution), the exponential suppression in the Fourier kernel implies that the integral converges when $\mathrm{Im}[q^\mu]$ lies in the forward timelike cone. Thus, the amplitude is analytic in the forward tube $\mathcal{T}_+$.

One might be afraid that the presence of the operators $(\Box + m^2)$ might spoil the argument. The key point is that the differential operators in the integrand do not affect

[2]This is one of the core assumptions of the axiomatic formulation of QFT.

[3]The third invariant, u, is related by $s + t + u = 4m^2$ for identical external masses.

[4]For the connected part of the amplitude, the difference between time-ordered and retarded correlators is purely a disconnected contribution and does not affect the connected part of scattering amplitude.

the support of the correlator, as they act locally in spacetime. Thus, the analyticity of the amplitude in the domain $\mathcal{T}_+$ follows directly from the analyticity of the retarded correlator, provided the integrand satisfies appropriate temperedness conditions.

However, *primitive domain* of analyticity corresponds to off-shell, complexified momenta and has no overlap with the physical, on-shell kinematics. This is seen explicitly by considering the forward kinematics $q = q_1 = q_2$ and attempting to satisfy the mass-shell condition $q^2 = m^2$ while keeping $\mathrm{Im}[q^\mu]$ timelike and future-directed. The constraints $\mathrm{Im}[q] \cdot \mathrm{Re}[q] = 0$ and $\mathrm{Re}[q]^2 - \mathrm{Im}[q]^2 = m^2$ imply that $\mathrm{Re}[q^\mu]$ must be spacelike, excluding on-shell momenta from $\mathcal{T}_+$.

To extend the domain of analyticity to include the physical region, we invoke analytic completion techniques [37,38]. The idea is to consider the amplitude for a crossed process, such as the scattering $p_1 + \bar{q}_1 \to p_2 + \bar{q}_2$, where $\bar{q}_{1,2}$ denote the momenta of the incoming/outgoing antiparticle. Changing the integration variable $z \to -z$, the corresponding connected amplitude becomes

$$\bar{T}^{\text{conn.}}_{p_1,\bar{q}_1\to p_2,\bar{q}_2} = -i \int d^4z, e^{-i\bar{q}\cdot z} \left(\Box z/2 + m^2\right) \left(\Box - z/2 + m^2\right) \theta(-z^0) \langle p_2|[\phi^\dagger(z/2), \phi(-z/2)]|p_1\rangle, \tag{2.1.8}$$

where $\bar{q} = (\bar{q}_1 + \bar{q}_2)/2$. This expression is analytic in the backward tube $\mathcal{T}_- \equiv \mathbb{R}^4 + iV_- = \{\mathrm{Im}[\bar{q}]^2 > 0\,,\ \mathrm{Im}[\bar{q}^0] < 0\}$, defined by complex momenta with past-directed timelike imaginary parts.

The difference between the original amplitude and the crossed one is the Fourier transform of the full commutator:

$$C(z) = \langle p_2|[(\Box_{z/2} + m^2)\phi^\dagger(z/2), (\Box_{-z/2} + m^2)\phi(-z/2)]|p_1\rangle = \langle p_2|[j(z/2)^\dagger, j(-z/2)]|p_1\rangle\ , \tag{2.1.9}$$

where we define the interpolating current $j(x) \equiv (\Box_x + m^2)\phi(x)$. Inserting a complete set of intermediate states, we obtain:

$$\begin{aligned} T^{\text{conn.}}(q) - \bar{T}^{\text{conn.}}(\bar{q})|_{q=-\bar{q}} &= i \int d^4z, e^{iq\cdot z} C(z) = \\ &= (2\pi)^4 \sum_n |\langle n|j(0)|0\rangle|^2 \left[\delta^4\left(q - p_n + \frac{p_1+p_2}{2}\right) - \delta^4\left(q + p_n - \frac{p_1+p_2}{2}\right)\right]\ . \end{aligned} \tag{2.1.10}$$

For a gapped theory, there exists an open neighborhood in real q-space where this difference vanishes, i.e., the support of the delta functions lies outside the allowed kinematic region. In this region, the two amplitudes coincide.

This coincidence allows us to invoke the Edge of the Wedge Theorem [39], a generalization of the Schwarz reflection principle to several complex variables. It states that if two holomorphic functions, defined in disjoint domains (e.g. the tubes $\mathcal{T}_+$ and $\mathcal{T}_-$) agree on a real submanifold with non-zero measure (the "edge"), then there exists a single analytic function in the convex hull of the two domains which extends both. The convex hull of $\mathcal{T}_+ \cup \mathcal{T}_-$ is the smallest convex set in $\mathbb{C}^4$ that contains both $\mathcal{T}_\pm$. Therefore it contains complex momenta whose imaginary part lies in the convex cone spanned by $V_+ \cup V_-$.

More concretely, the convex hull of the two disjoint tubes includes all the points of the form

$$p = \lambda p_+ + (1-\lambda)p_- \ , \ \lambda \in [0,1] \ , \ p_\pm \in \mathcal{T}_\pm \ . \tag{2.1.11}$$

The extended analyticity domain now contains points whose imaginary parts can be both spacelike and lightlike as well (i.e., not purely future or past timelike), and crucially it includes real momenta as the limit where $\mathrm{Im}[p^\mu] \to 0$. In particular, it includes a portion of the physical on-shell surface.

Consequently, one obtains analyticity of the amplitude in a real neighborhood of the on-shell kinematic configuration. Mapping this domain into the Mandelstam variables then allows to identify a region in the complex s-plane where the amplitude is analytic for fixed t. In particular, for gapped theories, it has been proven [40–42] that, as a function of the complexified Mandelstam invariants s and t, the amplitude $\mathcal{A}(s,t)$ is analytic in the complex s-plane, except for singularities (poles and branch points) which lie on the real s-axis, as dictated by Unitarity. This statement holds true for complex values of t within the Lehmann ellipse (whose size depends on the mass gap) [43, 44].

2.1.4 Unitarity

Unitarity is a fundamental principle of quantum theory, expressing the conservation of probability in the time evolution of states. In the context of scattering processes, it ensures that the total probability for all physically allowed outcomes of an initial state must sum to one. This condition is encoded in the requirement that the S-matrix is a unitary operator:

$$S^\dagger S = S S^\dagger = \mathbb{I}. \tag{2.1.12}$$

The S-matrix encapsulates the full dynamics of asymptotic scattering processes, mapping incoming free-particle states to outgoing ones:

$$|\mathrm{out}\rangle = S|\mathrm{in}\rangle. \tag{2.1.13}$$

To analyze the implications of unitarity more explicitly, it is standard to separate the S-matrix into a trivial (non-interacting) part and a non-trivial (interacting) part:

$$S = \mathbb{I} + iT, \tag{2.1.14}$$

where the operator T contains all the dynamical information about scattering. Substituting this decomposition into the unitarity condition yields:

$$i(T - T^\dagger) = -TT^\dagger. \tag{2.1.15}$$

This relation, known as the unitarity equation, expresses the anti-Hermitian part of the scattering operator in terms of the product $TT^\dagger$, which is manifestly positive semi-definite.

Taking matrix elements of this equation between two arbitrary asymptotic states $|a\rangle, |b\rangle$, and inserting a complete set of intermediate states, one obtains:

$$\langle b|T|a\rangle - \langle b|T^\dagger|a\rangle = i\sum_n \langle b|T|n\rangle\langle n|T^\dagger|a\rangle. \tag{2.1.16}$$

In particular, for forward matrix elements $|a\rangle = |b\rangle$, the imaginary part of the forward scattering amplitude becomes:

$$2\mathrm{Im}[\langle a|T|a\rangle] = \sum_n |\langle n|T|a\rangle|^2. \tag{2.1.17}$$

This expression is known as the optical theorem, a central consequence of unitarity. It equates the imaginary part of the forward scattering amplitude to the total transition probability into all allowed final states $|n\rangle$, and hence to the total cross section.

The right-hand side is strictly positive, implying that the imaginary part of the forward amplitude is also positive, a fact that will be crucial in deriving positivity bounds on effective field theories.

It is evident that Unitarity constrains the singularity structure of scattering amplitudes in the complex plane of kinematic invariants. In particular, poles and branch points on the real s-axis correspond to physical thresholds.

As (2.1.17) shows, the imaginary part of the forward amplitude becomes nonzero only above the energy thresholds where intermediate states can go on-shell. The right-hand side receives non-zero contributions only when the total center-of-mass energy s is sufficient to produce the intermediate state $|n\rangle$. For instance, in correspondence of a single-particle threshold, the amplitude develops a pole. Branch points, instead, correspond to the threshold for N-particle production ($N \geq 2$). If the lightest one-particle state state has mass

m, assuming that its production is physically allowed, then $\mathrm{Im}[\langle a|T|a\rangle] = 0$ for $s < m$, implying that the amplitude is purely real below this threshold. In particular, below the first unitarity thresholds, the forward amplitude satisfies

$$\langle a|T|a\rangle(s) \equiv \mathcal{A}(s) = \mathcal{A}^*(s^*) \tag{2.1.18}$$

The same property, known as *hermitian analyticity*, is enjoyed by the analytic continuation of the amplitude on the complex s-plane. This observation is crucial because it enables to link the discontinuity of the forward amplitude along the unitarity cuts to its imaginary part:

$$\mathrm{Disc}[\mathcal{A}](s) \equiv \lim_{\epsilon\to 0}(\mathcal{A}(s+i\epsilon)-\mathcal{A}(s-i\epsilon)) = \lim_{\epsilon\to 0}(\mathcal{A}(s+i\epsilon)-\mathcal{A}^*(s+i\epsilon)) = 2i\mathrm{Im}[\mathcal{A}](s) \tag{2.1.19}$$

Thus, Unitarity plays a dual role: it enforces conservation of probability and tightly constrains the analytic structure of scattering amplitudes. These features are essential ingredients in the derivation of dispersion relations, and they form a cornerstone of the modern analytic S-matrix bootstrap program.

2.1.5 Positivity at work: the Goldstone toy-model

Having reviewed the foundational assumptions underlying positivity bounds, we now illustrate their implications through a concrete example, reviewing the seminal work [11]. The proposed toy model is a Lorentz-invariant EFT describing a massless scalar field. Imposing a discrete $\mathbb{Z}_2$ symmetry (i.e., $\theta \to -\theta$) constrains the form of the Lagrangian to

$$\mathcal{L} = \frac{1}{2}(\partial\theta)^2 + \frac{c_4}{\Lambda^4}(\partial\theta)^4 + \dots \tag{2.1.20}$$

Here, the first term represents the canonical kinetic term, while the second is the leading-order irrelevant operator responsible for self-interactions of the scalar θ. The ellipsis denotes higher-dimensional operators consistent with the EFT symmetries.

As stated in the introduction, symmetry principles play a central role in the EFT expansion. In this case, the $\mathbb{Z}_2$ symmetry ensures that the Lagrangian contains only even powers of θ, while shift symmetry $\theta \to \theta + \mathrm{const}$ implies that each θ field must be accompanied by at least one derivative.[5]

[5] Operators with undifferentiated θ can still be consistent with shift symmetry if their variation under a shift transformation is a total derivative.

At the EFT level, the Wilson coefficient c_4 appears unconstrained by symmetry. However, assuming that the EFT admits a consistent, causal, and unitary UV completion imposes a nontrivial constraint: c_4 must be strictly positive. To demonstrate this, we compute the $2 \to 2$ scattering amplitude for the Goldstone bosons and analyze its analyticity properties.

At tree level, the leading-order amplitude is

$$\langle q_2, p_2|T|p_1, q_1\rangle \equiv \mathcal{A}(s,t) = \frac{c_4}{\Lambda^4}(s^2 + t^2 + u^2), \tag{2.1.21}$$

where p_1, q_1 and p_2, q_2 are the incoming/outgoing momenta of the Goldstones and $u = -s-t$ due to the masslessness of the external particles. In the forward limit ($t = 0$), this reduces to

$$\mathcal{A}(s,0) = \frac{2c_4}{\Lambda^4}s^2. \tag{2.1.22}$$

This expression is analytic in the entire complex s-plane. This means that the thrice-subtracted forward amplitude, $\mathcal{A}(s,0)/s^3$, is a meromorphic with a single pole at $s = 0$ whose residue is proportional to c_4. This pole structure is a feature of the EFT truncation; in a full UV completion, the amplitude would exhibit a richer analytic structure, including singularities associated with the production of heavy intermediate states.

To illustrate this, consider two representative UV completions:

- Linear sigma model: A $U(1)$-symmetric scalar field theory in the broken phase. The amplitude acquires poles in the s, t, and u channels due to tree-level exchange of the radial (Higgs) mode. When the center-of-mass energy reaches the threshold for on-shell Higgs production, the amplitude develops an imaginary part proportional to $\delta(s - m_h^2)$, where m_h is the Higgs mass.

- Heavy fermion loop: The scalar couples derivatively to a massive Dirac fermion. At one loop, the amplitude develops a branch point at the threshold $s_{\text{th}} = 4m_\psi^2$, corresponding to pair production of the fermion–antifermion state.

As discussed earlier, under the assumptions of unitarity, locality, Lorentz invariance, and a mass gap, the full forward amplitude $\mathcal{A}(s,0)$ is analytic in the complex s-plane, away from the real axis where branch cuts arise due to unitarity. At very low energies, the EFT provides a reliable approximation to the full theory. We now use dispersion relations to connect the low-energy coefficient c_4 to high-energy data.

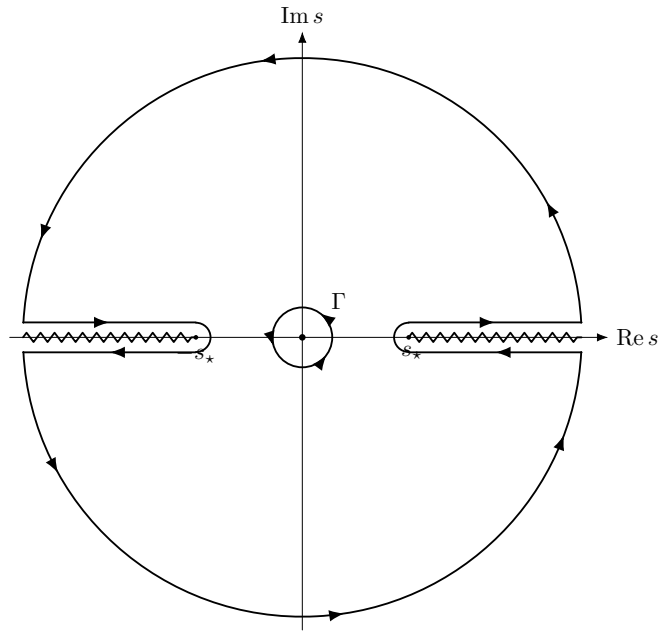

Figure 2.1 Analytic structure of $\mathcal{A}(s,0)$ in the complex s-plane. Once stretched to complex infinity, the contour consists of three contributions: the great semicircles and the integrals of $\mathrm{Disc}\mathcal{A}(s,0)$ along the two cuts.

Consider the following subtracted dispersion relation:

$$\frac{4\pi c_4}{\Lambda^4} = \oint_\Gamma \frac{\mathcal{A}(s,0)}{s^3} ds, \tag{2.1.23}$$

where the contour Γ encircles the origin in the complex s-plane.

The contour can be deformed into three contributions (see fig. 2.1):

Large semicircles at infinity, which vanish due to the Froissart-Martin bound [45]. This ensures that for gapped, unitary theories, $|\mathcal{A}(s,0)| \lesssim |s| \log^2 |s|$ at large $|s|$, implying that $|\mathcal{A}(s,0)|/|s|^3 \to 0$ sufficiently fast as $|s| \to \infty$. Integral along the positive real axis, where the discontinuity across the branch cut is given by

$$\int_{s_\star}^{\infty} \frac{\mathrm{Disc}\mathcal{A}(s,0)}{s^3} ds = 2i \int_{s_\star}^{\infty} \frac{\mathrm{Im}\mathcal{A}(s,0)}{s^3} ds, \tag{2.1.24}$$

using hermitian analyticity.

Integral along the negative real axis, associated with the u-channel branch cut. By crossing symmetry and changing variables $s \to -s$, this can be recast into another integral

along the positive real axis:

$$\int_{-\infty}^{-s_\star} \frac{\mathrm{Disc}\mathcal{A}(s,0)}{s^3} ds = \int_{s_\star}^{\infty} \frac{\mathrm{Disc}\mathcal{A}(-s,0)}{s^3} ds \quad = 2i \int_{s_\star}^{\infty} \frac{\mathrm{Im}\mathcal{A}(s,0)}{s^3} ds, \tag{2.1.25}$$

since $\mathcal{A}(s,0) = \mathcal{A}(-s,0)$ in the forward limit for identical scalars[6]

Combining all contributions, we find:

$$\frac{4\pi c_4}{\Lambda^4} = 4 \int_{s_\star}^{\infty} \frac{\mathrm{Im}\mathcal{A}(s,0)}{s^3} ds, \tag{2.1.26}$$

from which the positivity of the integrand immediately implies:

$$c_4 > 0. \tag{2.1.27}$$

This result demonstrates how low-energy Wilson coefficients are constrained by the requirement of a consistent UV completion. It exemplifies a dispersion relation, linking low-energy data (e.g., c_4) to an integral over high-energy spectral information.

Analogous positivity bounds can be derived for higher-derivative operators, e.g., those scaling as s^3, s^4, etc., by considering further subtractions in the dispersion relation. Each subtraction isolates the residue associated with a given operator.

Finally, we emphasize that the above argument crucially relies on the tree-level form of the low-energy amplitude. Including loop corrections involving massless Goldstones introduces branch points at $s = 0$, which obstruct the analytic continuation between the upper and lower half s-planes. In such gapless theories, standard dispersion relations in the forward limit may break down, and alternative approaches, such as dispersive representations in non-forward [26] kinematics or the use of "arc variables" [20], must be employed.

2.1.6 An EFT Argument for Positivity

While rigorous derivations of positivity bounds typically rely on dispersion relations for $2 \to 2$ scattering amplitudes and assumptions about the UV completion or high-energy behavior of the EFT, it is instructive to derive a weaker, but physically insightful, version of these bounds entirely within the low-energy EFT regime. This approach is based on studying the propagation of perturbations around nontrivial, translationally invariant background field configurations.

[6] This is a consequence of crossing symmetry, which enforces $\mathcal{A}(s,t) = \mathcal{A}(u,t)$.

Concretely, starting from the Lagrangian (2.1.20) one expands the Goldstone field $\theta = \bar{\theta} + \pi$, around a background profile $\bar{\theta}$ such that its gradient is constant and timelike:

$$\partial_\mu \bar{\theta} \equiv C_\mu \, , \; C^2 > 0 \, , \tag{2.1.28}$$

where $C^2 \ll \Lambda^4$ to ensure self-consistency of the EFT expansion.

Expanding the EFT Lagrangian to quadratic order in the fluctuations π leads to an effective equation of motion of the form

$$\left[\left(1 + 4 \frac{c_4 C^2}{\Lambda^4} \right) \Box + 8 \frac{c_4 C^\mu C^\nu}{\Lambda^4} \partial_\mu \partial_\nu \right] \pi = 0 \tag{2.1.29}$$

Translating the equation in Fourier space yields the dispersion relation

$$k^2 \sim -8 c_4 \frac{(C \cdot k)^2}{\Lambda^4}, \tag{2.1.30}$$

valid to leading order in C^2/Λ^4.

From this dispersion relation, it follows that, if $c_4 < 0$, the Goldstone fluctuations propagate with a superluminal speed of sound. To see this explicitly, write the dispersion relation in the standard form

$$\omega^2 = c_s^2 \vec{k}^2 \, , \tag{2.1.31}$$

where c_s is the phase velocity of the perturbation. When $c_4 < 0$, the modifications to the kinetic terms induce $c_s > 1$, signaling superluminal propagation.

Such superluminal behavior is pathological in a theory whose underlying Lorentz invariance is a global symmetry of the system. In this context, superluminality leads to violations of causality and allows, in principle, for the construction of closed timelike curves and related time paradoxes.

Therefore, to avoid these inconsistencies and preserve a well-defined causal structure, one must impose the positivity constraint $c_4 \geq 0$. This represents a weaker, EFT-internal version of the positivity bounds obtained from S-matrix dispersion relations, reflecting constraints arising purely from the low-energy regime without appeal to UV completions.

The origin of this bound can be traced to the interpretation of fluctuation propagation over the background as an effective sum over multiple microscopic scattering events. Although each individual scattering event produces a time advance or delay too small to be resolved within the EFT, the cumulative effect of many such events leads to a macroscopic shift in the propagation time of the perturbations. This accumulated time shift manifests as a modification of the propagation speed at the EFT level.

Superluminal propagation, in this context, reflects a net macroscopic time advance and is thus a genuine pathology incompatible with a causal EFT respecting Lorentz symmetry. However, several remarks clarify the scope and limitations of this argument:

- the argument crucially relies on the Goldstone fluctuations propagating exactly at the speed of light in vacuum. The addition of irrelevant operators can then shift this speed slightly inside or outside the light cone depending on the sign of c_4. If the initial field were massive, one would have to boost the fluctuations 4-momentum sufficiently close to the light-cone in order to appreciate the effect of the irrelevant deformations. But performing such a boost inevitably pushes the energy of the fluctuations beyonf the EFT regime. Thus a similar bound could not be drawn without accessing energies close to the EFT cutoff, beyond the EFT's regime of validity.

- Because the background gradient C_μ must satisfy $C^2 \ll \Lambda^4$ for the EFT expansion to hold, higher-dimensional operators corrections are suppressed by higher powers of C^2/Λ^4. Consequently, the speed of sound is sensitive only to the leading irrelevant operator with the least suppressed correction, here parameterized by c_4. This contrasts with positivity bounds derived from scattering amplitudes, where careful subtractions can isolate and constrain a broader set of higher dimensional operators.

- It was originally proposed [11] that, within the EFT framework, one can engineer background configurations that allow for the formation of closed timelike curves (CTCs). Such a scenario would imply that violations of positivity give rise not only to macroscopic time advances but also to more severe issues of global causality. This argument, however, is not entirely robust. More recent work [46] demonstrates that quantum effects can safeguard the causal structure of quantum field theory at low energies, even in the presence of superluminal propagation. In particular, the backreaction of low-energy modes can obstruct the formation of CTCs, thereby preserving the predictivity of the effective field theory.

In summary, superluminality arguments can provide a complementary and physically intuitive route to positivity bounds within the EFT regime, relying on causality and Lorentz invariance. While less stringent than full dispersion relation methods, they impose nontrivial constraints on the signs of leading irrelevant operators, thereby constraining the EFT parameter space consistent with a causal and unitary UV completion.

2.2 dRGT Massive Gravity

The inclusion of higher-dimensional operators is standard practice in theories of Dark Energy, where they often serve as convenient parametrizations of potential deviations from General Relativity (GR) at cosmological scales. Their impact, however, depends crucially on how they are chosen: certain combinations can introduce instabilities, whereas carefully tuned interactions can instead guarantee theoretical consistency. For instance, in Horndeski models, higher-derivative terms are arranged so that the equations of motion remain second order, thereby avoiding Ostrogradsky instabilities. In other models, higher-derivative terms sustain screening mechanisms that enable to recover GR at small scales, preserving compatibility with solar system tests.

Among the many modified gravity proposals, massive gravity stands out for its conceptual simplicity and rich phenomenology. By endowing the graviton with a mass, the theory introduces three additional degrees of freedom in four dimensions, leading to observable features such as modified dispersion relations and a finite gravitational interaction range on scales $\sim m_g^{-1}$.

However, constructing a consistent theory of a massive spin-2 field is far from straightforward. The Fierz–Pauli theory [47], the first linear theory of massive gravity, exhibits a discontinuity in the massless limit, known as the van Dam–Veltman–Zakharov (vDVZ) discontinuity [48, 49]. This issue was addressed by Vainshtein [50], who emphasized the importance of nonlinear interactions in recovering GR predictions at short distances. Yet, attempts to construct a fully nonlinear theory of massive gravity ran into another problem: the presence of a sixth, ghost-like degree of freedom—the Boulware–Deser ghost [51].

A major breakthrough occurred with the work of de Rham, Gabadadze, and Tolley (dRGT), who formulated a nonlinear, ghost-free theory of massive gravity [32].

In what follows, we review the key steps leading to the construction of the dRGT model, beginning with the linear theory of a spin-2 field in Minkowski spacetime.

2.2.1 Massive Fierz-Pauli

The kinetic term for a massless spin-2 field on flat space is uniquely determined, up to normalization, by Lorentz invariance, locality, and absence of ghosts. It takes the form

$$\mathcal{K}_h = -\frac{1}{4} h^{ab} \mathcal{E}_{ab}{}^{cd} h_{cd}, \tag{2.2.1}$$

where $\mathcal{E}_{ab}{}^{cd}$ is the Lichnerowicz operator, defined as

$$\mathcal{E}^{ab}{}_{cd}h_{ab} = -\frac{1}{2}\left(\Box h_{cd} - 2\partial_{(c}\partial^a h_{d)a} + \partial_c\partial_d h - \eta_{cd}(\Box h - \partial_a\partial_b h^{ab})\right). \tag{2.2.2}$$

This is the result obtained by expanding the Einstein–Hilbert action around flat space to quadratic order in the metric perturbation. Alternatively, from a bottom-up perspective, this is the unique quadratic action that is ghost-free and propagates the correct number of degrees of freedom for a massless spin-2 field.

The symmetric tensor h_{ab} contains 10 components. Gauge invariance under linear diffeomorphisms

$$h_{ab} \to h_{ab} + \partial_{(a}\xi_{b)} \tag{2.2.3}$$

removes 4 components, while other 4 are non-dynamical (they enter the action without time derivatives and hence do not propagate). This leaves 2 physical degrees of freedom, corresponding to the ± 2 helicities of the massless graviton.

The spin-2 field couples to matter via

$$\frac{1}{2M_{\rm Pl}}h_{ab}T^{ab}, \tag{2.2.4}$$

which leads to the field equation

$$\mathcal{E}_{ab}{}^{cd}h_{cd} = \frac{1}{M_{\rm Pl}}T_{ab}. \tag{2.2.5}$$

In de Donder gauge, defined by

$$\partial^a h_{ab} = \frac{1}{2}\partial_b h, \tag{2.2.6}$$

this equation simplifies to

$$\Box h_{ab} = -\frac{2}{M_{\rm Pl}}\left(T_{ab} - \frac{1}{2}\eta_{ab}T\right), \tag{2.2.7}$$

and the propagator takes the form

$$G_{abcd} = \frac{\eta_{a(c}\eta_{|b|d)} - \frac{1}{2}\eta_{ab}\eta_{cd}}{\Box}. \tag{2.2.8}$$

To describe a massive spin-2 particle, one adds the Fierz-Pauli mass term to the action:

$$\mathcal{L}_m = -\frac{1}{8}m^2\left(h_{ab}h^{ab} - \alpha h^2\right), \tag{2.2.9}$$

which inevitably breaks the gauge symmetry. However, one can use a Stueckelberg trick to restore it, introducting into the description an extra vector field χ_a, and replacing h_{ab} with $h_{ab} + 2\partial_{(a}\chi_{b)}$. This way, the mass term becomes

$$-\frac{1}{8}m^2\left[\left(h_{ab} + 2\partial_{(a}\chi_{b)}\right)^2 - \alpha\left(h + 2\partial_c\chi^c\right)^2\right]. \tag{2.2.10}$$

and it can be checked that it is invariant under the gauge transformations

$$h_{ab} \to h_{ab} + \partial_{(a}\xi_{b)}, \quad \chi_a \to \chi_a - \frac{1}{2}\xi_a. \tag{2.2.11}$$

Setting $\alpha = 1$, so that the kinetic term of the vector field χ_a reduces to the Maxwell Lagrangian, one can make the field content more explicit by decomposing

$$\chi_a = \frac{1}{m}A_a + \frac{1}{m^2}\partial_a\pi, \tag{2.2.12}$$

and writing

$$h_{ab} = \tilde{h}_{ab} + \eta_{ab}\pi. \tag{2.2.13}$$

The full quadratic action then acquires the form

$$\begin{aligned}\mathcal{L}_h = &-\frac{1}{4}\tilde{h}^{ab}\mathcal{E}_{ab}{}^{cd}\tilde{h}_{cd} - \frac{1}{8}F_{ab}F^{ab} - \frac{3}{4}\partial_a\pi\partial^a\pi - \frac{1}{8}m^2(\tilde{h}_{ab}\tilde{h}^{ab} - \tilde{h}^2) + \frac{3}{2}m^2\pi^2 \\ &- \frac{1}{2}m\partial_{(a}A_{b)}\left(\tilde{h}^{ab} - \tilde{h}\eta^{ab}\right) + 3m\pi\partial_a A^a + \frac{3}{2}m^2\pi\tilde{h},\end{aligned} \tag{2.2.14}$$

where the first three terms are nothing but the kinetic terms of the tensor, the vector and the scalar degrees of freedom of the theory. Thus, the above Lagrangian correctly describes the 5 degrees of freedom of a massive spin-2 field: 2 from the tensor $\tilde{h}_{ab}$, 2 from the transverse polarizations of the vector A_a, and 1 scalar π. In particular, looking at the mass eigenstates reveals that all d.o.f.s have the same mass m.

Using (2.2.13) in the coupling to matter yields to different contributions

$$h_{ab}T^{ab} = \tilde{h}_{ab}T^{ab} + \pi T, \tag{2.2.15}$$

where the second extra term involves the coupling between the helicity-0 mode of the graviton and the trace of the stress-energy tensor. Extracting the evolution equations

$$(\Box - m^2)h_{ab} = \frac{1}{M_{Pl}}\left(\tilde{\eta}_{a(c}\tilde{\eta}_{d)b} - \frac{1}{3}\tilde{\eta}_{ab}\tilde{\eta}_{cd}\right)T^{cd}, \tag{2.2.16}$$

reveals the form of the propagator of a massive spin-2 field to be

$$G^m_{abcd} = \frac{\tilde{\eta}_{a(c}\tilde{\eta}_{|b|d)} - \frac{1}{3}\tilde{\eta}_{ab}\tilde{\eta}_{cd}}{\Box - m^2}, \quad \text{with} \quad \tilde{\eta}_{ab} = \eta_{ab} - \frac{1}{m^2}\partial_a\partial_b. \tag{2.2.17}$$

It it straightforward to check that, in the massless limit $m \to 0$, the above expression does not match (2.2.8). This mismatch, also called *van Dam–Veltman–Zakharov (vDVZ) discontinuity* is a manifestation of the fact that the massless limit of the massive theory does not reproduce the predictions of massless linearized General Relativity. Such discontinuity is a peculiarity of the spin-2 field and it is entirely due to the fact that one of the physical polarizations of the massive graviton couples directly to matter at the linear level. In the case of a spin-1 field, on the contrary, the extra polarizations decouple smoothly in the $m \to 0$ limit, yielding back the exact form of the massless propagator.

The resolution of this discontinuity was later identified by Vainshtein, who pointed out the necessity to incorporate nonlinear interactions. At nonlinear level, indeed, a *Vainshtein screening* mechanism leads to a heavy suppression of the the dynamics of the helicity-0 mode, which is effectively decoupled. Thus, to wash away the vDVZ disconinuity it is necessary to look for a nonlinear completion of the Fierz-Pauli Lagrangian. This demands a nonlinear completion not only of the kinetic term, which is just the Einstein-Hilbert action, but also of the mass term, ultimately leading to the dRGT action.

2.2.2 Full dRGT

To get a nonlinear completion of Fierz-Pauli, one should map the mass terms of h_{ab} into mass terms for the metric tensor g_{ab}. However, one immediately realizes that,besides δ^a_b and $\sqrt{-g}$, no nontrivial scalar density can be built out of g_{ab} only[7]. It is therefore necessary to introduce an extra auxiliary object, a reference metric f_{ab}, in order to be able to build non-trivial candidates for the mass term. On physical grounds, the reference metric f_{ab} can be thought of as the background over which the graviton field propagates.

It is important to notice that the generic reference metric f_{ab} does not, in general, transform as a tensor under a general change of coordinates. Nonetheless, one can covariantize the reference metric introducing four Stückelberg fields ϕ_a and defining the object

$$\tilde{f}_{ab} \equiv \partial_a\phi^c\partial_b\phi^d f_{cd}. \tag{2.2.18}$$

The covariant reference metric $\tilde{f}_{ab}$ will indeed transform as a tensor provided each ϕ^a transforms as a scalar under a general coordinate transformation. The tensor $\tilde{f}_{ab}$ can be

[7]Provided the covariant derivative operator is defined with respect to the Levi-Civita connection.

thought of as the push-forward of the reference metric f_{ab} from the manifold on which f_{ab} is defined (whose coordinates are nothing but the Stueckelberg fields) to the physical manifold, inhabited by g_{ab}.

The same covariantization procedure can be carried for the metric fluctuations $h_{ab} = M_{\rm Pl}(g_{ab} - f_{ab})$. Concretely speaking, this means promoting h_{ab} to the tensor

$$H_{ab} \equiv M_{\rm Pl}(g_{ab} - \tilde{f}_{ab}),$$

which correctly embodies all the five degrees of freedom of the massive graviton. This can be seen more explicitly specializing to the case where $f_{ab} = \eta_{ab}$ (and, consequently, $\tilde{f}_{ab} = \partial_a\phi^c\partial_b\phi_c$). In this situation it is convenient to write the Stückelberg fields in the following manner[8]

$$\phi^a = x^a - \frac{1}{M_{\rm Pl}}\chi^a,$$

where a has to be intended as a Lorentz index. If a further helicity decomposition of the vector χ_a

$$\chi_a = \frac{1}{m}A_a + \frac{1}{m^2}\partial_a\pi$$

is performed, the explicit form of the perturbation H_{ab} acquires the form

$$\begin{aligned} H_{ab} = M_{\rm Pl}(g_{ab} - \tilde{f}_{ab}) = h_{ab} + \frac{2}{M_{\rm Pl}m}\partial_{(a}A_{b)} + \frac{2}{M_{\rm Pl}m^2}\Pi_{ab} + \frac{1}{M_{\rm Pl}^2m^2}\partial_aA^c\partial_bA_c \\ - \frac{2}{M_{\rm Pl}^2m^3}\partial_aA^c\Pi_{bc} - \frac{1}{M_{\rm Pl}^2m^4}\Pi_{ac}\Pi^c_b, \end{aligned} \tag{2.2.19}$$

where $\Pi_{ab} \equiv \partial_a\partial_b\pi$. The equation above shows the explicit appearance of the helicity modes of the massive graviton: A_a identifies the helicity-1 degrees of freedom of the massive spin-2 field, while π encodes the helicity-0 mode information.

The introduction of an additional metric f_{ab} in the form of a generic reference metric might not sound too tasty. To convince ourselves that this is indeed a necessity, we must think about the possible ways to construct a nontrivial mass term to include in the nonlinear Lagrangian of the graviton. Indeed, the only possible scalar that can be built out of the physical metric, g_{ab}, alone is $g_{ab}g^{ab} = 4$, which contributes in the form of a cosmological constant. The presence of the additional tensor $\tilde{f}_{ab}$ enables to construct nontrivial mass

[8]The notation is motivated by the fact that, in the Unitary gauge, $\phi^a = x^a$ and the two metrics f_{ab} and $\tilde{f}_{ab}$ do coincide.

terms for the graviton. Indeed, the fundamental building block adopted in the extensions of the Fierz-Pauli mass term is

$$\mathcal{X}^a_b \equiv g^{ac}\tilde{f}_{cb}, \tag{2.2.20}$$

from which the covariant spacetime perturbation H_{ab} can be rewritten as

$$H^a_b = M_{\rm Pl}(\delta^a_b - \mathcal{X}^a_b).$$

It follows, then, that the most straightforward nonlinear extension of the Fierz-Pauli mass term is

$$\mathcal{L}_m = -m^2 M_{\rm Pl}^2\sqrt{-g}\left([(1-\mathcal{X})^2] - [1-\mathcal{X}]^2\right), \tag{2.2.21}$$

where square brackets denote the trace.

Clearly, this is not the only possible way to nonlinearly extend the Fierz-Pauli mass term. More general functions of the perturbation H_{ab} have been proposed to provide a mass term for the graviton, but it turned out that they possessed ghost instabilities [51]. Eq. (2.2.21) makes no exception. To see more clearly the appearance of such pathology, we restrict to the helicity-0 mode sector of the tensor $\mathcal{X}^a_b$,

$$\mathcal{X}^a_b = \delta^a_b - \frac{2}{M_{\rm Pl}m^2}\Pi^a_b + \frac{1}{M_{\rm Pl}^2 m^4}\Pi^a_c\Pi^c_b\,,$$

where $\Pi^a_b \equiv \partial^a\partial_b\pi$ and look at the structure of the corresponding Lagrangian:

$$\mathcal{L}_\pi = -\frac{4}{m^2}\left([\Pi^2]-[\Pi]^2\right) + \frac{4}{M_{\rm Pl}m^4}\left([\Pi^3]-[\Pi][\Pi^2]\right) + \frac{1}{M_{\rm Pl}^2 m^6}\left([\Pi^4]-[\Pi^2]^2\right). \tag{2.2.22}$$

It is not difficult to notice that the quadratic term acquires the form of a total derivative. The actual problem lies in the fact that this property is not enjoyed by the cubic and quartic operators, which therefore induce the presence of higher derivative terms in the equation of motion of the helicity-0 mode of the graviton, signaling the presence of a ghost-like instability. To get rid of such pathology, the mass term must be constructed in a clever manner, in order to enable recasting the helicity-0 mode operators into the form of total derivatives.

In 2010, a considerable breakthrough was achieved when de Rham, Gabadadze and Tolley [32] succeeded in constructing a mass term that was not plagued by ghost pathologies, obtaining the first ghost-free nonlinear model of Massive Gravity. Although the original construction was carried through the introduction of an auxiliary extra dimension [52], the same structure of the mass term operators can be obtained by means of a nonlinear

algebraic equation. In particular, the mass term turns out to consist of a finite sum of polynomials in the tensor

$$\mathcal{K}^a_b \equiv \delta^a_b - \left(\sqrt{g^{-1}f}\right)^a_b = \delta^a_b - (\delta^a_b - H^a_b) = -\sum_{i=1}^{\infty} d_i (H^i)^a_b, \tag{2.2.23}$$

where $(H^i)^a_b = H^a_{c_1} H^{c_1}_{c_2} \cdots H^{c_{i-1}}_b$ and

$$d_i = \frac{(2i)!}{(1-2i)(i!)^2 4^i}.$$

More specifically, it is a linear combination of the elementary symmetric polynomials of the eigenvalues of the above matrix:

$$\begin{aligned}
e_0(\mathcal{K}) &= \epsilon^{abcd}\epsilon_{abcd} = 4!, \\
e_1(\mathcal{K}) &= \epsilon^{abcd}\epsilon_{a'bcd}\mathcal{K}^{a'}_a = 3![\mathcal{K}], \\
e_2(\mathcal{K}) &= \epsilon^{abcd}\epsilon_{a'b'cd}\mathcal{K}^{a'}_a\mathcal{K}^{b'}_b = 2!\left([\mathcal{K}]^2 - [\mathcal{K}^2]\right), \\
e_3(\mathcal{K}) &= \epsilon^{abcd}\epsilon_{a'b'c'd}\mathcal{K}^{a'}_a\mathcal{K}^{b'}_b\mathcal{K}^{c'}_c = [\mathcal{K}]^3 - 3[\mathcal{K}][\mathcal{K}^2] + 2[\mathcal{K}^3], \\
e_4(\mathcal{K}) &= \epsilon^{abcd}\epsilon_{a'b'c'd'}\mathcal{K}^{a'}_a\mathcal{K}^{b'}_b\mathcal{K}^{c'}_c\mathcal{K}^{d'}_d = \det[\mathcal{K}].
\end{aligned} \tag{2.2.24}$$

Higher order poylnomials do not contribute since they are zero in $d = 4$ spacetime dimensions. More generally, given a fixed number of dimensions d, $e_k(\mathcal{K})$ is identically vanishing for $k > d$ [53]. Actually, not all the above scalars bring a nontrivial contribution to the mass term of the graviton. The e_0 polynomial describes the presence of a cosmological constant term, while $e_1(\mathcal{K})$ corresponds to a tadpole. The structure of $e_2(\mathcal{K})$ resembles the quadratic term that appeared in eq. (2.2.22), and the scalars $e_3(\mathcal{K})$ and $e_4(\mathcal{K})$ are genuine nonlinear potentials.

Being a linear combination of the scalars $e_n(\mathcal{K})$, the mass term can then be written as

$$\mathcal{U}[g,f] = -\frac{m^2}{2}\sum_{n=0}^{4}\alpha_n e_n(\mathcal{K}), \tag{2.2.25}$$

with α_n the string of parameters of the theory. The full Lagrangian of the dRGT model results to be

$$\mathcal{L}_{\text{dRGT}} = \frac{M^2_{\text{Pl}}}{2}\sqrt{-g}\left(R[g] - \mathcal{U}[g,f]\right). \tag{2.2.26}$$

The above expression provides a mathematically consistent description of the physics of the massive graviton. As it was previously emphasized, the mass term possesses a

very special structure. Indeed, it can be recast, at every order, into the form of a total derivative, generalizing, thus, the Fierz-Pauli structure of (2.2.21). The clever construction of $\mathcal{U}$ ensures the absence of the Boulware-Deser ghost riding on top of the helicity-0 mode of the massive spin-2 field. Actually, it was proved that the dRGT model of Massive Gravity is fully ghost-free [54,55]. The key observation lies in the fact that not all the Stueckelberg fields are independent. In particular, the Hessian matrix

$$\mathcal{H}_{ab} \equiv \frac{\delta^2 \mathcal{L}_{\mathrm{dRGT}}}{\delta \dot{\phi}^a \delta \dot{\phi}^b}$$

turns out to have a vanishing determinant, and therefore it is not invertible[9]. This condition ensures that the dynamics of one of the Stueckelberg fields can be completely determined by solving the equation of motion of the remaining three. As a consequence, the introduction of the Stückelbergs ϕ^a brings three (instead of four) additional degrees of freedom into play, for a total of five physical degrees of freedom for the theory, which is consistent with the number of independent polarizations possessed by a massive spin-2 field.

It is important to notice that, even at the nonlinear level, the inclusion of the Stueckelberg fields is necessary to restore nonlinear diffeomorphism invariance, which is inevitably broken when the graviton mass term is introduced in the Lagrangian. As it was previously mentioned, this results in the promotion of the reference metric f_{ab} to the tensor $\tilde{f}_{ab}$.

Phenomenologically speaking, the possibility to rely on a consistent Massive Gravity model gives the opportunity to consider interesting scenarios. As an example, the additional degrees of freedom stored in the graviton result in new potential gravitational wave polarizations. In particular, two new vector modes and a scalar mode.

On the cosmological side, a nonvanishing graviton mass would imply a finite range for the gravitational interaction: the gravitational potential profile would acquire a Yukawa-like suppression, leading to a weakening of the interaction itself. Heuristically, this suppression might mimic the observed cosmic accelerated expansion. As a consequence, Massive Gravity may be able to provide an alternative explanation for the late time cosmic acceleration.

Although the potentially interesting cosmological implication of the theory, it has been shown that no dynamical flat/closed FLRW solutions are admitted for the dRGT graviton [56]. More precisely, the choice of a Minkowski reference metric, together with an FLRW-compatible ansatz for the Stueckelberg fields ϕ^a, results in a staticity constraint on the

[9] Alternatively, one may exploit the ADM language and show that the lapse function is the only non-dynamical variable, whose associated constraint removes the ghost degree of freedom.

scale factor

$$\dot{a} = 0 \ . \tag{2.2.27}$$

Progress was made (see [57, 58]) when it was realized that the aforementioned No-Go theorem was a consequence of the poorly chosen ansatz for the Stueckelberg fields. Indeed, different authors showed that relaxing homogeneity or isotropy [58–60] of the Stueckelbergs gave access to dynamical FLRW backgrounds, even when the extra metric f_{ab} was chosen to be Minkowski. Among them, a potentially interesting self-accelerating solution, in which the Stueckelberg sector behaves as a cosmological constant. It was later highlighted that, on this background, three of the five degrees of freedom of the theory are strongly coupled (see [57, 61–64]).

Despite its pathologies, the extraction of the self-accelerating background teaches an interesting lesson: inhomogeneous Stueckelberg configurations can behave as an effective perfect fluid and sustain a dynamical flat FLRW background solution. Chapter 5 will exploit and extends the approach proposed in [58,65] to classify the most general dynamical flat FLRW solutions of dRGT massive gravity.

Chapter 3

Non-analyticity of the S-matrix with spontaneously broken Lorentz invariance

As mentioned in the introduction, the spontaneous breaking of Lorentz invariance introduces new conceptual challenges for the formulation of positivity bounds. A natural first guess would be to rely on the properties the S-matrix, following methods used in Lorentz-invariant theories [11, 20]. However, as noted in [66], the S-matrix framework is not generally suitable for UV completions without Lorentz invariance.

When Lorentz invariance is preserved, in- and out-states are well defined at all energies. Single-particle states remain free, and boosts connect their low- and high-energy versions, ensuring that the S-matrix is consistently defined: at low energies it can be computed within the EFT, while at high energies the UV completion is required. In the absence of Lorentz invariance, this structure breaks down. As the scattering energy increases, there is no boost symmetry guaranteeing that well-defined low-energy excitations extend to high energies. Indeed, in systems with spontaneously broken Lorentz invariance the low-energy excitations (such as phonons, inflaton perturbations, or black-hole quasinormal modes) simply do not exist at arbitrarily high energies. As a result, the S-matrix cannot be defined in full generality, and one must instead rely on alternative observables, such as conserved currents, to derive universal bounds [66].

In this chapter, we study the S-matrix in a minimal model exhibiting spontaneous Lorentz breaking: a renormalizable complex scalar with a U(1) symmetry at finite charge.

Boost invariance is broken, but spatial and temporal translations remain intact. The model has two modes, a massless Goldstone and a massive radial excitation, whose dispersion relations are analyzed in Section 3.1. Being weakly coupled, the Goldstone S-matrix can be studied at all energies, providing a valuable explicit example of S-matrix physics without Lorentz invariance before making broader claims.

Before calculating the S-matrix and evaluating it in various limits of physical interest (section 3.3 and appendices A.2 and A.3), in section 3.2 (and appendix A.1) we will derive an LSZ reduction formula that connects the S-matrix to correlation functions. Here we encounter a striking difference compared to the Lorentz invariant case: the relation between the S-matrix and correlation functions involves operators that are non-local in space. This spatial non- locality arises from the mixing of the two modes, which depends on the momentum. The presence of this non-locality spoils the analyticity properties of the S-matrix compared to the Lorentz invariant case. We conclude that even in cases where the S-matrix exists at all energies one cannot derive positivity bounds using the conventional dispersive arguments. The same result was obtained by the authors of [67], who addressed the same questions focusing on the same model. In section 3.4 and appendix A.4 we study the decay rate of Goldstones, while conclusions and future directions are discussed in section 3.5.

3.1 The $U(1)$ model

We start with the renormalizable Lagrangian (we use the mostly-minus signature)

$$\mathcal{L} = \partial\Phi^\dagger \cdot \partial\Phi + m^2\,\Phi^\dagger\Phi - \lambda(\Phi^\dagger\Phi)^2\,. \tag{3.1.1}$$

We set

$$\Phi = \frac{\rho}{\sqrt{2}} e^{i\theta/v}\,, \tag{3.1.2}$$

where v is a constant with dimensions of energy that will be defined in (3.1.6). This way we obtain

$$\mathcal{L} = \frac{1}{2}(\partial\rho)^2 + \frac{1}{2v^2}(\partial\theta)^2\rho^2 + \frac{m^2}{2}\rho^2 - \frac{\lambda}{4}\rho^4\,. \tag{3.1.3}$$

We are going to study this model around a time-dependent solution $\theta = \mu^2 t/2$, i.e. with spontaneous breaking of Lorentz invariance. Expanding as $\theta = \mu^2 t/2 + \pi$, we get

$$\mathcal{L} = \frac{1}{2}(\partial\rho)^2 + \frac{1}{2v^2}\left(\mu^2\dot{\pi} + (\partial\pi)^2\right)\rho^2 + \frac{1}{2}\left(m^2 + \frac{\mu^4}{4v^2}\right)\rho^2 - \frac{\lambda}{4}\rho^4\,, \tag{3.1.4}$$

which can be rewritten as

$$\mathcal{L} = \frac{1}{2}(\partial\rho)^2 + \frac{1}{2v^2}\left(\mu^2\dot{\pi} + (\partial\pi)^2\right)\rho^2 - \frac{\lambda}{4}(\rho^2 - v^2)^2 + \text{constant}\,, \tag{3.1.5}$$

where v is implicitly defined through

$$v^2 = \frac{1}{\lambda}\left(m^2 + \frac{\mu^4}{4v^2}\right)\,. \tag{3.1.6}$$

It is useful to notice that for $\mu \ll m/\lambda^{1/4}$, $v \approx m/\lambda^{1/2}$, i.e. the Lorentz invariant result, while for $\mu \gg m/\lambda^{1/4}$, $v \approx \mu/(4\lambda)^{1/4}$. Expanding around the minimum by setting $\rho = v+h$, up to the constant and a total derivative we find

$$\mathcal{L} = \frac{1}{2}(\partial h)^2 + \frac{1}{2}(\partial\pi)^2 + \frac{1}{2v^2}\left(\mu^2\dot{\pi} + (\partial\pi)^2\right)(h^2 + 2vh) - \frac{\lambda}{4}(h^2 + 2vh)^2\,. \tag{3.1.7}$$

Let us focus on the quadratic part of the Lagrangian,

$$\mathcal{L}_{(2)} = \frac{1}{2}(\partial h)^2 + \frac{1}{2}(\partial\pi)^2 + \frac{\mu^2}{v}\dot{\pi}h - \lambda v^2 h^2\,, \tag{3.1.8}$$

which in Fourier space reads

$$\mathcal{L}_{(2)} = \frac{1}{2}\begin{pmatrix} \tilde{\pi}_{-k} & \tilde{h}_{-k} \end{pmatrix}\begin{pmatrix} k^2 & i\mu^2\omega/v \\ -i\mu^2\omega/v & k^2 - M^2 \end{pmatrix}\begin{pmatrix} \tilde{\pi}_k \\ \tilde{h}_k \end{pmatrix}\,, \tag{3.1.9}$$

where

$$M^2 \equiv 2\lambda v^2\,. \tag{3.1.10}$$

By looking at the zeros of the determinant one can find the spectrum of the theory, namely one can find the dispersion relations for the various particles:

$$(\omega^2 - \boldsymbol{k}^2)(\omega^2 - \boldsymbol{k}^2 - M^2) - \frac{\mu^4\omega^2}{v^2} = 0\,. \tag{3.1.11}$$

There are two branches of solutions,

$$\omega^2 = E_\pm(\boldsymbol{k})^2 \equiv \boldsymbol{k}^2 + \frac{1}{2}\left(M^2 + \frac{\mu^4}{v^2}\right) \pm \sqrt{\frac{\mu^4}{v^2}\boldsymbol{k}^2 + \frac{1}{4}\left(M^2 + \frac{\mu^4}{v^2}\right)^2}\,. \tag{3.1.12}$$

Thus the Fock space contains two types of particles which are labelled by their three-momentum $\boldsymbol{k}$ and by an extra label $\pm$ indicating which dispersion relates their energy and momentum, see figure 3.1. The $-$ state is the Goldstone: for small enough $\boldsymbol{k}$ its dispersion

relation is linear, with a speed of propagation smaller than unity. The + state is gapped and, for energies much smaller than this gap, one integrates out this state and writes an EFT for the Goldstone only: we will come back to this in section 3.3.1.

Now that we have established what the asymptotic states are we must choose which fields to use to interpolate such states. One possibility is to use h and π. They clearly can interpolate both $\pm$ states. The purpose of the next section is to quantify how much they actually do.

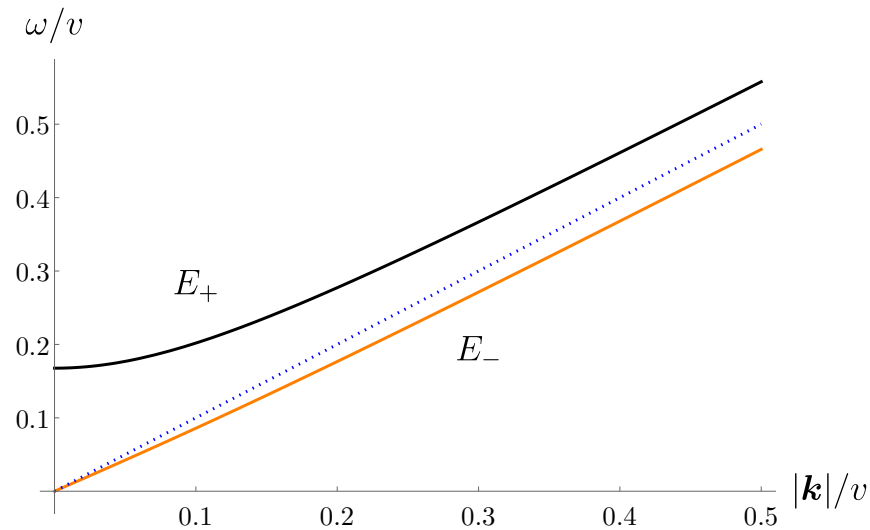

Figure 3.1Plot of the dispersion relations of the + (black) and − (orange) states in units of v for $\lambda = 10^{-2}$ and $\mu/v = 3/10$. The blue dotted line is the null curve $\omega(\boldsymbol{k}) = |\boldsymbol{k}|$, and we have $E_\pm(\boldsymbol{k}) = |\boldsymbol{k}| \pm \mu^2/2v + \mathcal{O}\left(|\boldsymbol{k}|^{-1}\right)$ as $|\boldsymbol{k}| \to \infty$. Thus the + branch is always timelike while the − branch is spacelike.

3.1.1 Canonical quantization

We begin by introducing the ladder operators of the asymptotic states with commutation relations

$$[a_l(\boldsymbol{k}), a_m^\dagger(\boldsymbol{q})] = (2\pi)^3 2E_l(\boldsymbol{k})\delta_{lm}\delta^{(3)}(\boldsymbol{k}-\boldsymbol{q}) \tag{3.1.13}$$

so that a single particle state of type l with three-momentum $\boldsymbol{k}$ is obtained by

$$|l, \boldsymbol{k}\rangle = a_l^\dagger(\boldsymbol{k})\,|0\rangle\ , \quad l \in \{-,+\}\,. \tag{3.1.14}$$

The fields can be written as[1]

$$\phi^a(t,\boldsymbol{x}) \equiv \sum_{l=\pm} \int \frac{\mathrm{d}^3\boldsymbol{k}}{(2\pi)^3 2E_l(\boldsymbol{k})} \left(Z_l^a(\boldsymbol{k}) a_l(\boldsymbol{k}) e^{-i(E_l(\boldsymbol{k})t - \boldsymbol{k}\cdot\boldsymbol{x})} + \text{h.c.} \right) , \quad a \in \{\pi, h\} . \tag{3.1.15}$$

We will now obtain an expression for the Z-factors using the canonical commutation relations and the free equations of motion. The momenta conjugate to π and h are

$$\Pi^\pi = \dot{\pi} + \frac{\mu^2}{2v} h , \quad \Pi^h = \dot{h} - \frac{\mu^2}{2v} \pi , \tag{3.1.16}$$

so that[2]

$$\Pi^b(t,\boldsymbol{x}) = \sum_{l=\pm} \int \frac{\mathrm{d}^3\boldsymbol{k}}{(2\pi)^3 2E_l(\boldsymbol{k})} \left[\left(-iE_l(\boldsymbol{k}) Z_l^b(\boldsymbol{k}) + \epsilon^{bc} \frac{\mu^2}{2v} Z_l^c(\boldsymbol{k}) \right) a_l(\boldsymbol{k}) e^{-i(E_l(\boldsymbol{k})t - \boldsymbol{k}\cdot\boldsymbol{x})} + \text{h.c.} \right] . \tag{3.1.17}$$

The equal-time commutation relations are

$$\begin{aligned} &[\phi^a(t,\boldsymbol{x}), \phi^b(t,\boldsymbol{y})] = 0 , \\ &[\phi^a(t,\boldsymbol{x}), \Pi^b(t,\boldsymbol{y})] = i\delta^{ab}\delta^{(3)}(\boldsymbol{x}-\boldsymbol{y}) , \\ &[\Pi^a(t,\boldsymbol{x}), \Pi^b(t,\boldsymbol{y})] = 0 . \end{aligned} \tag{3.1.18}$$

The first and second equations read[3]

$$\begin{aligned} &\sum_{l=\pm} \frac{Z_l^a \bar{Z}_l^b - \bar{Z}_l^a Z_l^b}{E_l} = 0 , \\ &\sum_{l=\pm} Z_l^a \bar{Z}_l^b + \bar{Z}_l^a Z_l^b = 2\delta^{ab} , \end{aligned} \tag{3.1.19}$$

where we have suppressed the $\boldsymbol{k}$-dependence and indicated with $\bar{Z}$ the complex conjugate of Z. The third equation boils down to

$$\sum_{l=\pm} \frac{E_l}{2} \left(Z_l^a \bar{Z}_l^b - \bar{Z}_l^a Z_l^b \right) = -i \frac{\mu^2}{v} \epsilon^{ab} . \tag{3.1.20}$$

The free equations of motion imply that for fixed l the vector Z_l^a is an eigenvector of the matrix in Eq. (3.1.9). This gives

$$Z_l^h = \frac{iE_l \mu^2}{v k_l^2} Z_l^\pi , \tag{3.1.21}$$

[1] $\phi^\pi \equiv \pi, \phi^h \equiv h$.

[2] $\epsilon^{\pi h} \equiv 1 \equiv -\epsilon^{h\pi}$ and zero otherwise.

[3] Here we use invariance under spatial rotations – that $Z_l^a(\boldsymbol{k})$ is only a function of $|\boldsymbol{k}|$.

where $k_l^2 = E_l(\boldsymbol{k})^2 - \boldsymbol{k}^2$ and this equation holds for $l \in \{-,+\}$ separately. Using Eq. (3.1.21) in (3.1.19) gives

$$\sum_{l=\pm} \frac{|Z_l^\pi|^2}{k_l^2 - M^2} = 0\,, \quad \sum_{l=\pm} |Z_l^\pi|^2 = 1\,, \tag{3.1.22}$$

whose solutions are

$$|Z_l^\pi|^2 = l\frac{k_l^2 - M^2}{k_+^2 - k_-^2}\,, \quad l \in \{-,+\}\,. \tag{3.1.23}$$

Explicitly in terms of the spatial momentum,

$$|Z_\pm^\pi(\boldsymbol{k})|^2 = \frac{1}{2} \pm \frac{\mu^4/v^2 - M^2}{2\sqrt{4\mu^4\boldsymbol{k}^2/v^2 + (\mu^4/v^2 + M^2)^2}}\,, \tag{3.1.24}$$

$$|Z_\pm^h(\boldsymbol{k})|^2 = \frac{1}{2} \pm \frac{\mu^4/v^2 + M^2}{2\sqrt{4\mu^4\boldsymbol{k}^2/v^2 + (\mu^4/v^2 + M^2)^2}}\,. \tag{3.1.25}$$

With the relations (3.1.21), there are two remaining unfixed phases in the solution. These correspond to our freedom in (3.1.15) to rotate $a_\pm(\boldsymbol{k})$. Choosing Z_-^π and Z_+^h to be positive real, the explicit expressions for the interpolating factors are

$$Z_-^\pi(\boldsymbol{k}) = \sqrt{\frac{1}{2} - \frac{\mu^4/v^2 - M^2}{2\sqrt{4\mu^4\boldsymbol{k}^2/v^2 + (\mu^4/v^2 + M^2)^2}}}\,, \tag{3.1.26}$$

$$Z_-^h(\boldsymbol{k}) = -i\sqrt{\frac{1}{2} - \frac{\mu^4/v^2 + M^2}{2\sqrt{4\mu^4\boldsymbol{k}^2/v^2 + (\mu^4/v^2 + M^2)^2}}}\,, \tag{3.1.27}$$

$$Z_+^\pi(\boldsymbol{k}) = -i\sqrt{\frac{1}{2} + \frac{\mu^4/v^2 - M^2}{2\sqrt{4\mu^4\boldsymbol{k}^2/v^2 + (\mu^4/v^2 + M^2)^2}}}\,, \tag{3.1.28}$$

$$Z_+^h(\boldsymbol{k}) = \sqrt{\frac{1}{2} + \frac{\mu^4/v^2 + M^2}{2\sqrt{4\mu^4\boldsymbol{k}^2/v^2 + (\mu^4/v^2 + M^2)^2}}}\,. \tag{3.1.29}$$

From these expressions we see

$$Z_-^\pi(\boldsymbol{k}) \sim Z_+^h(\boldsymbol{k}) \sim \frac{1}{\sqrt{2}}\,, \quad Z_+^\pi(\boldsymbol{k}) \sim Z_-^h(\boldsymbol{k}) \sim -\frac{i}{\sqrt{2}} \quad \text{as } |\boldsymbol{k}| \to \infty\,. \tag{3.1.30}$$

This means that at high energies the two fields π, h interpolate the two asymptotic states $-,+$ equally well. This can also be understood by considering the quadratic Lagrangian

(3.1.8) and noticing that, in the high energy limit, the splitting is dominated by the one-derivative operator $(\mu^2/v)h\dot{\pi}$ while the mass can be neglected. So at high energies the quadratic Lagrangian reads

$$\mathcal{L}_{(2)} \sim \frac{1}{2}\begin{pmatrix} \pi & h \end{pmatrix}\begin{pmatrix} -\partial^2 & -(\mu^2/v)\partial_t \\ (\mu^2/v)\partial_t & -\partial^2 \end{pmatrix}\begin{pmatrix} \pi \\ h \end{pmatrix} \tag{3.1.31}$$

which can be diagonalized yielding

$$\mathcal{L}_{(2)} \sim \frac{1}{2}\times\frac{1}{\sqrt{2}}\begin{pmatrix} \pi - ih & h - i\pi \end{pmatrix}\begin{pmatrix} -\partial^2 + i(\mu^2/v)\partial_t & 0 \\ 0 & -\partial^2 - i(\mu^2/v)\partial_t \end{pmatrix}\frac{1}{\sqrt{2}}\begin{pmatrix} \pi + ih \\ h + i\pi \end{pmatrix}. \tag{3.1.32}$$

In the two eigenvalues we recognize the high energy limits of the dispersion relations (3.1.12) and in the eigenvectors we recognize the high energy limits of the Z-factors (3.1.30). Since the leading splitting operator $(\mu^2/v)h\dot{\pi}$ is Lorentz-breaking, going to very high energies one does not recover the same eigenvectors as in the Lorentz invariant limit $\mu \to 0$. At low energies, conversely, the splitting is dominated by the mass. The crossover between the two regimes happens at

$$\frac{\mu^2\omega}{v} \sim M^2 \quad \Rightarrow \quad \omega_c \sim \frac{M^2 v}{\mu^2} \sim \lambda\frac{v^3}{\mu^2}\,. \tag{3.1.33}$$

For $\mu \lesssim m/\lambda^{1/4}$, this crossover scale is $\omega_c \sim m^3/(\mu^2\lambda^{1/2})$, otherwise, for $\mu \gtrsim m/\lambda^{1/4}$, $\omega_c \sim \lambda^{1/4}\mu$.

3.2 LSZ reduction formula and lack of analyticity

In this section we will derive the LSZ reduction formula [68], following Weinberg's "polology" arguments [34].[4] This is well-known material in the Lorentz invariant case, and we will highlight the differences in the absence of Lorentz invariance.

We want to prove the following relation between time-ordered Green's functions and

[4] We acknowledge Riccardo Rattazzi for clarifying certain aspects of Weinberg's "polology" arguments and their link to the LSZ reduction formula, during the "Advanced Quantum Field Theory" course given at EPFL in 2020.

S-matrix elements:

$$\prod_{i=1}^{n}\int \mathrm{d}^4 y_i\, e^{ip_i\cdot y_i}\prod_{j=1}^{m}\int \mathrm{d}^4 x_j\, e^{-ik_j\cdot x_j}\langle 0|T(\pi(y_1)\dots\pi(y_n)\pi(x_1)\dots\pi(x_m))|0\rangle \cong \\ \prod_{i=1}^{n}\frac{iZ_-^\pi(\boldsymbol{p}_i)}{(p_i^0)^2-E_-(\boldsymbol{p}_i)^2+i\varepsilon}\prod_{j=1}^{m}\frac{i\bar{Z}_-^\pi(\boldsymbol{k}_j)}{(k_j^0)^2-E_-(\boldsymbol{k}_j)^2+i\varepsilon}\langle \boldsymbol{p}_1\dots\boldsymbol{p}_n|S|\boldsymbol{k}_1\dots\boldsymbol{k}_m\rangle\,. \tag{3.2.1}$$

The $\cong$ symbol indicates the equality holds in the limit all particles go on-shell: $p_i^0\to E_-(\boldsymbol{p}_i)$ and $k_j^0\to E_-(\boldsymbol{k}_j)$. Notice we are taking the convention that $p_i^0,k_j^0>0$. The matrix elements were defined in (3.1.15) as

$$Z_\pm^a(\boldsymbol{k})\equiv\langle 0|\phi^a(0)|\pm,k\rangle\ ,\quad a\in\{h,\pi\}\,. \tag{3.2.2}$$

(In the standard Lorentz invariant treatment, these would reduce to a factor $\sqrt{Z}$, which describes the wavefunction normalization.) Here we are considering the scattering of $-$ particles; if one were interested in $+$ particles, one should use Z_+'s and also use the dispersion relations $E_+(\,\cdot\,)^2$. In this way of deriving the LSZ reduction formula, one is free to use any field to interpolate the particles of interest provided there is a nonzero overlap. For instance, one could write a similar formula by replacing some (or all) the fields π with h. Since the overlap between a $-$ particle and the h-field goes to zero at low energies (see (3.1.29)), it is more natural to use π.

To prove (3.2.1) one focuses on the regions of integration $y_i^0\to+\infty$ and $x_i^0\to-\infty$ since this is the region that gives rise to the poles [34]. In this regime all the y's are after all the x's and the time-ordered product factorizes as

$$\langle 0|T(\pi(y_1)\dots\pi(y_n))T(\pi(x_1)\dots\pi(x_m))|0\rangle\,. \tag{3.2.3}$$

We can thus insert a complete set of states (twice) in the middle,

$$\sum_{\alpha,\beta}\langle 0|T(\pi(y_1)\dots\pi(y_n))|\alpha_{\rm out}\rangle\langle\alpha_{\rm out}|\beta_{\rm in}\rangle\langle\beta_{\rm in}|T(\pi(x_1)\dots\pi(x_m))|0\rangle\,. \tag{3.2.4}$$

The object $\langle\alpha_{\rm out}|\beta_{\rm in}\rangle$ is the S-matrix. In the late-time limit, after the wave packets of the various particles are separated, the matrix element on the left is dominated by a state with n particles:

$$\lim_{y_i^0\to+\infty}\langle 0|T(\pi(y_1)\dots\pi(y_n))|\alpha_{\rm out}\rangle\cong\langle 0|T(\pi(y_1)\dots\pi(y_n))|\boldsymbol{q}_1\dots\boldsymbol{q}_n\rangle_{\rm out}\cong \\ \cong\prod_{i=1}^{n}\langle 0|\pi(y_i)|\boldsymbol{q}_i\rangle_{\rm out}\cong\prod_{i=1}^{n}Z_-^\pi(\boldsymbol{q}_i)e^{-iq_i\cdot y_i}\,. \tag{3.2.5}$$

(The resolution of identity contains also + particles, but those would not contribute to the pole when one goes on-shell for − states.) Notice that if the theory were invariant under boosts, Z would not depend on $\boldsymbol{q}$: as we will see, this is a crucial difference. (We have been sloppy here with permutations, which will eventually cancel with the normalization of states with identical particles.) Each term in the product gives

$$\int \mathrm{d}^4 y_i \, e^{ip_i\cdot y_i} Z_-^\pi(\boldsymbol{q}_i) e^{-iq_i\cdot y_i} = \int \mathrm{d}y_i^0 (2\pi)^3 \delta^{(3)}(\boldsymbol{p}_i - \boldsymbol{q}_i) Z_-^\pi(\boldsymbol{q}_i) e^{i(p_i^0 - q_i^0)y_i^0} \,, \tag{3.2.6}$$

where we did the integral over the spatial variables. Then doing the integral over the phase space, $\int \mathrm{d}^3\boldsymbol{q}_i/((2\pi)^3 2E_-(\boldsymbol{q}_i))$, one gets

$$\int \mathrm{d}y_i^0 \frac{1}{2E_-(\boldsymbol{p}_i)} Z_-^\pi(\boldsymbol{p}_i) e^{i(p_i^0 - E_-(\boldsymbol{p}_i))y_i^0} \cong \frac{iZ_-^\pi(\boldsymbol{p}_i)}{(p_i^0)^2 - E_-(\boldsymbol{p}_i)^2 + i\varepsilon} \,, \tag{3.2.7}$$

where the last equality is valid up to terms that vanish as one goes close to the pole. To make the time integral well-defined one has to slightly deform the contour of integration, hence the $i\varepsilon$. The same arguments work for the incoming particles, proving the LSZ formula (3.2.1).

We can now proceed to study the analyticity of the $2 \to 2$ S-matrix. In this case the LSZ formula, in which only one in-going and one out-going leg is reduced, gives

$$S = -\int \mathrm{d}^4x \, \mathrm{d}^4y \, e^{i(q_2\cdot y - q_1\cdot x)} \frac{-\partial_{y^0}^2 - E_-(-i\partial_{y_i})^2}{Z_-^\pi(-i\partial_{y_i})} \frac{-\partial_{x^0}^2 - E_-(-i\partial_{x_i})^2}{\bar{Z}_-^\pi(-i\partial_{x_i})} \langle \boldsymbol{p}_2 | T(\pi(y)\pi(x)) | \boldsymbol{p}_1 \rangle \,. \tag{3.2.8}$$

We slightly changed the notation calling $\boldsymbol{q}_1$ and $\boldsymbol{p}_1$ the incoming momenta ($\boldsymbol{q}_2$ and $\boldsymbol{p}_2$ are outgoing). This simplifies the comparison with Itzykson & Zuber's book [35], whose logic we will follow. As in the Lorentz invariant case one can replace the time-ordered correlation function with the retarded two-point function: the difference only contributes to a disconnected piece of the S-matrix. Therefore one has

$$S = -\int \mathrm{d}^4x \, \mathrm{d}^4y \, e^{i(q_2\cdot y - q_1\cdot x)} \frac{-\partial_{y^0}^2 - E_-(-i\partial_{y_i})^2}{Z_-^\pi(-i\partial_{y_i})} \frac{-\partial_{x^0}^2 - E_-(-i\partial_{x_i})^2}{\bar{Z}_-^\pi(-i\partial_{x_i})} \langle \boldsymbol{p}_2 | \theta(y^0 - x^0)[\pi(y), \pi(x)] | \boldsymbol{p}_1 \rangle \,. \tag{3.2.9}$$

Using translation invariance one can then factor out the delta function of energy and momentum conservation,

$$S = (2\pi)^4 \delta^{(4)}(p_2 + q_2 - p_1 - q_1) i\mathcal{M} \,, \tag{3.2.10}$$

so that, in terms of $q \equiv \frac{1}{2}(q_1 + q_2)$, one has

$$\mathcal{M} = i \int \mathrm{d}^4 z \, e^{iq\cdot z} \langle \boldsymbol{p}_2 | \theta(z^0) \left[\frac{\partial^2_{z^0/2} + E_-(-i\partial_{z_i/2})^2}{Z^\pi_-(-i\partial_{z_i/2})} \pi\left(\frac{z}{2}\right), \frac{\partial^2_{z^0/2} + E_-(-i\partial_{z_i/2})^2}{\bar{Z}^\pi_-(-i\partial_{z_i/2})} \pi\left(-\frac{z}{2}\right) \right] |\boldsymbol{p}_1\rangle \,. \tag{3.2.11}$$

In the Lorentz invariant case the Z's are just constants and the differential operators are the Klein-Gordon ones, $\Box + m^2$. Since these operators are local, the integrand is nonzero only for z^μ in the forward lightcone. Therefore $\mathcal{M}(q^\mu)$ is analytic if Im q^μ lies in the forward lightcone. (In this region all the derivatives of $\mathcal{M}$ are convergent integrals, assuming polynomial boundedness of the matrix elements, and it thus defines an analytic function.) This primitive domain of analyticity is the stepping stone for the use of dispersive arguments in the S-matrix [35,37]. Here, however, the differential operators acting on the fields are non-local. In particular, from the explicit expressions of Z^π_- and E^2_- one sees the presence of branch points for complex spatial momenta. These singularities are present for any value of the time components of the momenta. This means there is no cone of analyticity for Im q^μ, contrary to the Lorentz invariant case. The only guaranteed region of analyticity, which is universal and independent of the model at hand, is for Im $q^0 > 0$: this is just a consequence of the fact the integrand above is retarded, i.e. different from zero only for $z^0 \geq 0$.

Another way to see the absence of analyticity is to consider fields built only out of creation/annihilation operators of $-$ (or respectively $+$) states:

$$\varphi_l(t, \boldsymbol{x}) \equiv \int \frac{\mathrm{d}^3\boldsymbol{k}}{(2\pi)^3 2E_l(\boldsymbol{k})} \left(a_l(\boldsymbol{k}) e^{-i(E_l(\boldsymbol{k})t - \boldsymbol{k}\cdot\boldsymbol{x})} + \text{h.c.} \right) \,, \; l \in \{-, +\} \,. \tag{3.2.12}$$

These fields interpolate only one of the two eigenstates, so that $\langle 0|\varphi_l(0)|l, q\rangle_{\text{out}} = 1$. The φ's however are not microcausal, i.e. *they do not commute outside the lightcone*. The simplest way to see this is to look at the Fourier representation of the retarded Green's function,

$$G_{R,l}(\omega, \boldsymbol{k}) = \frac{i}{(\omega + i\varepsilon)^2 - E_l(\boldsymbol{k})^2} \,. \tag{3.2.13}$$

A necessary and sufficient condition for the vanishing of the retarded Green's function outside the forward lightcone is that its Fourier representation is analytic when the imaginary part of the 4-vector $(\omega, \boldsymbol{k})$ is in the forward lightcone. This property does not hold here since $E_l(\boldsymbol{k})$ has branch points, as we saw above. On the other hand, the fields $\pi(x)$ and

$h(x)$ commute outside the lightcone.[5] In order to create a single energy eigenstate, one has to act non-locally in the fields and this is the ultimate reason for the absence of analyticity.

The relation between the S-matrix and correlation functions is uniquely defined only in the limit when the external momenta are real and on-shell. Therefore the definition of Eq. (3.2.11) is ambiguous for generic complex q^μ.[6] In appendix A.1 we derive an LSZ reduction formula starting from the explicit expression of the creation and annihilation operators of the $+$ and $-$ states. The final reduction formula gives the same S-matrix, but it is different from the one obtained above. The conclusion about the lack of analyticity remains the same, however. Given this ambiguity, one may wonder whether a "clever" LSZ procedure exists that gives an analytic off-shell S-matrix. In particular analyticity is preserved if one acts on each external leg with a local differential operator, i.e. a polynomial in Fourier space. This is indeed what happens in the Lorentz invariant case. We will now prove that this does not work: there is no way to extract the correct S-matrix by acting with local differential operators.

Let us assume that such an operator exists. This corresponds to a polynomial $P(\omega, |\boldsymbol{k}|^2)$ that multiplies each external leg. (For rotational invariance P must depend only on $|\boldsymbol{k}|^2$.) In order to give the correct S-matrix this polynomial must satisfy

$$P(\omega, |\boldsymbol{k}|^2) = \frac{2E_-(|\boldsymbol{k}|)}{Z_-^\pi(|\boldsymbol{k}|)}\,(\omega - E_-(|\boldsymbol{k}|)) + \mathcal{O}\left((\omega - E_-(|\boldsymbol{k}|))^2\right) \quad \text{as } \omega \to E_-(|\boldsymbol{k}|)\,. \tag{3.2.14}$$

At fixed $|\boldsymbol{k}|$, the polynomial in ω must have $E_-(|\boldsymbol{k}|)$ as a simple root. This is surely possible: indeed the dispersion relations in the model at hand are solutions of the polynomial equation (3.1.11). To get also the correct normalization, P must satisfy

$$\frac{\partial}{\partial\omega} P(\omega, |\boldsymbol{k}|^2)\bigg|_{\omega=E_-(|\boldsymbol{k}|)} = \frac{2E_-(|\boldsymbol{k}|)}{Z_-^\pi(|\boldsymbol{k}|)}\,. \tag{3.2.15}$$

Taking the partial derivative with respect to ω of the polynomial P gives another polynomial $Q(\omega, |\boldsymbol{k}|^2)$, which should satisfy

$$Q(\omega = E_-(|\boldsymbol{k}|), |\boldsymbol{k}|^2) = \frac{2E_-(|\boldsymbol{k}|)}{Z_-^\pi(|\boldsymbol{k}|)}\,. \tag{3.2.16}$$

[5] Notice that $\pi(x)$ is not a Lorentz scalar, since Lorentz invariance is spontaneously broken. However the relation between the original Lorentz invariant field $\Phi(x)$ and $\pi(x), h(x)$ is local, so that microcausality is preserved.

[6] For fixed $\boldsymbol{p}_1$ and $\boldsymbol{p}_2$ the S-matrix depends on 3 real variables, for instance the vector $\boldsymbol{q}_1$ (in the presence of Lorentz invariance it would depend on a single real variable). Therefore there is no unique analytic extension to a function of $q^\mu \in \mathbb{C}^4$.

Let us look at the two sides of this equation as a function of the complex variable $|\boldsymbol{k}|^2$. The RHS is analytic around the positive real axis $|\boldsymbol{k}|^2 > 0$: if the two sides of the equation above coincide for physical values $|\boldsymbol{k}|^2 > 0$, they must have the same analytic extension in the complex $|\boldsymbol{k}|^2$ plane (properly extended to take into account branch points). However it is impossible that the two functions coincide in the complex plane. The RHS has poles at the zeros of $Z_-^\pi(|\boldsymbol{k}|)$, while the LHS has no poles being a polynomial in $|\boldsymbol{k}|^2$ and $E_-(|\boldsymbol{k}|)$ (see its explicit expression Eq. (3.1.12)). Therefore P cannot exist.

In conclusion, one cannot extract the S-matrix from correlation functions acting with local differential operators, preserving in this way the analyticity of the retarded Green's function. One cannot exclude some more exotic way of defining the S-matrix for complex momenta that preserves analyticity.

3.3 The S-matrix

The object of interest in this work is the scattering amplitude for the process $|-,\boldsymbol{p}_1\rangle\,|-,\boldsymbol{q}_1\rangle$ into $|-,\boldsymbol{p}_2\rangle\,|-,\boldsymbol{q}_2\rangle$. In what follows we will denote this scattering amplitude by $\mathcal{M}$ (details about the calculation are deferred to appendix A.2.) This scattering amplitude has four

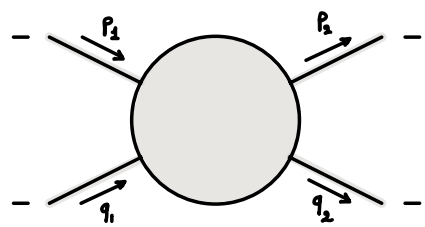

contributions, from contact interactions and from exchange diagrams in the three channels:

$$\mathcal{M} = \mathcal{M}_c + \mathcal{M}_s + \mathcal{M}_t + \mathcal{M}_u\,. \tag{3.3.1}$$

These terms read

$$\begin{aligned}\mathcal{M}_c = -\frac{\mu^4}{v^4}\prod_{i=1}^{2}\left(\frac{Z_-^\pi(\boldsymbol{p}_i)^{-1}}{(p_i^0)^2 - E_+(\boldsymbol{p}_i)^2}\frac{Z_-^\pi(\boldsymbol{q}_i)^{-1}}{(q_i^0)^2 - E_+(\boldsymbol{q}_i)^2}\right)\Big[&6\lambda\mu^4 p_1^0 q_1^0 p_2^0 q_2^0 + \\ &- 2p_1\cdot q_1(p_1^2 - M^2)(q_1^2 - M^2)p_2^0 q_2^0 - 2p_1\cdot q_2(p_1^2 - M^2)(q_2^2 - M^2)q_1^0 p_2^0 + \\ &- 2p_1\cdot p_2(p_1^2 - M^2)(p_2^2 - M^2)q_1^0 q_2^0 - 2q_1\cdot q_2(q_1^2 - M^2)(q_2^2 - M^2)p_1^0 p_2^0 + \\ &- 2p_2\cdot q_1(p_2^2 - M^2)(q_1^2 - M^2)p_1^0 q_2^0 - 2q_2\cdot p_2(p_2^2 - M^2)(q_2^2 - M^2)p_1^0 q_1^0\Big]\,,\end{aligned} \tag{3.3.2}$$

$$\mathcal{M}_s = \prod_{i=1}^{2}\left(\frac{Z_-^\pi(\boldsymbol{p}_i)^{-1}}{(p_i^0)^2 - E_+(\boldsymbol{p}_i)^2}\frac{Z_-^\pi(\boldsymbol{q}_i)^{-1}}{(q_i^0)^2 - E_+(\boldsymbol{q}_i)^2}\right)\frac{v^{-9}}{(p_1+q_1)^2((p_1+q_1)^2 - M^2) - \frac{\mu^4}{v^2}(p_1^0+q_1^0)^2}$$
$$\Big[2\lambda v^3\mu^4 B(p_1,q_1)B(p_2,q_2) + [B(p_1,q_1)A(p_2,q_2) + B(p_2,q_2)A(p_1,q_1)]\mu^4(p_1^0+q_1^0) -$$
$$v[A(p_1,q_1)A(p_2,q_2) + \mu^4 B(p_1,q_1)B(p_2,q_2)](p_1+q_1)^2\Big]\,, \tag{3.3.3}$$

$$\mathcal{M}_t = \prod_{i=1}^{2}\left(\frac{Z_-^\pi(\boldsymbol{p}_i)^{-1}}{(p_i^0)^2 - E_+(\boldsymbol{p}_i)^2}\frac{Z_-^\pi(\boldsymbol{q}_i)^{-1}}{(q_i^0)^2 - E_+(\boldsymbol{q}_i)^2}\right)\frac{v^{-9}}{(q_1-q_2)^2((q_1-q_2)^2 - M^2) - \frac{\mu^4}{v^2}(q_1^0-q_2^0)^2}$$
$$\Big[2\lambda v^3\mu^4 B(q_1,-q_2)B(-p_1,p_2) + [B(q_1,-q_2)A(-p_1,p_2) + B(-p_1,p_2)A(q_1,-q_2)]\mu^4(q_1^0-q_2^0) -$$
$$v[A(q_1,-q_2)A(-p_1,p_2) + \mu^4 B(q_1,-q_2)B(-p_1,p_2)](q_1-q_2)^2\Big]\,, \tag{3.3.4}$$

and

$$\mathcal{M}_u = \prod_{i=1}^{2}\left(\frac{Z_-^\pi(\boldsymbol{p}_i)^{-1}}{(p_i^0)^2 - E_+(\boldsymbol{p}_i)^2}\frac{Z_-^\pi(\boldsymbol{q}_i)^{-1}}{(q_i^0)^2 - E_+(\boldsymbol{q}_i)^2}\right)\frac{v^{-9}}{(q_1-p_2)^2((q_1-p_2)^2 - M^2) - \frac{\mu^4}{v^2}(q_1^0-p_2^0)^2}$$
$$\Big[2\lambda v^3\mu^4 B(q_1,-p_2)B(q_2,-p_1) + [B(q_1,-p_2)A(q_2,-p_1) + B(q_2,-p_1)A(q_1,-p_2)]\mu^4(q_1^0-p_2^0) -$$
$$v[A(q_1,-p_2)A(q_2,-p_1) + \mu^4 B(q_1,-p_2)B(q_2,-p_1)](q_1-p_2)^2\Big]\,. \tag{3.3.5}$$

Here, as specified in section 3.1.1, we have chosen Z_-^π to be real, so we do not make distinction between Z_-^π and $\bar{Z}_-^\pi$. In order to write the blocks in a slightly more compact form we have defined the functions

$$A(p_1,q_1) \equiv 2v^3(p_1^2 - M^2)(q_1^2 - M^2)p_1\cdot q_1 - v\mu^4 p_1^0 q_1^0(p_1^2 + q_1^2 + M^2)\,, \tag{3.3.6}$$

and

$$B(p_1,q_1) \equiv \mu^4(p_1^0)^2 q_1^0 - 2v^2 q_1^0(p_1^2 - M^2)(p_1^2 + p_1\cdot q_1) + (p_1 \leftrightarrow q_1)\,. \tag{3.3.7}$$

It is straightforward to check that the amplitude would be analytic in $q \equiv \frac{1}{2}(q_1+q_2)$ for Im q^μ in the forward lightcone, if the LSZ procedure did not introduce the non-analyticities discussed the previous section. Notice that under the exchange $p_1 \leftrightarrow -q_2$ we have $\mathcal{M}_s \leftrightarrow \mathcal{M}_t$ and under $p_1 \leftrightarrow -p_2$ we have $\mathcal{M}_s \leftrightarrow \mathcal{M}_t$, whereas $\mathcal{M}_c$ is always unchanged. This shows that $\mathcal{M}$ is invariant under the exchange of the external momenta, i.e. it is crossing symmetric.

3.3.1 Interesting limits

Given the complexity of the scattering amplitude it is useful to study it in some interesting limits.

$\mu = 0$

As a sanity check we want to be sure to recover the usual Lorentz invariant form of the S-matrix when we switch off the breaking μ. It is straightforward to see that for $\mu = 0$,

$$\begin{aligned} &Z_-^\pi = 1\,, \quad E_-(\boldsymbol{k})^2 = \boldsymbol{k}^2\,, \quad E_+(\boldsymbol{k})^2 = \boldsymbol{k}^2 + M^2\,, \\ &A(p_1, q_1) = 2v^3 M^4 p_1 \cdot q_1\,, \quad B(p_1, q_1) = 2v^2 M^2 (p_1^0 + q_1^0) p_1 \cdot q_1\,. \end{aligned} \tag{3.3.8}$$

As a consequence, the various contributions to the tree-level amplitude reduce to

$$\mathcal{M}_c = 0\,,\ \mathcal{M}_s = -\frac{s^2}{v^2(s - M^2)}\,,\ \mathcal{M}_t = -\frac{t^2}{v^2(t - M^2)}\,,\ \mathcal{M}_u = -\frac{u^2}{v^2(u - M^2)}\,, \tag{3.3.9}$$

using the usual Maldelstam variables. The full amplitude is thus

$$\mathcal{M} = -\frac{1}{v^2}\left[\frac{s^2}{s - M^2} + \frac{t^2}{t - M^2} + \frac{u^2}{u - M^2}\right]. \tag{3.3.10}$$

The amplitude reproduces its Lorentz invariant counterpart as soon as the breaking is switched off.

High energies

Another interesting limit to explore is the "high-energy limit", intended as the limit achieved when the energies of the scattered states are much larger than all the other scales involved in the problem. In order to take this limit, for convenience, we specialize to the kinematical configuration in which the energies of the scattering states are all the same

$$q_1^0 = q_2^0 = p_1^0 = p_2^0 \equiv \omega\,, \tag{3.3.11}$$

and in which the angle between $\vec{q}_1$ and $\vec{p}_1$ is not zero. The high-energy limit is therefore realized by

$$\lim_{\omega/\Omega \to \infty} \mathcal{M} \tag{3.3.12}$$

where

$$\Omega \gg v, M, \mu, \omega_c \tag{3.3.13}$$

is a reference scale whose value is much larger than all the other scales of the problem. In this limit, the behavior of the different contributions to the amplitude is

$$\begin{aligned}\mathcal{M}_c =& -\frac{\omega^2(\hat{p_1}\cdot\hat{q_1}+\hat{p_1}\cdot\hat{q_2}+\hat{q_1}\cdot\hat{q_2}-3)}{v^2}-\frac{3\mu^2\omega}{v^3}\\ &+\frac{9\mu^8-3M^4v^4+(\hat{p_1}\cdot\hat{q_1}+\hat{p_1}\cdot\hat{q_2}+\hat{q_1}\cdot\hat{q_2})\left(\mu^4+M^2v^2\right)^2-6\lambda\mu^4v^4}{4\mu^4v^4}+\mathcal{O}\left(\frac{\Omega}{\omega}\right),\end{aligned} \tag{3.3.14}$$

$$\begin{aligned}\mathcal{M}_s =& \frac{5\omega^2(\hat{p_1}\cdot\hat{q_1}-1)}{2v^2}+\frac{\omega\left(6\mu^4+M^2v^2\hat{p_1}\cdot\hat{q_1}-M^2v^2\right)}{2\mu^2v^3}\\ &+\frac{1}{8}\left(16\lambda+\frac{3M^4}{\mu^4}+\frac{8M^2}{v^2}+\hat{p_1}\cdot\hat{q_1}\left(-\frac{3M^4}{\mu^4}-\frac{10M^2}{v^2}-\frac{5\mu^4}{v^4}\right)-\frac{19\mu^4}{v^4}\right)+\mathcal{O}\left(\frac{\Omega}{\omega}\right),\end{aligned} \tag{3.3.15}$$

$$\begin{aligned}\mathcal{M}_t =& \frac{\omega^2(1-\hat{q_1}\cdot\hat{q_2})}{2v^2}+\frac{M^2\omega(1-\hat{q_1}\cdot\hat{q_2})}{2\mu^2v}\\ &+\frac{-\mu^8+M^4v^4-16\mu^4M^2v^2+\hat{q_1}\cdot\hat{q_2}\left(\mu^8-M^4v^4+2\mu^4M^2v^2\right)}{8\mu^4v^4}+\mathcal{O}\left(\frac{\Omega}{\omega}\right),\end{aligned} \tag{3.3.16}$$

$$\begin{aligned}\mathcal{M}_u =& \frac{\omega^2(1-\hat{p_1}\cdot\hat{q_2})}{2v^2}+\frac{M^2\omega(1-\hat{p_1}\cdot\hat{q_2})}{2\mu^2v}\\ &+\frac{-\mu^8+M^4v^4-16\mu^4M^2v^2+\hat{p_1}\cdot\hat{q_2}\left(\mu^8-M^4v^4+2\mu^4M^2v^2\right)}{8\mu^4v^4}+\mathcal{O}\left(\frac{\Omega}{\omega}\right)\ \text{as}\ \frac{\omega}{\Omega}\to\infty\,.\end{aligned} \tag{3.3.17}$$

where $\hat{p_i}\cdot\hat{q_j}=\boldsymbol{p}_i\cdot\boldsymbol{q}_j/|\boldsymbol{p}_i||\boldsymbol{q}_j|$. Momentum conservation enforces the condition

$$1+\hat{p_1}\cdot\hat{q_1}-\hat{q_2}\cdot\hat{q_1}-\hat{p_1}\cdot\hat{q_2}=0\,,$$

which ensures the cancellation of the divergent terms in the above blocks, yielding a constant asymptotic value for the full amplitude:

$$\mathcal{M}=-2\frac{M^2}{v^2}+\mathcal{O}\left(\frac{\Omega}{\omega}\right)=-4\lambda+\mathcal{O}\left(\frac{\Omega}{\omega}\right)\quad\text{as}\quad\frac{\omega}{\Omega}\to\infty\,. \tag{3.3.18}$$

Interestingly, the amplitude asymptotes to the Lorentz-invariant amplitude for the scattering of $U(1)$ eigenstates (quanta of Φ) in the unbroken phase and not to the $s\to+\infty$ limit of the Lorentz-invariant amplitude that describes the finite-angle scattering of Goldstones in the broken phase[7]. Indeed, making use of (3.1.1), it is possible to check that the $\Phi\Phi\to\Phi\Phi$ scattering amplitude is given by

$$\mathcal{M}_{\Phi\Phi\to\Phi\Phi}=-4\lambda\,, \tag{3.3.19}$$

[7]We thank the authors of [**?**] for pointing out a mistake in the first version of our paper.

in agreement with (3.3.18). (On the other hand, the Lorentz-invariant amplitude of the Goldstones, Eq. (3.3.10), asymptotes to -6λ in the $s \to +\infty$ limit at finite angle.) As discussed at the end of section 3.1.1, for $\omega \gg \omega_c$ the quanta of Φ are indeed the correct eigenstates. We refer the reader to reference [**?**] for a more comprehensive treatment and explanation.

Low energies

As a final check we explore the low-energy limit of the amplitude to show that it agrees with the amplitude computed within the EFT of π. This EFT is obtained by integrating out the radial mode h at tree level and at leading order in the derivative expansion. Starting from the equation of motion of h,

$$\Box h - \frac{\mu^2\dot{\pi} + (\partial\pi)^2}{v^2}(h+v) + \lambda(h^2+2hv)(h+v) = 0\,, \tag{3.3.20}$$

at leading order in the derivative expansion we have

$$h^2 + 2hv = \frac{\mu^2\dot{\pi} + (\partial\pi)^2}{\lambda v^2}\,. \tag{3.3.21}$$

Plugging this expression into Eq. (3.1.7) yields the low-energy Lagrangian of π at leading order in the derivative expansion (neglecting a total derivative):

$$\mathcal{L}_{\rm EFT} = \frac{(\partial\pi)^2}{2} + \frac{(\mu^2\dot{\pi} + (\partial\pi)^2)^2}{4\lambda v^4}\,. \tag{3.3.22}$$

Canonically normalizing by setting $\pi = \pi_c c_s$ yields

$$\mathcal{L}_{\rm EFT} = \frac{1}{2}\left(\dot{\pi}_c^2 - c_s^2(\boldsymbol{\nabla}\pi_c)^2\right) + \frac{\mu^2 c_s^3}{2\lambda v^4}\dot{\pi}_c(\partial\pi_c)^2 + \frac{c_s^4}{4\lambda v^4}(\partial\pi_c)^4\,, \tag{3.3.23}$$

where

$$c_s^2 = \frac{1}{1+\mu^4/2\lambda v^4} \equiv \frac{1}{1+\alpha}\,. \tag{3.3.24}$$

The S-matrix for $\pi\pi \to \pi\pi$ can be computed easily and its explicit expression is reported in appendix A.3. We will now check that the low-energy limit of the full S-matrix (3.3.1) agrees with the expression obtained within the EFT. As before we specialize to a kinematical configuration with all energies equal. In this configuration, the low energy limit of the S-matrix is realized by considering energies much smaller than the mass of the

radial mode. Keeping only the leading order terms in the derivative expansion and making use of

$$Z_-^\pi(0) = c_s\,,\ E_-(0)^2 - E_+(0)^2 = -\frac{M^2}{c_s^2}\,, \tag{3.3.25}$$

the amplitude contributions reduce to ($s \equiv (p_1+q_1)^2$, $t \equiv (q_2-q_1)^2$ and $u \equiv (p_2-q_1)^2$)

$$\mathcal{M}_c \to -\alpha^2 \frac{c_s^4}{\mu^4}\omega^2\left(7\alpha\omega^2 - 2s + 2t + 2u\right)\,, \tag{3.3.26}$$

$$\mathcal{M}_s \to -\frac{16c_s^4\alpha^2\omega^2}{\mu^4}\frac{(s+\alpha\omega^2)^2}{s+4\alpha\omega^2} + c_s^4\frac{\alpha\left(\alpha\omega^2+s\right)^2}{\mu^4}\,, \tag{3.3.27}$$

$$\mathcal{M}_u \to c_s^4\frac{\alpha\left(3\alpha\omega^2+u\right)^2}{\mu^4}\,, \tag{3.3.28}$$

$$\mathcal{M}_t \to c_s^4\frac{\alpha\left(3\alpha\omega^2+t\right)^2}{\mu^4}\,. \tag{3.3.29}$$

As a consequence, they sum up to give

$$\mathcal{M}_{\text{low-energy}} = \frac{c_s^4\alpha\left(s^2+t^2+u^2-4\alpha\omega^2\right)}{\mu^4} - \frac{16c_s^4\alpha^2\omega^2}{\mu^4}\frac{(s+\alpha\omega^2)^2}{s+4\alpha\omega^2}\,, \tag{3.3.30}$$

in agreement with the EFT computation (see Eq. (A.3.1) in appendix A.3).

3.4 Decay rate of the Goldstone

The states $-$ and $+$ are unstable, so they are not exact asymptotic states. Therefore, the S-matrix we calculated makes sense only if the typical time of interaction, which is of order ω^{-1}, is much shorter than the lifetime of the states. In terms of the decay rate one needs

$$\frac{\Gamma(\omega)}{\omega} \ll 1\,. \tag{3.4.1}$$

Before delving into the estimates of the decay rate, it is important to notice that the model at hand is weakly coupled at all energies. As such, we expect all interactions to be suppressed by powers of the coupling constant λ: also Γ is thus λ-suppressed. Therefore we expect that, for $\lambda \ll 1$, the condition (3.4.1) is satisfied. We will now check this expectation computing the decay width in the two regimes $\omega \ll M$ and $\omega \gg M$, where M is the mass of the radial mode h.

3.4.1 $\omega \ll M$

The gap of the + branch, $E_+(0)$, is always of the same order as M. For $\omega \ll M$ the only allowed decay process with a 2-particle final state is $- \to --$ and in this low-energy regime we can rely on the EFT Lagrangian (3.3.23): the decay is induced by the operator

$$\frac{\mu^2 c_s^3}{2\lambda v^4}\dot{\pi}_c(\partial\pi_c)^2 \,. \tag{3.4.2}$$

The ratio (3.4.1) can be estimated as

$$\frac{\Gamma}{\omega}(\omega \ll M) \sim (1-c_s^{-2})^2 \left(\frac{\omega}{M}\right)^4 \frac{\mu^4\lambda^2}{M^4} \sim \lambda \left(\frac{\omega}{M}\right)^4 \left(\frac{\lambda\mu^4}{M^4}\right)^3 \ll \lambda \,. \tag{3.4.3}$$

We have used $1 - c_s^{-2} \approx -\mu^4/\lambda v^4$, $M^2 \geq \sqrt{\lambda}\mu^2$ and the low-energy condition $\omega \ll M$. The kinematical suppression $(1-c_s^{-2})^2$ requires some explanation. For small frequency the dispersion relation is linear, so that the kinematics of the decay is collinear. The scalar product $p_1^\mu p_{2\,\mu}$, which arises from the operator (3.4.2), is thus proportional to $1 - c_s^{-2}$.

3.4.2 $\omega \gg M$

To tackle the high-energy side of the problem we begin by performing a convenient change of basis. In the UV it is useful to use a field basis where renormalizability is manifest. In this basis we will not need to worry about cancellations among various terms and it is thus simpler to make estimates. Such a basis is easy to find: the Lagrangian (3.1.1) we started with is manifestly renormalizable and we simply need to expand around a symmetry breaking solution[8]

$$\Phi = \phi_b(t) + \frac{\phi_1 + i\phi_2}{\sqrt{2}} \,, \qquad \phi_b(t) \equiv \frac{v}{\sqrt{2}} e^{i\mu^2 t/2v} \,. \tag{3.4.6}$$

Notice that one is allowed to treat ϕ_b as approximately constant in the regime $\omega \gg M$: indeed the frequency of ϕ_b is of order μ^2/v, which is at most of order M. For our estimates

[8] Another natural choice of fields would have been

$$\Phi \equiv \phi_b(t) + e^{i\mu^2 t/2v}\frac{\sigma_1 + i\sigma_2}{\sqrt{2}} \,. \tag{3.4.4}$$

The Lagrangian written in this basis reads

$$\mathcal{L} = \frac{(\partial\sigma_1)^2}{2} + \frac{(\partial\sigma_2)^2}{2} - \frac{\mu^2}{2v}\left(\dot{\sigma}_1\sigma_2 - \dot{\sigma}_2\sigma_1\right) - \frac{\lambda}{4}\left(2v\sigma_1 + \sigma_1^2 + \sigma_2^2\right)^2 . \tag{3.4.5}$$

we need to know how much these new fields interpolate the two asymptotic states. As already discussed at the end of section 3.1.1 it is easy to see that, above the crossover scale ω_c, both ϕ_1 and ϕ_2 interpolate to order one for $+$ and $-$, i.e.

$$|\langle 0|\phi_{1,2}|\pm\rangle| = \mathcal{O}(1)\,. \tag{3.4.7}$$

(Using this in the regime $M \ll \omega \ll \omega_c$ will give an upper bound for the decay rate, as we will discuss.) By plugging (3.4.6) into (3.1.1), setting $t = 0$ and focusing on the cubic part of the Lagrangian we obtain

$$\mathcal{L}_{(3)} \sim -\lambda v \phi_1^2 \phi_2 - \lambda v \phi_1^3\,. \tag{3.4.8}$$

As expected this operator is relevant and we do not need to worry about cancellations. We can simply write

$$\frac{\Gamma}{\omega}(\omega \gg M) \sim \lambda^2 \frac{v^2}{\omega^2} \sim \lambda \frac{M^2}{\omega^2}\,. \tag{3.4.9}$$

As expected, the ratio between the interaction time and the decay lifetime of $-$ is always suppressed by λ. Notice that the two estimates (3.4.3) and (3.4.9) do not agree when evaluated at $\omega = M$. Indeed, approaching $\omega = M$ from the low and the high-energy regime gives respectively

$$\frac{\Gamma}{\omega}(\omega \ll M) \to \lambda \left(\frac{\lambda \mu^4}{M^4}\right)^3\,, \quad \frac{\Gamma}{\omega}(\omega \gg M) \to \lambda\,. \tag{3.4.10}$$

This difference is a consequence of the fact that (3.4.9) actually yields an overestimate of the Γ/ω ratio within the window of energies $M \ll \omega \ll \omega_c$. Even if these estimates are enough to conclude that the S-matrix is well defined since the decay is always perturbative, i.e. suppressed by λ, it is instructive to work out a finer estimate for Γ/ω in the intermediate regime $M \ll \omega \ll \omega_c$. We will do this in Appendix A.4.

The careful reader might wonder why we only paid attention to the $- \to --$ process among the possible decay channels. What about the decay into $-+$ and $++$? The decay into $++$ is kinematically forbidden: by energy and momentum conservation we should have

$$p^2 = (p_1 + p_2)^2 \qquad \text{where } p^2 < 0\,, \quad p_i^2 > 0\,. \tag{3.4.11}$$

Given that the sum of two timelike future-directed four-momenta, see eq. (3.1.12), is always timelike future-directed, we see that this channel is kinematically prohibited. We can try to repeat the same argument for $-$ decaying into $-$ and $+$. In this case we have

$$(p - p_1)^2 = p_2^2\,, \tag{3.4.12}$$

where we have taken the first outgoing particle to be gapless. Generically now we cannot conclude anything because the sum of two spacelike vectors is not necessarily spacelike. If we restrict our attention to $\omega_1, \omega_2 < \omega < \omega_c$, we can approximate the dispersion relation as linear and then

$$\begin{aligned}(p-p_1)^2 &= p^2 + p_1^2 - 2p_1 \cdot p_2 \simeq (c_s^2-1)(\boldsymbol{p}^2+\boldsymbol{p}_1^2) - 2(c_s^2|\boldsymbol{p}_1||\boldsymbol{p}_2| - \boldsymbol{p}_1\cdot\boldsymbol{p}_2) \\ &< (c_s^2-1)(\boldsymbol{p}^2+\boldsymbol{p}_1^2) - 2(c_s^2|\boldsymbol{p}_1||\boldsymbol{p}_2| - |\boldsymbol{p}_1||\boldsymbol{p}_2|) = (c_s^2-1)(|\boldsymbol{p}_1|-|\boldsymbol{p}_2|)^2 < 0\,.\end{aligned} \tag{3.4.13}$$

Since $p_2^2 > 0$ we conclude that for $\omega < \omega_c$ this decay does not happen and the only kinematically allowed process in this regime is $- \to --$. The decay $- \to -+$ only happens for $\omega \gtrsim \omega_c$. In this range of energies, the cubic part of the Lagrangian is again given by (3.4.8), leading to the same estimate for the Γ/ω ratio of the $- \to -+$ process:

$$\frac{\Gamma}{\omega}(\omega \gtrsim \omega_c) \sim \lambda \frac{M^2}{\omega^2} \ll \lambda\,. \tag{3.4.14}$$

It is important to stress that the non-analyticities studied in this paper are not a consequence of the absence of absolutely stable asymptotic states. Indeed, one can send the coupling $\lambda \to 0$ while keeping μ^2/v fixed. In this limit, $\Gamma \to 0$ while the discontinuity in $\mathcal{M}/\lambda$ remains constant.

3.5 Discussion and future directions

We calculated the S-matrix for Goldstone scattering in a complex $\lambda|\Phi|^4$ model in a state at finite charge, i.e. with spontaneous breaking of Lorentz invariance. This is arguably the simplest model that gives a Lorentz-violating S-matrix that is well-defined at all energies, and it may be a good testing ground to discuss general properties of the S-matrix when Lorentz invariance is broken. A general lesson that emerged from this calculation is that the S-matrix does not enjoy the same analyticity properties as in the Lorentz invariant case: the relation between the S-matrix and correlation functions introduces non-analyticities which are a consequence of the breaking of boosts.

It seems thus quite difficult to obtain general positivity bounds using the S-matrix, at least in the most naive way. It would be worth exploring whether one gains something looking at the limit of small breaking $\mu \to 0$: this would correspond to studying the S-matrix on a *weak* Lorentz-breaking background, similarly to the analysis of the propagation of signals on a background, pioneered in [11]. Alternatively, one could abandon the S-matrix and use other objects which are well-defined both in the UV and in the IR: one

example are conserved currents as discussed in [66], where some bounds were already derived.

Perhaps the more general lesson is that we have a very limited understanding of the basic properties of QFT when Lorentz is spontaneously broken.

Chapter 4

Analyticity and positivity properties of Green functions

The preceding discussion elucidated the breakdown of the S-matrix framework in providing a coherent interpolation between the infrared (IR) and ultraviolet (UV) regimes in theories where Lorentz boosts are spontaneously broken. This necessitates the exploration of alternative positivity conditions that are not reliant on standard S-matrix analyticity assumptions.

In the Lorentz-invariant case, the Fourier transform of retarded two-point functions is analytic in a single variable, namely the complexified squared momentum. Once boost invariance is broken, the Fourier-transformed retarded correlators then become analytic functions of at least two independent variables, making the analysis substantially more involved. This situation is conceptually closer to the study of analyticity properties of Lorentz-invariant $2 \to 2$ scattering amplitudes. Within this context, retarded two-point correlation functions represent a natural class of objects to consider, given their well-understood analytic structure in complex momentum space.

We proceed by reviewing essential results that establish the necessary and sufficient criteria linking analyticity domains to the causal and retarded nature of correlation functions. In particular, we derive generalized multivariable dispersion relations for retarded two-point functions and rigorously prove that, in passive (i.e., dissipative or stable) systems, all zeros of these functions must reside outside their primitive domain of analyticity, thereby imposing stringent spectral constraints. Crucially, the absence of such zeros also guarantees the analyticity of the retarded polarization tensor $\Pi^{\mu\nu}$. This property is non-

trivial, as it does not follow directly from microcausality ($\Pi^{\mu\nu}$ is not itself a commutator of local operators). Physically, this analyticity is inherited by the electric and magnetic response functions: ε and $1/\mu$ are analytic functions of ω and $\vec{k}$.

4.1 Causality and Analyticity

The connection between causality and analyticity is fundamental in physics. Broadly speaking, the Fourier transform of a microcausal response function, which that vanishes outside the light cone, is expected to display well-defined analytic properties. More precisely, if a retarded Green's function in real space is microcausal (vanishing outside the forward light cone) and exhibits suitable late-time asymptotics, then its Fourier transform is analytic within a corresponding complex domain.

This naturally prompts the following question: *What are the necessary and sufficient conditions that an analytic function in Fourier space must satisfy to be the Fourier transform of a causal real-space distribution?* In this section, we discuss theorems addressing this question. We will mainly follow the treatment in Bogolubov's work [69], extending the results to the context in which Lorentz transformations are nonlinearly realized and illustrating them with explicit examples.

4.1.1 $0+1$ Dimensions

As a warm-up, consider $0+1$-dimensional spacetime, where the response is local in space and depends only on time, a common simplification in condensed matter physics.

In this case, the linear response to a time-dependent source is described by a retarded Green's function $G_R(t)$. Causality is equivalent to the condition

$$G_R(t) = 0, \quad t < 0. \tag{4.1.1}$$

This ensures that the system's configuration at time t_0 depends only on sources at earlier times $t < t_0$.

Taking the Fourier transform,

$$\tilde{G}_R(\omega) = \int dt\, e^{i\omega t} G_R(t), \tag{4.1.2}$$

we see that if $G_R(t)$ grows no faster than polynomially at large t, then $\tilde{G}_R(\omega)$ is analytic in the upper half-plane

$$\mathrm{UHP} = \{\omega \in \mathbb{C} \mid \mathrm{Im}[\omega] > 0\}.$$

This follows because $G_R(t)$ has support only for $t > 0$, and for $\omega \in$ UHP the factor $e^{i\omega t}$ provides exponential suppression. The integral is convergent, and $\tilde{G}_R(\omega)$ satisfies the Cauchy–Riemann equations in the UHP. The polynomial growth condition is crucial for $\tilde{G}_R(\omega)$ to be well-defined on the real axis, a condition satisfied by stable systems.[1]

Conversely, suppose $\tilde{G}_R(\omega)$ is analytic in the UHP and polynomially bounded as $|\omega| \to \infty$. Its inverse Fourier transform,

$$G_R(t) = \frac{1}{2\pi} \int d\omega \, e^{-i\omega t} \tilde{G}_R(\omega), \tag{4.1.3}$$

vanishes for $t < 0$: for such t, the contour may be closed in the UHP, and the contribution from the arc at infinity vanishes, leaving $G_R(t)$ supported only for $t \geq 0$.

In most physical applications, "Green's functions" are not ordinary functions but *tempered distributions* (see Appendix B.1). A tempered distribution belongs to the dual space $S'(\mathbb{R}^n)$ of Schwartz functions, smooth functions whose derivatives of all orders decay faster than any polynomial. Tempered distributions are natural objects in constructive or axiomatic quantum field theories (QFTs), and they enjoy the following key properties:

1. They are polynomially bounded.

2. The Fourier transform of a tempered distribution is itself a tempered distribution.

For the rest of the discussion, we will assume all Green's functions are tempered distributions. This assumption ensures that their Fourier transforms are well-defined in the sense of tempered distributions, allowing us to meaningfully characterize their analytic and support properties in momentum space. In particular, the causal structure of such distributions is encoded in precise analyticity properties of their Fourier transforms, as captured by the following theorem.

Theorem 4.1.1. *A tempered distribution $G \in S'(\mathbb{R})$ is retarded if and only if its Fourier transform is analytic in the UHP and satisfies*

$$|\tilde{G}(\omega)| \leq A \frac{(1 + |\omega|)^n}{|\omega_I|^m}, \quad \omega \in \text{UHP}, \quad n, m \in \mathbb{N}, \tag{4.1.4}$$

where $A > 0$ and n, m depend on G.

[1] For example, the retarded Green's function of a harmonic oscillator diverges exponentially for $m^2 < 0$, signalling instability: initially small disturbances get exmponentially amplified with time.

The main message of the theorem is that if a tempered distribution is retarded, then its Fourier transform will be analytic in the upper half-plane. Moreover, the estimate ensures that the Fourier transform of G is polynomially bounded not only on the real line (a consequence of temperedness) but also on the whole domain of analyticity. Therefore, for fixed $\omega_I > 0$, the Fourier transform of G defines a tempered distribution wrt ω_R. On the other hand, an analytic function on the UHP can be identified as the analytic continuation of the Fourier transform of a retarded Green's function only if it satisfies the estimate of the theorem.

It is interesting to notice how the bound contains information about the behaviour of $\tilde{G}$ not only in the large $|\omega|$ limit but also in the $\omega_I \to 0^+$ limit. In particular, the theorem ensures that $\tilde{G}$ cannot diverge faster than $|\omega_I|^{-n}, n > 0$, as we approach the real axis from above. To better clarify these statements, we will now discuss some instructive examples.

Examples

- *Necessity of polynomial boundedness:* Retardedness alone does not ensure the Fourier transform satisfies Theorem 4.1.1. If $G_R(t)$ grows faster than polynomially, $\tilde{G}_R(\omega)$ develops severe singularities. For example,

$$G_R(t) = \begin{cases} e^{\sqrt{t}}, & t \geq 0, \\ 0, & t < 0, \end{cases} \to \tilde{G}_R(\omega) = \frac{(-1)^{3/4}\pi e^{\frac{i}{4\omega}}\left(\mathrm{erf}\left(\frac{\sqrt[4]{-1}}{\sqrt{2}\sqrt{\omega}}\right)+1\right)}{2\omega^{3/2}} + \frac{i}{\omega}. \tag{4.1.5}$$

  has a Fourier transform with an essential singularity at $\omega = 0$, violating the bound as $\omega_I \to 0^+$.

- *Essential singularities are not always problematic:* The above example links a super-polynomial growth in $G_R(t)$ with an essential singularity in $\tilde{G}_R(\omega)$ that violates the theorem's bound. However, essential singularities can be compatible with causality and polynomial boundedness provided their divergent behaviour is not accessible in the $\omega_I \to 0^+$ limit. For instance,

$$F_\pm(\omega) = e^{\pm i/\omega} \tag{4.1.6}$$

  both have an essential singularity at $\omega = 0$, yet only F_- corresponds to a retarded tempered distribution, while F_+ does not.

A Comment

For a retarded Green's function $G_R(t)$, it may be tempting to write

$$G_R(t) = \theta(t) G_R(t) \tag{4.1.7}$$

to express that it vanishes for $t < 0$. Strictly speaking, the product $\theta(t)G_R(t)$ is meaningful only when $G_R(t)$ can be written as a first-order derivative of a continuous function [70]. Another way to see that the above expression is not well-defined for a general tempered distribution is to look at its Fourier space version:

$$\tilde{G}_R(\omega) = \frac{i}{\pi} \tilde{G}_R \star P(1/\omega) = \frac{i}{\pi} \text{P.V.} \int d\omega' \frac{\tilde{G}_R(\omega')}{\omega' - \omega}. \tag{4.1.8}$$

The above expression involves a convolution between tempered distributions, which is not well-defined in general. In particular, eq. (4.1.8) makes sense only if $\tilde{G}_R(\omega) \sim \omega^{-\alpha}$, $\alpha > 0$, in the $\omega \to \infty$ limit. This condition is not always satisfied, otherwise one could write unsubtracted dispersion relations for the Fourier transform of any tempered distribution.

4.1.2 $d+1$ Dimensions

We now extend the discussion to higher dimensions. Consider a retarded two-point function $G_R(x)$ in a spatially homogeneous $(d+1)$-dimensional system. For now, we do not assume rotational invariance. In this setting, $G_R(x)$ describes the linear response of a state with spontaneously broken boost symmetry (which is the typical situation that arises in condensed matter systems).

Microcausality requires that $G_R(x)$ vanish for spacelike separations, while retardedness requires support only for $x^0 \geq 0$. Together, these imply that a microcausal, retarded tempered distribution is supported within the forward light cone:

$$\text{FLC}_x = \{x \in \mathbb{R}^{d,1} \mid x^2 \geq 0,\, x^0 \geq 0\}.$$

The Fourier transform

$$\tilde{G}_R(k) = \int dt \int d^d x\, e^{ik\cdot x} G_R(x), \tag{4.1.9}$$

then, enjoys analyticity in the *forward tube*

$$T_+ = \mathbb{R}^{d+1} + iV_+ \subset \mathbb{C}^{d+1},$$

where V_+ is the interior of the forward light cone in imaginary momentum space:

$$V_+ \equiv \{\mathrm{Im}[k] \in \mathbb{R}^{d,1} \mid \mathrm{Im}[k]^2 > 0,\, \mathrm{Im}[k^0] > 0\}.$$

In other words, $\tilde{G}_R(k)$ is analytic whenever $\mathrm{Im}[k]$ is timelike and future-directed.[2]

The argument parallels the $0+1$ case: the exponential factor in (4.1.9) suppresses the integral whenever $\mathrm{Im}[k] \cdot x > 0$. Since $G_R(x)$ is supported inside the FLC, taking $\mathrm{Im}[k^0] > |\mathrm{Im}[\vec{k}]|$ guarantees convergence if $G_R(x)$ is polynomially bounded, which is ensured by temperedness.

Conversely, if $\tilde{G}_R(k)$ is analytic in T_+ and polynomially bounded as $|k^0| \to \infty$, its inverse Fourier transform $G_R(x)$ is supported inside the FLC. This can be seen explicitly in $1+1$ dimensions: introducing light-cone coordinates $(z_1, z_2) = (k^0 + k^1, k^0 - k^1)$, the domain of analyticity becomes

$$D = \{(z_1, z_2) \in \mathbb{C}^2 \mid \mathrm{Im}[z_1] > 0,\, \mathrm{Im}[z_2] > 0\}.$$

For $t^2 - x^2 > 0$ and $t < 0$, both exponentials in the Fourier kernel suppress the integrand, allowing contour closure and showing G_R vanishes in the backward light cone. For spacelike separation $t^2 - x^2 < 0$, one exponential still provides suppression, yielding the same conclusion. Thus analyticity plus polynomial boundedness imply microcausality and retardedness, and vice versa.

The multidimensional generalisation of Theorem 4.1.1, adapted from Bogolubov (see theorem B.9 in [69]) to the case without Lorentz invariance, is as follows

Theorem 4.1.2. *A tempered distribution $G \in S'(\mathbb{R}^{d,1})$ is retarded and microcausal if and only if its Fourier transform $\tilde{G}$ is analytic in the tube $T_+ = \mathbb{R}^{d+1} + iV_+$ and satisfies*

$$|\tilde{G}(k)| \leq A \frac{(1 + |\mathrm{Re}[k] + i\mathrm{Im}[k]|)^n}{\left(\sqrt{\mathrm{Im}[k]^2}\right)^m}, \tag{4.1.10}$$

for all $\mathrm{Re}[k] \in \mathbb{R}^{d+1}$, $\mathrm{Im}[k] \in V_+$, with constants $A > 0$ and integers $m, n \in \mathbb{N}$ depending on G.

The bound constrains growth both in the limit of large $|k|$ and of $\mathrm{Im}[k]^2 \to 0^+$, ensuring $\tilde{G}$ remains polynomially bounded throughout its domain. Moreover, the theorem gives a

[2] When time-translation invariance is broken, it is useful to work in a mixed representation where only spatial coordinates are Fourier transformed. In that case, $\tilde{G}_R(t, \vec{k})$ is analytic for any $\vec{k} \in \mathbb{C}^d$ [71].

bound on growth of $\tilde{G}_R$ not only when k approaches physical values but also when one approaches boundary of V_+. The presence of more spatial dimensions makes it possible to perform the $\mathrm{Im}[k]^2 \to 0^+$ limit in different ways[3].

4.1.3 Rotational Invariance

Many interesting systems possess rotational symmetry, which reduces the problem to an effective $1+1$-dimensional form. In this case, a retarded, microcausal distribution $G_R(t,r)$ has support on

$$\mathrm{FLC} = \{(t,r) \in \mathbb{R} \times \mathbb{R}^+ \mid t^2 - r^2 \geq 0,\, t \geq 0\},$$

where $r = |\vec{x}|$. Its Fourier transform depends only on ω and $k = |\vec{k}|$:

$$\begin{aligned}\tilde{G}_R(\omega,k) &= \int dt\, d^d x\, e^{i\omega t - i\vec{k}\cdot\vec{x}} G_R(t,r) \\ &= \frac{2\pi^{(d-1)/2} i}{k\,\Gamma\left(\frac{d-1}{2}\right)} \int_0^\infty dt \int_0^t dr\, r^{d-2}\, G_R(t,r)\, e^{i\omega t} \left(e^{-ikr} - e^{ikr}\right),\end{aligned} \tag{4.1.12}$$

where angular integration has been performed.

As expected, we can parametrize the Green function as a function of ω and k rather than $\vec{k}$, i.e. $\tilde{G}_R(\omega,k)$. Eq. (4.1.12) implies that we can consider the Green function as a function of complex k, rather than $\vec{k}$. Taking $\omega = \omega_R + i\omega_I$ and $k = k_R + ik_I$, the same argument as before reveals that the region of analyticity is

$$D = \{(\omega,k) \in \mathbb{C}^2 \mid \omega_I > |k_I| > 0\}\,. \tag{4.1.13}$$

The reality condition implies $\tilde{G}_R(\omega,k)^* = \tilde{G}_R(-\omega^*,-k^*)$, and symmetry under $k \to -k$ allows extension to all $k_R \in \mathbb{R}$.

In summary, the interplay between causality and analyticity is encoded in the geometry of the domain of analyticity in complex momentum space and in bounds on the growth of $\tilde{G}_R$ both at infinity and near the boundary of this domain. These constraints are sharp: violating them corresponds to non-causal behaviour in real space.

[3] As a simple example, consider the following family of functions in $1+1$-dimensions:

$$F_{\sigma_1\sigma_2} \equiv e^{i\left(\frac{\sigma_1}{z_1} + \frac{\sigma_2}{z_2}\right)}\,,\; z_1 \equiv \omega + k, z_2 = \omega - k\,,\; \sigma_{1,2} = \pm \tag{4.1.11}$$

All the functions above posses essential singularities along the null directions $\mathrm{Im}[\omega] = |\mathrm{Im}[k]|$, however, only one of them is compatible with retardedness and microcausality when mapped back to real space.

4.2 Multi-variable dispersion relations

For analytic functions of a single complex variable that decay suitably at infinity, the real and imaginary parts are related via dispersion relations, the well-known Kramers–Kronig relations. As discussed in the previous section, any retarded Green's function is in fact an analytic function of several complex variables. In that case, one can tackle the problem of writing a multivariable dispersion relation by parametrizing all the variables in terms of a single one, effectively writing a single variable dispersion relation. This leads to a corresponding family of Kramers–Kronig-type relations, known as *Leontovich relations*, first derived by M. Leontovich [72] (see also [66, 73, 74]).

In this section we present another generalisation of standard dispersion relations to the multi-variable case, involving integration over *all* variables simultaneously, rather than along one-dimensional slices. This approach is, in a sense, a more natural extension of the Kramers–Kronig relation to several variables, and it will prove useful later for establishing the absence of zeros within the primitive domain of analyticity. For simplicity, we first focus on the rotationally symmetric case, where, as we saw earlier, the independent variables reduce to $(\omega, k) \in \mathbb{C}^2$. The non-rotational case will be discussed in section 4.4.2.

The key idea is to introduce new variables (z_1, z_2) such that the domain of analyticity maps to a product of upper half-planes (UHPs) in each variable, or at least contains them. In this form, one can write dispersion relations one variable at a time, holding the others fixed. To keep the discussion simple, we choose the transformation to be linear,[4] and require that taking, say, z_1 to complex infinity with z_2 fixed corresponds to approaching infinity in the (ω_I, k_I) plane along a timelike direction. This ensures control over the ultraviolet (UV) behaviour of the function.

A convenient choice is

$$z_1 \equiv \omega + \alpha k, \qquad z_2 \equiv \omega - \alpha k, \tag{4.2.1}$$

with $\alpha > 1$ real. The original analyticity domain $\omega_I > |k_I|$ then maps to

$$D = \left\{ (z_1, z_2) \in \mathbb{C}^2 \,\middle|\, z_{2I} > -\frac{\alpha - 1}{\alpha + 1} z_{1I}, \quad z_{2I} > -\frac{\alpha + 1}{\alpha - 1} z_{1I} \right\}. \tag{4.2.2}$$

For $\alpha > 1$, this region always contains the *generalised upper half-plane* (GUHP),

$$\tilde{D} = \{(z_1, z_2) \in \mathbb{C}^2 \mid z_{1I} > 0,\, z_{2I} > 0\}, \tag{4.2.3}$$

as illustrated in fig. 4.1. In the limit $\alpha \to 1$, $\tilde{D}$ coincides with D.

[4] More general transformations are possible; see [66] for discussion.

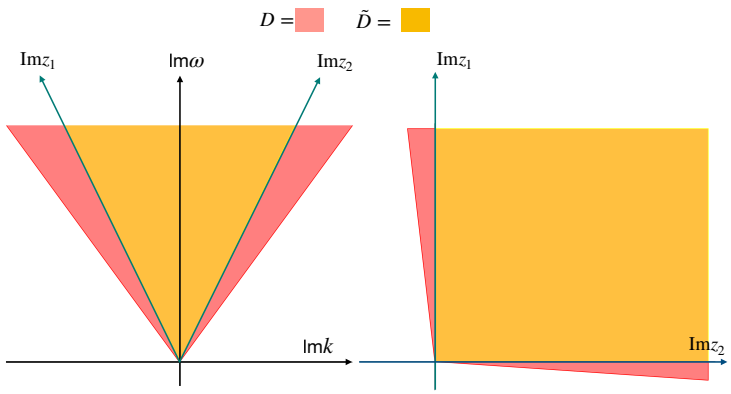

Figure 4.1Analyticity domain in the (ω_I, k_I) plane (left), and its image in the (z_{1I}, z_{2I}) plane (right). For $\alpha > 1$, the analyticity region D always includes the GUHP.

The parameter α has a useful interpretation in terms of UV behaviour. In the new variables, the Fourier transform reads

$$\tilde{G}(z_1, z_2) = \frac{\alpha}{2} \int du_1\, du_2\, e^{i(z_1 u_1 + z_2 u_2)/2}\, \tilde{G}(u_1, u_2), \tag{4.2.4}$$

where

$$u_1 \equiv t - \frac{x}{\alpha}, \quad u_2 \equiv t + \frac{x}{\alpha},$$

and $\tilde{G}(u_1, u_2) = G(t, x)$; the prefactor is the Jacobian of the transformation.[5]

Taking $|z_1| \to \infty$ with z_2 fixed forces $z_{1I} \to \infty$, producing an exponential suppression $e^{-z_{1I} u_1}$ in the integrand. The integral is dominated by $u_1 \approx 0$, which (since $\alpha > 1$) corresponds to $t, x \to 0$. We conclude that the $z_{1I} \to +\infty$ limit probes the short distance regime of $\tilde{G}(u_1, u_2)$, or, equivalently, its UV behavior (see also footnote 11 of [66]). The same reasoning holds with z_1 and z_2 exchanged.

For $\alpha = 1$, this property is lost: $u_1 = t - x$ corresponds to a null separation, which is not necessarily equivalent to short-distance.[6]

Since an analytic function of several variables is analytic in each variable separately (see, e.g., [75]), one can apply Cauchy's theorem successively. For $(z_1, z_2) \in \tilde{D}$, integrating

[5]We use the same notation G for the Green's function in both real and Fourier space.

[6]For example, $G(\omega, k) = \frac{i\omega}{\omega^2 - k^2}$, the retarded two-point function of a massless field with its conjugate momentum, vanishes at high frequencies. For $\alpha = 1$, $\tilde{G}(z_1, z_2) = i(z_1 + z_2)/(4 z_1 z_2)$ approaches a constant as $z_1 \to \infty$ with fixed z_2, while for $\alpha > 1$ it follows the same asymptotic decay as G.

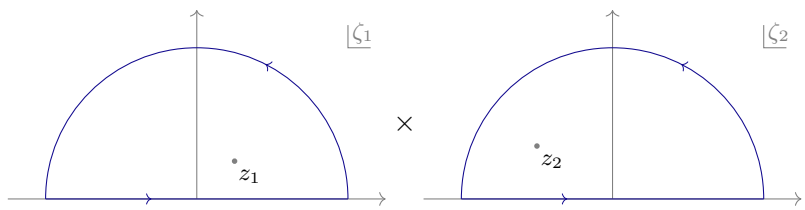

Figure 4.2Integration contour used in eq. (4.2.5).

over the contour shown in fig. 4.2 yields

$$\begin{aligned}\tilde{G}(z_1, z_2) &= \frac{1}{2\pi i}\int \frac{d\zeta_1\, \tilde{G}(\zeta_1, z_2)}{\zeta_1 - z_1 - i\epsilon} \\ &= \frac{1}{(2\pi i)^2}\int \frac{d\zeta_1\, d\zeta_2\, \tilde{G}(\zeta_1, \zeta_2)}{(\zeta_1 - z_1 - i\epsilon)(\zeta_2 - z_2 - i\epsilon)},\end{aligned} \tag{4.2.5}$$

where integration is along the real axis in each variable, and arcs at infinity have been neglected under the assumption $\tilde{G} \to 0$ there. The explicit $i\epsilon$ specifies the contour when a variable approaches the real axis.

A particularly useful relation follows by noting that, for $(z_1, z_2) \in \tilde{D}$, moving the poles in (4.2.5) to the lower half-plane yields zero:

$$\frac{1}{(2\pi i)^2}\int \frac{d\zeta_1\, d\zeta_2\, \tilde{G}(\zeta_1, \zeta_2)}{(\zeta_1 - z_1^* + i\epsilon)(\zeta_2 - z_2^* + i\epsilon)} = 0. \tag{4.2.6}$$

Subtracting (4.2.6) (after complex conjugation) from (4.2.5) gives

$$\tilde{G}(z_1, z_2) = -\frac{i}{2\pi^2}\int \frac{d\zeta_1\, d\zeta_2\, \operatorname{Im}\tilde{G}(\zeta_1, \zeta_2)}{(\zeta_1 - z_1 - i\epsilon)(\zeta_2 - z_2 - i\epsilon)}, \tag{4.2.7}$$

the direct multi-variable analogue of the standard dispersion relation for a single variable.

Expressing (4.2.7) in the original Fourier variables, with $\zeta_1 = \omega' + \alpha k'$ and $\zeta_2 = \omega' - \alpha k'$, gives

$$G(\omega, k) = -\frac{i\alpha}{\pi^2}\int \frac{d\omega'\, dk'\, \operatorname{Im} G(\omega', k')}{(\omega' - \omega - i\epsilon)^2 - \alpha^2(k' - k)^2}. \tag{4.2.8}$$

This form is far from obvious without the (z_1, z_2) parametrisation.

The multi-variable dispersion relation (4.2.7) is equivalent to the Leontovich relations, both following directly from analyticity (and assumptions about decay at infinity). For instance, in the rotationally invariant case, $G(\omega, k + \omega\xi)$ is analytic in ω for $|\xi| < 1$,[7] so

[7] More generally, one can take $\vec{k} \to \vec{k} + \omega\vec{\xi}$ with $|\vec{\xi}| < 1$.

that

$$G(\omega, k) = \frac{1}{2\pi i} \int \frac{d\zeta}{\zeta - \omega - i\epsilon} G\big(\zeta, k + (\zeta - \omega)\xi\big), \tag{4.2.9}$$

which corresponds to the single-variable dispersion relation in z_1 (or z_2) with $\xi = 1/\alpha$. Repeated application of (4.2.9) with $\xi = 1/\alpha$ and $\xi' = -1/\alpha$ reproduces (4.2.7) after a change of variables.

Single-variable dispersion relations on the real axis yield the familiar Hilbert transform relations:

$$\operatorname{Re} \tilde{G}(z_1, z_2) = \frac{1}{\pi} \operatorname{PV}_{z_1} \int \frac{d\zeta_1 \operatorname{Im} \tilde{G}(\zeta_1, z_2)}{\zeta_1 - z_1}, \tag{4.2.10}$$

$$\operatorname{Im} \tilde{G}(z_1, z_2) = -\frac{1}{\pi} \operatorname{PV}_{z_1} \int \frac{d\zeta_1 \operatorname{Re} \tilde{G}(\zeta_1, z_2)}{\zeta_1 - z_1}, \tag{4.2.11}$$

and similarly with $z_1 \leftrightarrow z_2$.

Applying (4.2.7) on the real plane, using Sokhotski–Plemelj and (4.2.10), yields the double principal value relations

$$\operatorname{Im} \tilde{G}(z_1, z_2) = -\frac{1}{\pi^2} \operatorname{PV}_{z_1, z_2} \int \frac{dt_1\, dt_2 \operatorname{Im} \tilde{G}(t_1, t_2)}{(t_1 - z_1)(t_2 - z_2)}, \tag{4.2.12}$$

$$\operatorname{Re} \tilde{G}(z_1, z_2) = -\frac{1}{\pi^2} \operatorname{PV}_{z_1, z_2} \int \frac{dt_1\, dt_2 \operatorname{Re} \tilde{G}(t_1, t_2)}{(t_1 - z_1)(t_2 - z_2)}, \tag{4.2.13}$$

where the principal value prescription applies to both integrals. These show that, in several variables, the real and imaginary parts are not only related as in the single-variable case, but are also constrained by the additional consistency conditions (4.2.12) and (4.2.13).

4.3 Positivity and its implications

Imaginary part of the response function in Fourier space specifies dissipation of the energy of an external source coupled to the system.[8] See for example [74, 76] for more details. For passive systems, that can only absorb energy from the source, the imaginary part is necessarily always positive for $\omega > 0$, and by reality condition, negative for $\omega < 0$, for all

[8] This is true only if we are studying the two point function of a single observable. In cases that there are many observables, dissipative part of the linear response (matrix) will be $(G - G^\dagger)/2i$. This coincides with the imaginary part, if the system has spacetime parity symmetry.

k. This is true for stable systems in their ground state and also for thermal states, among others.[9]

This positivity condition of the imaginary part can be shown to extend to complex frequencies and momenta by using dispersion relations. Consider first the single-variable case, after taking imaginary part of the dispersion relation, assuming no subtractions, we obtain

$$\mathrm{Im}G(\omega) = \frac{\mathrm{Im}\,\omega^2}{\pi}\int_0^{+\infty}\frac{\mathrm{d}z^2}{|z^2-(\omega)^2|^2}\mathrm{Im}G(z)\,, \tag{4.3.1}$$

where we have re-written the kernel $(z-\omega)^{-1} = (z-\omega^*)|z-\omega|^{-2}$, suppressing the $i\epsilon$ as ω is taken to be in the UHP, and then used the reality condition to integrate over positive frequencies. Positivity condition implies that the integral in eq. (4.3.1) is strictly positive, unless there is no response at all, and therefore the sign of $\mathrm{Im}G(\omega)$ is the same as the sign of $\mathrm{Im}\,\omega^2 = 2\mathrm{Im}\,\omega\,\mathrm{Re}\,\omega$ in the UHP, i.e. positive for $\mathrm{Re}\,\omega > 0$, negative for $\mathrm{Re}\,\omega < 0$, and zero on the imaginary axis, which is the extension of the real frequencies.

For multiple variables, it is useful to define $F(\omega,k) \equiv \omega G(\omega,k)$, for which the imaginary part $\mathrm{Im}\,F(\omega,k) = \omega\,\mathrm{Im}\,G(\omega,k)$ is positive for all real ω and k.[10] The new function is analytic in the same region, therefore, switching to z_1 and z_2 defined in eq. (4.2.1), we can write dispersion relations for $\tilde{F}(z_1,z_2) = F(\omega,k)$. Notice that the infinity behavior of F is worse than G by one factor of ω. Assuming, for the moment, that no subtractions required in a dispersion relation for $\tilde{F}(z_1,z_2)$, fixing z_2 to be some real point t_2, we can write

$$\tilde{F}(z_1,t_2) = \frac{1}{\pi}\int\frac{\mathrm{d}t_1}{t_1-z_1-i\epsilon}\mathrm{Im}\tilde{F}(t_1,t_2)\,, \tag{4.3.2}$$

which after taking an imaginary part, suppressing $i\epsilon$, gives a manifestly positive result

$$\mathrm{Im}\tilde{F}(z_1,t_2) = \frac{\mathrm{Im}z_1}{\pi}\int\frac{\mathrm{d}t_1}{|t_1-z_1|^2}\mathrm{Im}\tilde{F}(t_1,t_2) > 0\,. \tag{4.3.3}$$

Now, for z_2 in the UHP, this time we fix z_1 in the UHP, and write a dispersion relation with respect to z_2, which after taking an imaginary part gives

$$\mathrm{Im}\tilde{F}(z_1,z_2) = \frac{\mathrm{Im}z_2}{\pi}\int\frac{\mathrm{d}t_2}{|t_1-z_2|^2}\mathrm{Im}\tilde{F}(z_1,t_2) > 0\,, \tag{4.3.4}$$

[9] More generally, the positivity property holds for a system described by a density matrix for which occupancy of the energy eigen-states is monotonically decreasing with energy [74].

[10] It is completely natural to define F, as $\mathrm{Im}\,F(\omega,k)$, is in fact what appears in the energy dissipation formula.

where right hand side is strictly positive, because of eq. (4.3.3). This proves positivity of $\mathrm{Im}\tilde{F}(z_1, z_2)$ in the GUHP. Remember that from eq. (4.2.2) we see that the GUHP is a subset of the whole region of analyticity for $\alpha > 1$ (see fig. 4.1). However, for every point in the region of analyticity, there exist a suitable $\alpha > 1$ such that it is included in the GUHP in terms of z_1 and z_2 variables.[11] This concludes the claim, i.e. $F(\omega, k)$ has positive imaginary part in the whole region of analyticity.

The derivation presented above assumes $\tilde{F}(z_1, z_2) \to 0$ at complex infinity, which is a stronger assumption compared to $\tilde{G}(z_1, z_2) \to 0$. We can do better, starting from the double Cauchy integral, eq. (4.2.5), for $\tilde{G}(z_1, z_2)$ which we copy here, replacing $\tilde{G}(z_1, z_2) = 2\tilde{F}(z_1, z_2)/(z_1 + z_2)$,

$$\tilde{F}(z_1, z_2) = \frac{1}{(2\pi i)^2} \int \mathrm{d}t_1\, \mathrm{d}t_2\, \frac{(z_1 + z_2)}{(t_1 - z_1)(t_2 - z_2)(t_1 + t_2)} \tilde{F}(t_1, t_2)\,, \tag{4.3.5}$$

and suppressing the $i\epsilon$ to avoid clutter. The integral can be simplified using analticity of $\tilde{F}$. Using the trick of putting a pole at z_1^* (or z_2^*), same as what we did in eq. (4.2.6), we obtain

$$0 = \int \mathrm{d}t_1\, \frac{1}{(t_1 - z_1^*)(t_1 + t_2)} \tilde{F}(t_1, t_2) = \int \mathrm{d}t_1\, \frac{t_1 - z_1}{|t_1 - z_1|^2 (t_1 + t_2)} \tilde{F}(t_1, t_2)\,, \tag{4.3.6}$$

and similar expression with $z_1 \to z_2$ and $t_1 \leftrightarrow t_2$. This means that we can simplify the integral kernel of eq. (4.3.5), in multiple steps as follows

$$\begin{aligned}
\frac{(z_1 + z_2)}{(t_1 - z_1)(t_2 - z_2)(t_1 + t_2)} &= \frac{(z_1 + z_2)(t_1 - z_1^*)(t_2 - z_2^*)}{|t_1 - z_1|^2 |t_2 - z_2|^2 (t_1 + t_2)} \\
&= \frac{(z_1 + z_2)(t_1 - z_1 + 2i\mathrm{Im}z_1)(t_2 - z_2 + 2i\mathrm{Im}z_2)}{|t_1 - z_1|^2 |t_2 - z_2|^2 (t_1 + t_2)} \\
&\to (2i)^2 \mathrm{Im}z_1 \mathrm{Im}z_2 \frac{(z_1 + z_2)}{|t_1 - z_1|^2 |t_2 - z_2|^2 (t_1 + t_2)} \\
&= (2i)^2 \mathrm{Im}z_1 \mathrm{Im}z_2 \frac{-(t_1 - z_1) - (t_2 - z_2) + (t_1 + t_2)}{|t_1 - z_1|^2 |t_2 - z_2|^2 (t_1 + t_2)} \\
&\to (2i)^2 \mathrm{Im}z_1 \mathrm{Im}z_2 \frac{1}{|t_1 - z_1|^2 |t_2 - z_2|^2}\,.
\end{aligned} \tag{4.3.7}$$

The first equality follows from $(t_1 - z_1)^{-1} = (t_1 - z_1^*)|t_1 - z_1|^{-2}$ and similarly for the other variable. In the next step, we simply re-write $t_1 - z_1^* = (t_1 - z_1) + (z_1 - z_1^*) = (t_1 - z_1) + 2i\mathrm{Im}z_1$

[11] This amounts to taking the limit $\alpha \to 1^+$, which in principle should be well-defined, regarding the statement of positivity, since the imaginary part is assumed to be positive on the real plane.

and similarly for the other one. For each variable, fixing the other one, the integral over the first parenthesis, i.e. (t_1-z_1), vanishes due to analyticity, as in eq. (4.3.6), which reduces the kernel to the third line. In the forth line, we re-write $z_1+z_2 = -(t_1-z_1)-(t_2-z_2)+(t_1+t_2)$, in which, following the same logic, the first two terms drop out and simplifies the kernel further in the last line of eq. (4.3.7). This last form is particularly useful, since after taking an imaginary part of eq. (4.3.5) gives

$$\mathrm{Im}\tilde{F}(z_1,z_2) = \frac{\mathrm{Im}z_1\mathrm{Im}z_2}{\pi^2}\int \mathrm{d}t_1\,\mathrm{d}t_2\,\frac{\mathrm{Im}\tilde{F}(t_1,t_2)}{|t_1-z_1|^2|t_2-z_2|^2} > 0\,, \tag{4.3.8}$$

which is manifestly positive in the GUHP. Notice that this is the same result as before, i.e. combination of eq. (4.3.3) and eq. (4.3.4), starting from weaker assumptions on the infinity behavior.

Mathematically, the above shows that $\tilde{F}(z_1,z_2)$ belongs to the class of *Herglotz–Nevanlinna functions* in several complex variables: analytic functions on the product of upper half-planes whose imaginary part is non-negative in that domain. In one complex variable, such functions are completely characterized by the classical Herglotz representation theorem [77, 78], which states that any analytic function $f:\mathbb{C}^+\to\mathbb{C}$ with $\mathrm{Im}\,f\geq 0$ can be written as

$$f(z) = a + bz + \frac{1}{\pi}\int_{\mathbb{R}}\left(\frac{1}{t-z} - \frac{t}{1+t^2}\right)d\mu(t),$$

where $a\in\mathbb{R}$, $b\geq 0$, and μ is a positive measure satisfying the growth condition

$$\int_{\mathbb{R}}\frac{1}{1+t^2}\,d\mu(t) < \infty.$$

In several variables, however, the theory is subtler: pointwise positivity of the measure is not suffient to provide a good multidimensional representation of Herglotz–Nevanlinna functions. Indeed, the multidimensional integral representation becomes richer, as it requires the measure not only to satisfy the previous growth condition but also additional integral constraints which have no 1-dimensional analogue [79]. In our context, positivity of $\mathrm{Im}\,\tilde{F}$ ensures the existence of such a representation, with the associated measure encoding the spectral density of the underlying retarded correlator.

4.3.1 Implications for Passive Systems

Positivity of $\mathrm{Im}\,F$ throughout the primitive analyticity domain implies that F has no zeros there, so F^{-1} is analytic in the same domain. In passive electromagnetic media, F is

directly related to the linear electromagnetic response of the system. Following [74], the inverse current response function (which relates the induced current to the applied external field) can be written as

$$(G^{-1})^{\mu\nu} = \Pi^{\mu\nu} + g^2 \Delta^{\mu\nu},$$

where $\Delta^{\mu\nu}$ is the free photon propagator, $\Pi^{\mu\nu}$ is the self-energy tensor and g is the electromagnetic coupling. Unlike $G^{\mu\nu}$, $\Pi^{\mu\nu}$ is not itself given by a commutator of local operators, so its microcausality is not guaranteed *a priori*.

However, since $(F^{-1})^{\mu\nu}$ and $\Delta^{\mu\nu}$ share the same analyticity domain, and

$$\omega\,(F^{-1})^{\mu\nu} - g^2 \Delta^{\mu\nu} = \Pi^{\mu\nu},$$

it follows that the same analyticity properties extend to $\Pi^{\mu\nu}$. The Herglotz–Nevanlinna property of $F^{\mu\nu} = \omega G^{\mu\nu}$ guarantees that even observables not directly expressible as causal commutators, such as the self-energy, obey the same analyticity constraints in passive, dissipative systems. The polarization components of $\Pi^{\mu\nu}$, which are directly related to the electromagnetic response functions ε and $1/\mu$, encode the effect of the medium on the propagation of electromagnetic fields. In fact, $\Pi^{\mu\nu}$ is precisely the object entering the effective Maxwell equations. Consequently, analyticity of $\Pi^{\mu\nu}$ in the forward tube $\mathcal{T}_+$ immediately implies analyticity of $\varepsilon(\omega, \vec{k})$ and $1/\mu(\omega, \vec{k})$ in the same domain. This observation is significant, as it permits the derivation of dispersion relations directly in terms of $\Pi^{\mu\nu}$, without the need to restrict to a specific subset of its analytic domain, thereby extending the results of [74].

4.3.2 Non-compactness

Another remarkable consequence of positivity is that the imaginary part of $\tilde{F}$ (and therefore of G) cannot have compact support as a function of the real variables. To see this, we assume that $\tilde{F}$ vanishes at complex infinity. Under this assumption, it satisfies an unsubtracted double dispersion relation of the form (4.2.7):

$$\tilde{F}(z_1, z_2) = \frac{-i}{2\pi^2} \int dt_1\, dt_2\, \frac{\operatorname{Im} \tilde{F}(t_1, t_2)}{(t_1 - z_1 - i\epsilon)(t_2 - z_2 - i\epsilon)}\,. \tag{4.3.9}$$

Specialising to real values of $z_{1,2}$ and taking the imaginary part yields

$$\operatorname{Im} \tilde{F}(z_1, z_2) = -\frac{1}{\pi^2}\, \mathrm{PV}_{z_1, z_2} \int dt_1\, dt_2\, \frac{\operatorname{Im} \tilde{F}(t_1, t_2)}{(t_1 - z_1)(t_2 - z_2)}\,. \tag{4.3.10}$$

Now suppose that the support of $\operatorname{Im}\tilde{F}(t_1,t_2)$ is contained in a compact set $\mathcal{C}\subset\mathbb{R}^2$, and choose $(z_1,z_2)\notin\mathcal{C}$. The LHS then vanishes by assumption, while the RHS becomes

$$-\frac{1}{\pi^2}\int_{\mathcal{C}} dt_1\,dt_2\,\frac{\operatorname{Im}\tilde{F}(t_1,t_2)}{(t_1-z_1)(t_2-z_2)}\,, \tag{4.3.11}$$

where the principal value prescription has been removed since there are no singularities in the integration domain.

This integral can be further rewritten as

$$-\frac{1}{\pi^2 z_1 z_2}\int_{\mathcal{C}} dt_1\,dt_2\,\frac{\operatorname{Im}\tilde{F}(t_1,t_2)}{(1-t_1/z_1)\,(1-t_2/z_2)} = -\frac{1}{\pi^2 z_1 z_2}\sum_{j_1,j_2\geq 0}\int_{\mathcal{C}} dt_1\,dt_2\,\left(\frac{t_1}{z_1}\right)^{j_1}\left(\frac{t_2}{z_2}\right)^{j_2}\operatorname{Im}\tilde{F}(t_1,t_2)\,, \tag{4.3.12}$$

where we have used the geometric series expansion for the factors $1/(1-t_i/z_i)$.[12]

Specialising to the limit $z_1,z_2\to\infty$, the RHS can be approximated by the first term in the series, leading to the contradiction

$$0=-\frac{A}{\pi^2 z_1 z_2}\,,\quad A\equiv\int_{\mathcal{C}} dt_1\,dt_2\,\operatorname{Im}\tilde{F}(t_1,t_2)>0\,. \tag{4.3.13}$$

This contradiction reveals that $\operatorname{Im}\tilde{F}(t_1,t_2)$ cannot be compactly supported. Importantly, the very same conclusion applies to $\operatorname{Im}\tilde{G}(t_1,t_2)$, since they are related by $\operatorname{Im}\tilde{F}(t_1,t_2)=\frac{t_1+t_2}{2}\operatorname{Im}\tilde{G}(t_1,t_2)$, and the factor t_1+t_2 is itself not compactly supported.

4.4 Generalizations

The previous discussion heavily relied on the assumption that $G(z_1,z_2)\to 0$ in the limit of $|z_1|,|z_2|\to\infty$. Although for condensed matter media the plasma behavior enables to close the contours before the electron mass, this assumption is not valid in general. Moreover, rotational invariance simplified the situation as it enabled us to deal with only two variables. We will now explore how to generalize the previous results in absence of those assumption. In particular, we will (i) obtain the general form of double dispersion relations in the presence of subtractions and (ii) show that positivity of the imaginary part of $\tilde{F}$ can be extended to the situation in which also rotational invariance is broken, even though we still require G to vanish at complex infinity.

[12] Recall that $|t_i/z_i|<1$ since we chose $(z_1,z_2)\notin\mathcal{C}$.

4.4.1 Subtractions

In case when the function does not vanish at complex infinity, we have to take into account the contribution from the large semi-circle. Equivalently, we write dispersion relations for a modified version of the function, perhaps using division by a polynomial, which goes to zero at infinity. This is known as dispersion relation with subtractions. Below, we first review this for the single-variable case (see [34, 70] for an extensive discussion) and then discuss several variables.

Consider $G(z)$ which is analytic in the UHP and does not vanish at infinity. Define $\hat{G}(z) \equiv \frac{G(z)}{P(z)}$ where $P(z)$ is a polynomial with a certain degree such that $\hat{G}(z) \to 0$ at infinity. Indeed it is more economic to choose the degree as minimum as possible to avoid unnecessary complications. The polynomial is otherwise arbitrarily and can have zeros both in the upper or lower half-plane. In case there is a real zero, we move it away from the real axis, i.e. by an $i\epsilon$ prescription. For the rest of the discussion, we will assume that $P(z)$ is of even degree and that it is real on the real line, so that its zeros come in pairs of complex numbers related by complex conjugation. Following the standard argument we obtain

$$G(z) = Q(z) + \frac{P(z)}{\pi} \int \frac{\mathrm{d}t}{t - z - i\epsilon} \frac{\mathrm{Im}G(t)}{P(t)} \,, \tag{4.4.1}$$

where $Q(z)$ is a polynomial, of one degree less that $P(z)$, given by

$$Q(z) = P(z) \sum_a \left(\frac{G(z_a)}{P'(z_a)(z - z_a)} + \frac{G^*(z_a)}{(P'(z_a))^*(z - z_a^*)} \right) \,, \tag{4.4.2}$$

where the sum is over the zeros of $P(z_a) = 0$ that lie in the UHP, thereby picked by the contour integration. It is easy to notice that $Q(z_a) = G(z_a)$. Therefore, in order to reconstruct the full function $G(z)$ in the UHP, we need to provide extra data i.e. specifying the value of $G(z)$ at the zeros of $P(z)$ which lie in the UHP.

Let us switch to multiple variables; in this case one has to distinguish between infinity behavior of z_1 and z_2. As an example, assume $\tilde{G}(z_1, z_2)$ goes to zero for $z_1 \to \infty$, while approaching a constant for $z_1 \to \infty$ for fixed z_2. In that case, single subtraction is required for z_1, not for z_2. We will be interested in obtaining a subtracted double dispersion relation for $\tilde{F}(z_1, z_2) = \omega \tilde{G}(z_1, z_2)$ without relying on any decay condition. To be more precise, we will assume that $\tilde{F}$ is polynomially bounded, so that $\hat{F}(z_1, z_2) \equiv \frac{\tilde{F}(z_1,z_2)}{P_1(z_1)P_2(z_2)}$ has the desired decay condition if the degress n_1, n_2 of the polynomials $P_1(z_1)$ and $P_2(z_2)$ are

chosen appropriately[13]. Following the same similar steps as before, we begin by writing a dispersion relation for $\tilde{F}(z_1, t_2)/(P_1(z_1)P_2(z_2))$ by performing Cauchy theorem first wrt z_1 and then wrt z_2. This way we arrive at (see appendix B.2)

$$\tilde{F}(z_1, z_2) = Q_{12}(z_1, z_2) + Q_1(z_1, z_2) + Q_2(z_1, z_2) - \frac{iP_1(z_1)P_2(z_2)}{2\pi^2} \int \frac{\mathrm{d}t_1\, \mathrm{d}t_2}{(t_1 - z_1 - i\epsilon)(t_2 - z_2 - i\epsilon)} \frac{\mathrm{Im}\tilde{F}(t_1, t_2)}{P_1(t_1)P_2(t_2)}, \tag{4.4.3}$$

in which $Q_{12}(z_1, z_2)$ is a polynomial in both z_1 and z_2, $Q_1(z_1, z_2)$ is a polynomial in z_1 but not in z_2. Similar holds for $Q_2(z_1, z_2)$ with z_1 and z_2 exchanged. Without loss of generality, we are assumuming that the polynomials $P_i(z_i)$ are real on teh real line and that they are of even degree. For example, we can chose them to be positive on the real line:

$$P_i(z_i) = \prod_{k=1}^{n_i} (z_i^2 + \tilde{z}_{i_k}^2) \tag{4.4.4}$$

As a consequence, their zeros are purely imaginary numbers of the form $z_{i_k} = \pm i\tilde{z}_{i_k}$. Specializing to real values of z_i and taking the imaginary part of the above equation we get

$$\frac{1}{2}\mathrm{Im}\tilde{F}(z_1, z_2) = \mathrm{Im}Q_{12}(z_1, z_2) + \mathrm{Im}Q_1(z_1, z_2) + \mathrm{Im}Q_2(z_1, z_2) - \frac{P_1(z_1)P_2(z_2)}{2\pi^2} \mathrm{PV}_{z_1, z_2} \int dt_1 dt_2 \frac{\mathrm{Im}\tilde{F}(t_1, t_2)}{P_1(t_1)P_2(t_2)(t_1 - z_1)(t_2 - z_2)}, \tag{4.4.5}$$

4.4.2 Breaking rotations

We now turn to the case in which rotational symmetry is also spontaneously broken. This situation is particularly interesting because the loss of isotropy enriches the analytic structure of correlation functions and leads to a wider set of response coefficients. Such configurations can be realized experimentally, for example by placing the system in a uniform electric or magnetic field, which selects a preferred spatial direction. In these settings, dispersive techniques provide a powerful tool to derive universal predictions for the anisotropic response of the system to external probes. A concrete illustration is given

[13] Notice that the most general polynomial $P(z_1, z_2)$ is not necessarily separable in the variables. We simplify the discussion by taking it to be of the form $P_1(z_1)P_2(z_2)$.

in [80], where dispersion relations were applied to conformal field theories in the presence of a large magnetic field.

In absence of rotational symmetry, it is still true that $\tilde{G}_R(\omega, \vec{k})$ is analytic in the tube $\mathcal{T}_+$, however, it is less straightforward to find a clever analog of the mapping 4.2.1. We will now discuss a way to generalize the previous construction to the case in which rotations are broken. Concretely speaking, we want to find a map between $\mathbb{R}^{d+1} + i\text{GUHP}$ and $\mathbb{R}^{d+1} + iD$, $D \subset V_+$: a linear transformation

$$\omega = \sum_i \alpha_i z_i \ , \ \vec{k} = \sum_i \vec{\beta}_i z_i \ , \ \alpha_i \in \mathbb{R}, \vec{\beta}_i \in \mathbb{R}^d \tag{4.4.6}$$

for which the $d+1$-dimensional generalized upper-half plane

$$\text{GUHP} \equiv \{\text{Im}[z_i] > 0, \forall\, i\} \tag{4.4.7}$$

is strictly contained inside the forward lightcone V_+

$$\text{Im}[\omega]^2 - (\text{Im}[\vec{k}])^2 > 0, \text{Im}[\omega] > 0 \tag{4.4.8}$$

As discussed in the appendix appendix B.3, the simplest class of transformations are those which map the orthant GUHP into the convex cone $D_{\gamma,\vec{\theta}} \subset V_+$ generated by $d+1$ future-directed timelike vectors. These cones are particularly regular in the sense that their constant ω sections correspond to regular simplexes centered at the origin in $\vec{k}$-space. This convenient choice ensures that only $1 + d(d-1)/2$ parameters are necessary in order to cover the whole interior of V_+. In particular, $\gamma \in (1, \infty)$ controls the spread of the cone; i.e. in the limit $\gamma \to 1^+$, the generators of the cone become null. The remaining freedom corresponds to the possibility of rotating the convex cone about the ω-axis.

Let us now pick a choice of $(\gamma, \vec{\theta})$ and write down a multiple dispersion relation for $\tilde{G}(z_1, ..., z_{d+1})$, assuming no subtractions are needed. To do this we perform Cauchy theorem in each variable and get, after neglecting the arcs at infinity,

$$\tilde{G}(z_1, ..., z_{d+1}) = \frac{1}{(2\pi i)^{d+1}} \int dt_1 ... dt_{d+1} \frac{\tilde{G}(t_1, t_2)}{(t_1 - z_1 - i\epsilon)...(t_{d+1} - z_{d+1} - i\epsilon)} \tag{4.4.9}$$

Doing the same procedure but putting the poles in the generalized lower-half plane, we also get

$$\frac{1}{(2\pi i)^{d+1}} \int dt_1 ... dt_{d+1} \frac{\tilde{G}(t_1, t_2)}{(t_1 - z_1^* + i\epsilon)...(t_{d+1} - z_{d+1}^* + i\epsilon)} = 0 \tag{4.4.10}$$

Subtracting (if d is odd) or adding (if d is even) eq. (4.4.10), after complex conjugation, from eq. (4.4.9), yields

$$\tilde{G}(z_1, ..., z_{d+1}) = \frac{1}{\pi(2\pi i)^d} \int dt_1 ... dt_{d+1} \frac{\mathrm{Im}G(t_1, ..., t_{d+1})}{(t_1 - z_1 - i\epsilon)...(t_{d+1} - z_{d+1} - i\epsilon)} \tag{4.4.11}$$

We can now use the definition of $\tilde{F}(z_1, ..., z_{d+1}) \equiv (z_1 + z_2 + ... + z_{d+1})\tilde{G}(z_1, ..., z_{d+1})/(d+1)$ to rewrite eq. (4.4.9) in terms of $\tilde{F}$:

$$\tilde{F}(z_1, ..., z_{d+1}) = \frac{1}{(2\pi i)^{d+1}} \int dt_1 ... dt_{d+1} \frac{(z_1 + ... + z_{d+1})\tilde{F}(t_1, ..., t_{d+1})}{(t_1 + ... + t_{d+1})(t_1 - z_1)...(t_{d+1} - z_{d+1})} \tag{4.4.12}$$

Following the very same steps of eq. (4.3.7), the integral kernel can be simplified as

$$\begin{aligned} &\frac{\sum_k z_k}{(\sum_l t_l)\Pi_m(t_m - z_m)} = \frac{(\sum_k z_k)\Pi_m(t_m - z_m^*)}{(\sum_l t_l)\Pi_n|t_n - z_n|^2} = \frac{(\sum_k z_k)\Pi_m(t_m - z_m + 2i\mathrm{Im}z_m)}{(\sum_l t_l)\Pi_n|t_n - z_n|^2} = \\ &= \Pi_m(2i\mathrm{Im}z_m)\frac{(\sum_k z_k)}{(\sum_l t_l)\Pi_n|t_n - z_n|^2} + \frac{\sum_{S\subset\{1,...,d+1\}}\left(\Pi_{m\in S}(t_m - z_m)\right)\left(\Pi_{n\notin S}2i\mathrm{Im}z_n\right)}{(\sum_l t_l)\Pi_r|t_r - z_r|^2} \end{aligned} \tag{4.4.13}$$

where the indices run from 1 to $d+1$. Notice that the first term would correspond to the case in which $S = \emptyset$, hence the second sum does not run over this possiblity. Notice that every term of the sum contains at least one factor of the kind $t_m - z_m^*$ at the denominator. Thus, they vanishes when integrated agains $\tilde{F}$, since by Cauchy theorem their contribution corresponds to an integral over a circle which encloses no pole. The remaining part of the kernel can be further simplified as follows:

$$\frac{\Pi_m(2i\mathrm{Im}z_m)(\sum_k z_k)}{(\sum_l t_l)\Pi_n|t_n - z_n|^2} = (2i)^{d+1}\Pi_m(\mathrm{Im}z_m)\frac{-\sum_k(t_k - z_k) + (\sum_k t_k)}{(\sum_l t_l)\Pi_n|t_n - z_n|^2} \to \Pi_m\frac{\mathrm{Im}z_m}{|t_m - z_m|^2} \tag{4.4.14}$$

where we used again analyticity of $\tilde{F}$ to drop the terms of the first sum. As a consequence, the dispersion relation for $\tilde{F}$ boils down to

$$\tilde{F}(z_1, ..., z_{d+1}) = \frac{\Pi_m\mathrm{Im}z_m}{(\pi)^{d+1}} \int dt_1 ... dt_{d+1} \frac{\tilde{F}(t_1, ..., t_{d+1})}{|t_1 - z_1|^2...|t_{d+1} - z_{d+1}|^2} \tag{4.4.15}$$

Finally, taking the imaginary part on both sides yields

$$\mathrm{Im}\tilde{F}(z_1, ..., z_{d+1}) = \frac{\Pi_m\mathrm{Im}z_m}{(\pi)^{d+1}} \int dt_1 ... dt_{d+1} \frac{\mathrm{Im}\tilde{F}(t_1, ..., t_{d+1})}{|t_1 - z_1|^2...|t_{d+1} - z_{d+1}|^2} \tag{4.4.16}$$

which is valid on the generalized $d+1$ dimensional upper-half plane. Hence, we conclude that $\tilde{F}$ has positive imaginary part in the region $D_{\gamma,\vec{\theta}} \subset V_+$. Varying the parameters of

the map enables one to cover all the interior of V_+, finally concluding that $\tilde{F}$ has positive imaginary part over the whole primitive domain of analyticity even when rotations are spontaneously brokne.

Chapter 5

To the problem of cosmic expansion in massive gravity

In cosmological frameworks, the explicit breaking of time-translation symmetry obstructs the straightforward application of the off-shell analytic techniques developed in previous chapters. Although initial progress [71] has been made through the usage of a mixed representation of retarded two-point correlation functions—combining temporal and frequency domain analyses, the comprehensive characterization of their analytic and causal properties remains largely unexplored. In this chapter, we shift focus to a complementary strategy by examining the perturbative stability of cosmological solutions within the dRGT massive gravity theory. By performing a linear stability analysis of perturbations around these nontrivial background metrics, we derive necessary conditions for the absence of ghosts and gradient instabilities, thereby assessing the internal consistency and physical viability of potential cosmological scenarios in this framework. The approach proposed in [58, 65] is exploited and extended in order to classify the most general dynamical flat FLRW solutions of dRGT massive gravity. Starting from the assumption that the building block of the theory, X^{μ}_{ν}, enjoys the FLRW symmetries of the physical metric, we find that the admissible dynamical backgrounds are the aforementioned self-accelerated solution and a scenario in which the Stueckelberg stress-energy tensor behaves as a mixture of perfect fluids. A similar idea was presented by [65][1], and by [58], under the assumption of a diagonal reference metric and of spherically symmetric configurations of the Stueckelberg fields.

[1] Unfortunately, their proposed solutions for the profiles of the Stueckelberg fields leads again to the aforementioned No-Go theorem.

We advance these results and show that the existence of these solutions is actually guaranteed for any possible choice of f_{ab} and ϕ^a which satisfy a set of consistency conditions (in the form of complicated partial differential equations). These consistency relations arise as a consequence of the symmetries imposed on X^μ_ν and they can be used, once a choice of f_{ab} is specified, to determine the available profiles of ϕ^a. We explore the perturbative stability of the solutions in the absence and in the presence of additional matter content.

Section 5.1 motivates the methodology in the context of a multi-scalar theory. The concrete application of the proposed approach is then implemented and discussed in Sec. 5.2 for the minimal and full theory of dRGT Massive Gravity. Finally, the perturbative stability of the relevant backgrounds, in the absence of matter, is explored in Sec. 5.3.

Appendix C.1 is devoted to the classification of the admissible Stueckelberg profiles, with a focus on the case $f_{ab} = \eta_{ab}$; while App. C.2 extends the perturbative analysis in the presence of additional matter.

5.1 Single-field $P(X)$ vs multi-field $P(\mathcal{X})$

As a motivating warm-up, let us study the following toy model: a $P(X)$ theory of a shift-symmetric scalar field minimally coupled to gravity. The action takes the compact form

$$S = \int \mathrm{d}^4x\sqrt{-g}P(X) \ . \tag{5.1.1}$$

with $X = -(\partial\phi)^2/2$ the canonical kinetic term of the scalar field. Varying the above action with respect to the metric tensor yields the stress-energy tensor of the field ϕ:

$$T_{\mu\nu} \equiv \frac{-2}{\sqrt{-g}}\frac{\delta S}{\delta g^{\mu\nu}} = P_X\partial_\mu\phi\partial_\nu\phi + g_{\mu\nu}P \ , \tag{5.1.2}$$

where P_X is the derivative of P with respect to X. The above expression tells us that ϕ behaves as a fluid with 4-velocity $u^\mu \propto \partial^\mu\phi$. If we want to do cosmology it is convenient to go to the comoving frame of the fluid and project Einstein equations along the direction of u^μ as well as on the directions orthogonal to the flow. It is clear that $T_{\mu\nu}$ will inherit the symmetries of the spacetime it lives in. This means that if we demand our spacetime to be of an FLRW type (say $g_{00} = -1$, $g_{ij} = a(t)^2h_{ij}$), the matter content shall enjoy the symmetries of an FLRW universe, which are homogeneity and isotropy. More concretely, for a flat FLRW background, these requirements impose the following restrictions on the stress-energy tensor

$$T_{00} = \rho(t) \ , \quad T_{0i} = 0 \ , \quad T_{ij} = a(t)^2p(t)\delta_{ij} \ , \tag{5.1.3}$$

where $\rho(t)$ and $p(t)$ are the energy density and pressure, respectively, of the scalar field ϕ.

The question we want to address now is the following: what are the possible field configurations $\phi(t, \boldsymbol{x})$ for which $T_{\mu\nu}$ enjoys the FLRW symmetries? Together with the homogeneity of $P(X)$, compatibility with the FLRW symmetries would require $T_{0i} = 0$, which ultimately strictly forces

$$\partial_i \phi = 0 \ . \tag{5.1.4}$$

Therefore, it can be concluded that, at least in a single-field model, only homogeneous field configurations behave as a perfect fluid. In particular, homogeneity of X is implied by FLRW compatibility of $T_{\mu\nu}$.

We now show that the situation can change as soon as multiple fields are included in the description: in the context of multi-field $P(X)$-like theories, inhomogeneous field configurations can effectively behave as a perfect fluid. To this end, let us take a collection of shift-symmetric scalar fields ϕ^a and replace the old kinetic term X with its multi-field version

$$\mathcal{X} = -\frac{1}{2}\partial^\mu \phi^a \partial_\mu \phi^b f_{ab} \ , \tag{5.1.5}$$

where f_{ab} is the metric in field space. The Lagrangian density is now given by $P(\mathcal{X})$ and the stress-energy tensor acquires the form

$$T_{\mu\nu} = P_{\mathcal{X}} \partial_\mu \phi^a \partial_\nu \phi^b f_{ab} + g_{\mu\nu} P \ . \tag{5.1.6}$$

It is interesting to look at how the previous constraints of homogeneity and isotropy change with the addition of extra fields:

$$\begin{aligned} T_{00} \ &: \ P_{\mathcal{X}} \dot{\phi}^a \dot{\phi}^b f_{ab} - P = \rho \ , \\ T_{0i} = 0 \ &: \ \partial_i \phi^a \dot{\phi}^b f_{ab} = 0 \ , \\ T_{ij} \ &: \ P_{\mathcal{X}} \partial_i \phi^a \partial_j \phi^b f_{ab} + a^2 \delta_{ij} P = a^2 p \delta_{ij} \ . \end{aligned}$$

The very presence of extra fields gives the chance to avoid the strict condition $\partial_i \phi$ that we hit previously. Of course, $\partial_i \phi^a = 0$ for all a satisfies the above constraints. However, having multiple fields leaves room, in principle, for inhomogeneous field configurations to satisfy the above system of equations. When this is the case, we are facing the peculiar situation in which the collection of fields, despite being inhomogeneous, effectively behaves as a perfect fluid (see [81]).

A concrete example in a $1+1$ setting with a constant diagonal field-space metric is given by the configurations

$$\phi^a = T^a(t) + A^a + B^a x \ , \quad \dot{T}^0 = -\dot{T}^1 \frac{B^1 f_{11}}{B^0 f_{00}} \ , \tag{5.1.7}$$

where A^a and B^a are contants. It is straightforward to check that the above choice of profiles yields a perfect fluid stress-energy tensor. The continuity equation

$$\partial_t(P_{\mathcal{X}} a \dot{T}^1) = 0 \ , \tag{5.1.8}$$

can then be used to determine $T^1(t)$, while the equation of state of the fluid is specified by the choice of $P(\mathcal{X})$. The careful reader will surely have noticed the formal similarity between the scalar $\mathcal{X}$ and the trace of the tensor $(X^2)^\mu_\nu$ appearing in the dRGT action. Indeed, the Stueckelberg fields ϕ^a are not just scalars under diffeomorphism, they also enjoy a global shift symmetry

$$\phi^a \to \phi^a + C^a \ , \tag{5.1.9}$$

being the Goldstone bosons of broken diffeomorphisms. This similarity motivates the implementation of the previous approach within the context of dRGT Massive Gravity: instead of starting by specifying an ansatz for the Stueckelberg fields and the reference metric we will impose the FLRW symmetries directly on X^μ_ν (and, as a consequence, on the tensor $(X^2)^\mu_\nu$), extracting some interesting cosmological predictions which will not rely (up to a certain degree) on a specific choice of ϕ^a and f_{ab}. The basic assumption that will be kept through the whole discussion is that there exist at least a choice of f_{ab} and an associated family of configurations ϕ^a that make $(X^2)^\mu_\nu$ compatible with the FLRW symmetries. We will address the task of finding nontrivial configurations, in the particular case of Minkowski reference metric, in App. C.1. For the time being, let us take homogeneity and isotropy of X^μ_ν as our starting point and explore the cosmological consequences in the framework of dRGT.

5.2 Applications to dRGT

5.2.1 dRGT: setup

We begin by considering the dRGT action

$$S_{\text{dRGT}} = \int \mathrm{d}^4x\sqrt{-g}\left[R - \frac{m^2}{2}\sum_{i=2}^{4}\alpha_i\,\mathcal{U}_i[\mathcal{K}]\right] \ , \tag{5.2.1}$$

where, as discussed in 2.2, the dRGT potentials $\mathcal{U}_i[\mathcal{K}]$ are the elementary symmetric polynomials of the tensor $\mathcal{K}^\mu_\nu \equiv \delta^\mu_\nu - X^\mu_\nu$, namely

$$\begin{aligned}
\mathcal{U}_2 &= [\mathcal{K}^2] - [\mathcal{K}]^2 \ , \\
\mathcal{U}_3 &= -2[\mathcal{K}^3] + 3[\mathcal{K}][\mathcal{K}^2] - [\mathcal{K}]^3 \ , \\
\mathcal{U}_4 &= 6[\mathcal{K}^4] - 3[\mathcal{K}^2]^2 + 6[\mathcal{K}^2][\mathcal{K}]^2 - 8[\mathcal{K}][\mathcal{K}^3] - [\mathcal{K}]^4 \ .
\end{aligned} \tag{5.2.2}$$

where m is the graviton mass, the α_2, α_3, α_4 are dimensionless coefficients[2] and $[\mathcal{K}^n]$ stands for the trace of the matrix $\mathcal{K}^n$. Moreover, the building block X^μ_ν is defined by

$$(X)^\mu_\rho (X)^\rho_\nu = (X^2)^\mu_\nu = g^{\mu\rho}\partial_\rho\phi^a\partial_\nu\phi^b f_{ab} \ . \tag{5.2.3}$$

For the present discussion, we specialize to a flat FLRW physical metric $g_{\mu\nu}$, which, in comoving coordinates, takes the form $ds^2 = -dt^2 + a(t)^2 d\vec{x}^2$. As previously stated, we impose homogeneity and isotropy on the tensor X^μ_ν, which is the building block of the dRGT action. This means that

$$X^0_0 = F(t) \ , \quad X^0_i = 0 \ , \quad X^i_j = G(t)\,\delta_{ij} \ , \tag{5.2.4}$$

where δ_{ij} is the Kronecker delta and $F(t)$ and $G(t)$ are generic functions of time. As a consequence, both $(X^2)^\mu_\nu$ and the stress-energy tensor of the Stueckelberg sector enjoys the same symmetries of X^μ_ν. Notice that, in general, the contrary is not true: an FLRW-compatible stress tensor for ϕ^a does not imply that X^μ_ν is of the form (5.2.4). Equation (5.2.3) results in a set of constraints on the Stueckelberg fields

$$F^2 = -\dot{\phi}^a\dot{\phi}^b f_{ab} \ , \quad 0 = \dot{\phi}^a\partial_i\phi^b f_{ab} \ , \quad G^2\delta_{ij} = \frac{1}{a^2}\partial_i\phi^a\partial_j\phi^b f_{ab} \ . \tag{5.2.5}$$

Combining the above system with the Euler-Lagrange equations of the Stueckelberg fields would enable us to determine ϕ^a in terms of F and G, identifying the family of configurations that support a dynamical cosmology and, at the same time, ensures the symmetry conditions (5.2.4). This step is however not strictly needed. Indeed, we are interested in the background cosmological evolution and this is determined by the behaviour of $F(t)$ and $G(t)$, the components of X^μ_ν. To proceed in this direction, we will need the trace of X^μ_ν:

$$[X] = F + 3G \ . \tag{5.2.6}$$

[2]Notice that a rescaling of the α_i is degenerate with a rescaling of the mass and therefore one is always free to set $\alpha_2 = 1$, for example.

Before moving on, we note that imposing the form (5.2.4) for the building block X^μ_ν implies that spatial translations and rotations are unbroken at the level of the perturbations. Indeed, any variation of the action is proportional to traces of X^μ_ν (and its powers) thus the inhomogeneous background components of ϕ^a do not appear directly. We will see this explicitly in Sec. 5.3. On the other hand, imposing FRLW symmetries directly on $T_{\mu\nu}$ would not be sufficient to preserve these symmetries at the level of perturbations.

5.2.2 dRGT: Minimal Model

Remembering that $\mathcal{K}^\mu_\nu = \delta^\mu_\nu - X^\mu_\nu$, the explicit form of the minimal potential is

$$\mathcal{U}_2 = [\mathcal{K}^2] - [\mathcal{K}]^2 = -12 + 6[X] - [X]^2 + [X^2] = -6\left(2 - F - 3G + G^2 + FG\right) \ . \tag{5.2.7}$$

In the presence of the dRGT potential, the Einstein equations are modified as

$$G_{\mu\nu} - \frac{m^2}{2} Y_{\mu\nu} = \frac{T_{\mu\nu}}{M_{\rm Pl}^2} \ , \tag{5.2.8}$$

where[3]

$$Y_{\mu\nu} \equiv [\mathcal{K}]\, g_{\mu\nu} - \mathcal{K}_{\mu\nu} + \left[(\mathcal{K}^2)_{\mu\nu} - [\mathcal{K}]\mathcal{K}_{\mu\nu} - \frac{1}{2}\mathcal{U}_2\, g_{\mu\nu}\right] \ , \tag{5.2.9}$$

so that $T^\phi_{\mu\nu} \equiv m^2 M_P^2 Y_{\mu\nu}/2$ can be interpreted as the stress-energy tensor of the Stueckelberg sector, while $T_{\mu\nu}$ is the stress-energy tensor associated with ordinary matter content. Diffeomorphism invariance implies the covariant conservation for the Stueckelberg stress-energy tensor, $\nabla_\mu Y^\mu_\nu = 0$. [4] As anticipated in Sec. 5.1, the imposition of the symmetry constraints on $(X^2)^\mu_\nu$ yields an effective perfect fluid stress-energy tensor for the Stueckelberg sector. More explicitly, it is easy to verify that the non-vanishing components of the Y^μ_ν tensor are given by

$$Y^0_0 = 3\left(2 - 3G + G^2\right) \qquad Y^i_j = \left(6 - 3F - 6G + G^2 + 2FG\right)\delta_{ij} \ . \tag{5.2.10}$$

Thus, we can identify the energy density and pressure of the Stueckelberg fluid as

$$\begin{aligned} \rho_\phi &= -\frac{3m^2 M_{\rm Pl}^2}{2}\left(2 - 3G + G^2\right) \ , \\ p_\phi &= \frac{m^2 M_{\rm Pl}^2}{2}\left(6 - 6G + G^2 - 3F + 2FG\right) \ . \end{aligned} \tag{5.2.11}$$

[3] Notice that, if $X_{\mu\nu}$ is not symmetric, the expression of $Y_{\mu\nu}$ would need to be symmetrized in μ and ν.

[4] Note that this equation is automatically satisfied when the Stueckelberg fields satisfy their Euler-Lagrange equations $\delta S/\delta\varphi^a = 0$, In particular, one can show that $\partial_\nu\phi^a \delta S/\delta\varphi^a = \nabla_\mu Y^\mu_\nu$. Therefore, covariant conservation of Y^μ_ν is actually implied by the Euler-Lagrange equations, and that the two equations are actually equivalent.

It is evident that both the energy density and pressure of the Stueckelberg sector are functions of $F(t)$ and $G(t)$ and therefore are homogeneous functions. In particular, ρ_ϕ only depends on $G(t)$. This fact is crucial to ensure the existence of a class of "massive cosmologies" which can be fully determined without relying on the details of the choice of ϕ^a and f_{ab}.

Making explicit the components of the Einstein tensor and of the stress-energy tensor of the extra matter content (defined in terms of its density ρ and pressure p), the Friedmann equations acquire the form:

$$\begin{aligned} H^2 &= -\frac{m^2}{2}\left(2-3G+G^2\right)+\frac{\rho}{3M_{\rm Pl}^2}\ , \\ \frac{\ddot{a}}{a} &= -\frac{m^2}{4}\left(4-3F-3G+2FG\right)-\frac{3p+\rho}{6M_{\rm Pl}^2}\ . \end{aligned} \tag{5.2.12}$$

The continuity equation of the Stueckelberg sector can be written instead as

$$(3-2G)\left[\dot{G}+H(G-F)\right]=0\ . \tag{5.2.13}$$

As already explained, this set of equations does not depend on the explicit form of the Stueckelberg fields or the choice of the reference metric. Interestingly, we can classify the possible cosmologies according to which of the two factors in Eq. (5.2.13) is imposed to vanish. As a result, we can identify two possible branches:

- Λ-Branch : $G=3/2$.
- Mixed Branch: $\dot{G}+H(G-F)=0$.

We are now going to study these two branches separately.

Λ-Branch

This class of solutions is quite peculiar, since the specific value that G takes cancels precisely any possible F dependence in the pressure of the Stueckelberg fluid. As a consequence, ρ_ϕ and p_ϕ happen to be related by a barotropic equation of state with $w=-1$. This means that the stress-energy tensor of the Stueckelberg fluid is given by

$$T^\phi_{\mu\nu}=\frac{m^2M_{\rm Pl}^2}{2}Y_{\mu\nu}=-\frac{3m^2M_{\rm Pl}^2}{8}g_{\mu\nu}\ , \tag{5.2.14}$$

which corresponds to a cosmological constant of energy density $3m^2M_{\rm Pl}^2/8$. As a result, the Friedmann equations acquire the form

$$H^2 = \frac{m^2}{8} + \frac{\rho}{3M_{\rm Pl}^2} \ , \quad \frac{\ddot{a}}{a} = \frac{m^2}{8} - \frac{3p+\rho}{6M_{\rm Pl}^2} \ . \tag{5.2.15}$$

It is interesting to notice that, once the residual matter content of the spacetime is specified, the cosmology is fully determined, in a way which seems to be insensitive to the details of the Stueckelberg configurations (as well as on the choice of the reference metric), provided we restrict only on families of configurations which satisfy the symmetry requirements[5] (5.2.5). At the moment, we are assuming that there exists at least one choice of f_{ab} and ϕ^a that realizes the initial symmetry conditions. Notice that, if more choices are possible, the background cosmology will not be able to distinguish between these different possibilities: the features of the Λ-Branch solution do not depend on the particular ansatz for f_{ab} and ϕ^a. As clarified in the introduction, the same self-accelerated solution was found by [56], even though the authors did start from a different ansatz for X^μ_ν[6].

Mixed Branch

The second branch can accommodate different kinds of solutions.

Case $\dot{G} = 0$

The equation of motion forces either $F = G =$ const. or $H = 0$. In the second case, we hit again the No-Go theorem, while in the first scenario, the Stueckelberg fields behave again as a cosmological constant, whose energy density is

$$\rho_\phi = -\frac{3m^2M_{\rm Pl}^2}{2}(2 - 3G + G^2) \ . \tag{5.2.16}$$

Case $\dot{G} \neq 0$

Assuming now that $\dot{G} \neq 0$, we have that G can be obtained in terms of F and $a(t)$ by setting to zero the square bracket in Eq. (5.2.13). The resulting solution is

$$G(t) = \frac{1}{a}\left(G_0 + \int_{t_0}^{t} F(t')\dot{a}(t')\,\mathrm{d}t'\right) \ , \tag{5.2.17}$$

[5] It is actually non-trivial to look for Stueckelberg profiles which fulfil homogeneity and isotropy of $(X^2)^\mu_\nu$ and, at the same time, support a dynamical cosmology.

[6] In [56], a spherically symmetric ansatz is made for the Stueckelberg fields and the reference metric is chosen to be Minkowski. As a consequence, X^μ_ν is not diagonal and it does not enjoy the FLRW symmetries.

where G_0 is a constant. In this case, more effort is needed to fully understand the cosmology of this family of solutions. Indeed, an extra relation between F and G is needed to express both F and G as functions of time and, subsequently, completely determine the evolution of the scale factor. Actually, this extra relation comes directly from the set of symmetry constraints (5.2.5) and, in the specific case of Minkowski reference metric $f_{ab} = \eta_{ab}$, it takes the form (see App. C.1 for the derivation of the following relation)

$$a^2 G^2 = \lambda_1 \left(\int_{t_0}^{t} F(t')\, \mathrm{d}t' + \sigma \right)^2 \implies G = \pm \frac{\sqrt{\lambda_1}}{a} \left| \int_{t_0}^{t} F(t')\, \mathrm{d}t' + \sigma \right| , \tag{5.2.18}$$

where λ_1 and σ are parameters that label the family of field configurations ϕ^a that satisfies the symmetry constraints.

Combining Eq. (5.2.18) with the equation of motion Eq. (5.2.17) yields the following constraint

$$\pm \frac{\sqrt{\lambda_1}}{a}\, s\, F = HF\,, \qquad s \equiv \mathrm{sgn}\left[\int_{t_0}^{t} F(t')\, \mathrm{d}t' + \sigma \right] . \tag{5.2.19}$$

The first possibility for solving the equation above is to set $F = 0$ and therefore have $G = g/a$, with $g \equiv \pm|\sigma|\sqrt{\lambda_1}$ [7]. In this case, the behaviour of the Stueckelberg fluid is characterized by the following energy density and pressure

$$\begin{aligned} \rho_\phi &= -\frac{3m^2 M_{\mathrm{Pl}}^2}{2} \left(2 - \frac{3g}{a} + \frac{g^2}{a^2} \right) , \\ p_\phi &= \frac{m^2 M_{\mathrm{Pl}}^2}{2} \left(6 - \frac{6g}{a} + \frac{g^2}{a^2} \right) . \end{aligned} \tag{5.2.20}$$

Notice, first of all, that the sign of ρ_ϕ is crucially dependent on the sign of G. Indeed, if $G < 0$, the energy density of the Stueckelberg fluid is forced to be negative for the whole history of the spacetime. Moreover, the Stueckelberg sector behaves like a mixture of perfect fluids whose equations of state are respectively $w = -1, -2/3, -1/3$. This means that at early times the Stueckelberg sector mainly contributes in the form of curvature, while the asymptotic behaviour at late times is the one of a negative cosmological constant, which is independent on σ and λ_1[8].

Generally, such a rich scenario ends up being potentially pathological, because the energy density of the Stueckelberg sector sees its sign varying throughout the history of

[7] It is assumed $\sigma \neq 0$, otherwise the Stueckelberg energy density would be negative.

[8] On phenomenological grounds, to have a curvature component $|\Omega_k| < 0.01$ today, one needs the combination $g^2 = \sigma^2 \lambda_1 \lesssim 0.01$. A stronger bound on g could be obtained by imposing the energy component scaling as $1/a$ in Eq. (5.2.20) to be below today's observational limit.

the universe. Indeed, the energy density is positive only in the interval $g/2 < a < g^2$. It will be shown that, in the context of the full theory, an additional perfect fluid component (with an equation of state $w = 0$) appears in the Stueckelberg sector.

In addition to the two previous scenarios, the Mix-Branch can accommodate for another class of solutions, which is identified by $F \neq 0$. In this case, Eq. (5.2.18) transforms into a constraint on the Hubble parameter:

$$H = \pm \frac{\sqrt{\lambda_1}}{a} s \ . \tag{5.2.21}$$

Note that, demanding $H > 0$ would impose that $\pm s = 1$. From Eq. (5.2.21) we see that, one more time, the Stueckelberg sector imposes a constraint on the cosmology. A No-Go theorem knocks again at the door, forcing the second derivative of the scale factor to vanish, $\ddot{a} = 0$, and leading to a universe that expands/contracts in a uniform way (as $a \propto t$). In this particular situation, the Friedmann equations in Eq. (5.2.12) become a set of algebraic equations for F and G.

If other matter components were present, both F and G would depend on the rest of the matter content of the spacetime. This behaviour is crucial to enable the Stueckelberg fluid to cancel the influence of the other fluids and impose the No-Go constraint on $\ddot{a}$.
It is worth stressing that the features of this Branch, when $\dot{G} \neq 0$, strongly rely on the choice of the reference metric. A different ansatz for f_{ab} would, in principle, lead to a different extra relation between F and G, resulting in a different behaviour of the Stueckelberg fluid. Notice that similar branches were obtained in the context of bi-gravity [82], with an FLRW ansatz for both metric tensors.

5.2.3 dRGT: Full Theory

It is now time to generalise the previous results to the full dRGT model, in which both the cubic and quartic potentials $\mathcal{U}_3$ and $\mathcal{U}_4$, defined in Eq. (5.2.2), are included. As before, the starting point is the imposition of the symmetry conditions (5.2.4) on X^μ_ν. It is not difficult to check that the explicit expressions of the potentials in terms of the functions F and G which encapsulate the net effect of the inhomogeneous Stueckelberg configurations are

$$\begin{aligned} \mathcal{U}_2 &= -6(G-1)(F+G-2) \ , \\ \mathcal{U}_3 &= 6(G-1)^2(3F+G-4) \ , \\ \mathcal{U}_4 &= -24(F-1)(G-1)^3 \ . \end{aligned} \tag{5.2.22}$$

Branches	G	F	f_{ab}	Cosmology
Λ-Branch	$3/2$	$F(G, f_{ab})$	$-$	Λ
Mixed	$\propto 1/a$	0	η_{ab}	Mix
	$\propto 1/a$	$\neq 0$	η_{ab}	$\ddot{a} = 0$
	const	G	$-$	Λ
	const	$\neq G$	$-$	$H = 0$

Table 5.1 Different branches and their cosmological behaviour. The Λ-Branch is the self-accelerated background solution, in which the Stueckelberg sector behaves as a cosmological constant. The Mixed Branch can accommodate different classes of solutions. Among them, a dynamical background in which the Stueckelberg fields behave as a mixture of perfect fluids is obtained once the choice $f_{ab} = \eta_{ab}$ is specified. Similarly, also the $\ddot{a} = 0$ scenario requires a specification of the reference metric. Indeed, once f_{ab} is specified, an extra relation between F and G is provided by the symmetry conditions imposed on X^μ_ν, enabling to determine F in terms of G. All the other scenarios do not rely on a specific ansatz for f_{ab} and ϕ^a (provided they satisfy the consistency relations (5.2.5)).

The contribution of the additional potentials to the Stueckelberg stress-energy tensor can be straightforwardly evaluated[9], yielding

$$\begin{aligned} Y_{\mu\nu} = \alpha_2 &\left[\mathcal{K}^2_{\mu\nu} - \mathcal{K}_{\mu\nu} + (g_{\mu\nu} - \mathcal{K}_{\mu\nu})[\mathcal{K}] - \frac{1}{2}\mathcal{U}_2 g_{\mu\nu}\right] + \\ + \alpha_3 &\left[-3(\mathcal{K}^\rho_\mu - [\mathcal{K}]\delta^\rho_\mu)(\mathcal{K}^2_{\rho\nu} - \mathcal{K}_{\rho\nu}) - \frac{3}{2}\mathcal{U}_2(g_{\mu\nu} - \mathcal{K}_{\mu\nu}) - \frac{1}{2}\mathcal{U}_3 g_{\mu\nu}\right] + \\ + \alpha_4 &\left[6(2\mathcal{K}^\sigma_\mu\mathcal{K}^\rho_\sigma - 2[\mathcal{K}]\mathcal{K}^\rho_\mu - \mathcal{U}_2\delta^\rho_\mu)(\mathcal{K}^2_{\rho\nu} - \mathcal{K}_{\rho\nu}) - 2\mathcal{U}_3(g_{\mu\nu} - \mathcal{K}_{\mu\nu}) - \frac{1}{2}\mathcal{U}_4 g_{\mu\nu}\right] . \end{aligned} \tag{5.2.23}$$

Given the symmetries we are imposing on X^μ_ν, the Stueckelberg sector effectively behaves as a perfect fluid also in the full theory. Making use of the explicit expressions for the potentials Eq. (5.2.22) and of Eq. (5.2.4), we obtain the following values for the non-

[9]Notice that $X_{\mu\nu} = X_{\nu\mu}$ as a consequence of our initial assumption about X^μ_ν being FLRW-compatible.

vanishing components of the $Y_{\mu\nu}$ tensor

$$Y_{00} = (-6\alpha_2 - 12\alpha_3 - 12\alpha_4) + (-3\alpha_2 - 18\alpha_3 - 36\alpha_4)\, G^2 + (9\alpha_2 + 27\alpha_3 + 36\alpha_4)\, G + (3\alpha_3 + 12\alpha_4)\, G^3 \ ,$$
$$Y_{ij} = \delta_{ij} a^2 \Bigg[(6\alpha_2 + 12\alpha_3 + 12\alpha_4) + (\alpha_2 + 6\alpha_3 + 12\alpha_4)\, G^2 + (-6\alpha_2 - 18\alpha_3 - 24\alpha_4)\, G +$$
$$+ F\Bigg((-3\alpha_2 - 9\alpha_3 - 12\alpha_4) + (-3\alpha_3 - 12\alpha_4)\, G^2 + (2\alpha_2 + 12\alpha_3 + 24\alpha_4)\, G \Bigg)\Bigg] \ . \tag{5.2.24}$$

These expressions can be mapped to the energy density and the pressure of the Stueckelberg fluid as

$$\rho_\phi = \frac{M_{\rm Pl}^2 m^2}{2} Y_{00} \ , \quad p_\phi = \frac{1}{3}\frac{M_{\rm Pl}^2 m^2}{2} Y_i^i \ . \tag{5.2.25}$$

Lastly, the continuity equation for the Stueckelberg fields leads to the following relation:

$$\Big[3\,(\alpha_3 + 4\alpha_4)\, G^2 - 2\,(\alpha_2 + 6\alpha_3 + 12\alpha_4)\, G + 3\,(\alpha_2 + 3\alpha_3 + 4\alpha_4) \Big] \Big[\dot{G} + H(G - F) \Big] = 0 \ . \tag{5.2.26}$$

Notice that, similarly to the minimal model case, the continuity equation factorizes. This fact will allow us to identify two different cosmological branches, obtained by setting each of the two square brackets in Eq. (5.2.26) to zero.

Remarkably, the structure of the equation is very similar to the case of the minimal model Eq. (5.2.13). In particular, the second factor in Eq. (5.2.26) is identical to the one we already encountered while the first, once again, does not depend on the function F. It can be expected, then, that the qualitative features of the different cosmological branches will be extremely similar to those discussed in the previous section. Explicitly, the two branches are identified by the following conditions:

- Λ-Branch: $3\,(\alpha_3 + 4\alpha_4)\, G^2 - 2\,(\alpha_2 + 6\alpha_3 + 12\alpha_4)\, G + 3\,(\alpha_2 + 3\alpha_3 + 4\alpha_4) = 0$.
- Mix Branch: $\dot{G} + H(G - F) = 0$.

Their properties are summarized in Tab. 5.1.

Λ-Branch

As before, the first branch is identified by the vanishing condition of the above algebraic equation for G. This is nothing but a quadratic equation for G, and its roots are simply given by

$$G_\pm = \frac{\alpha_2 + 6\alpha_3 + 12\alpha_4 \pm \Delta}{3\,(\alpha_3 + 4\alpha_4)} \ , \quad \Delta \equiv \sqrt{\alpha_2^2 + 3\,(\alpha_3 - 4\alpha_4)\,\alpha_2 + 9\alpha_3^2} \ . \tag{5.2.27}$$

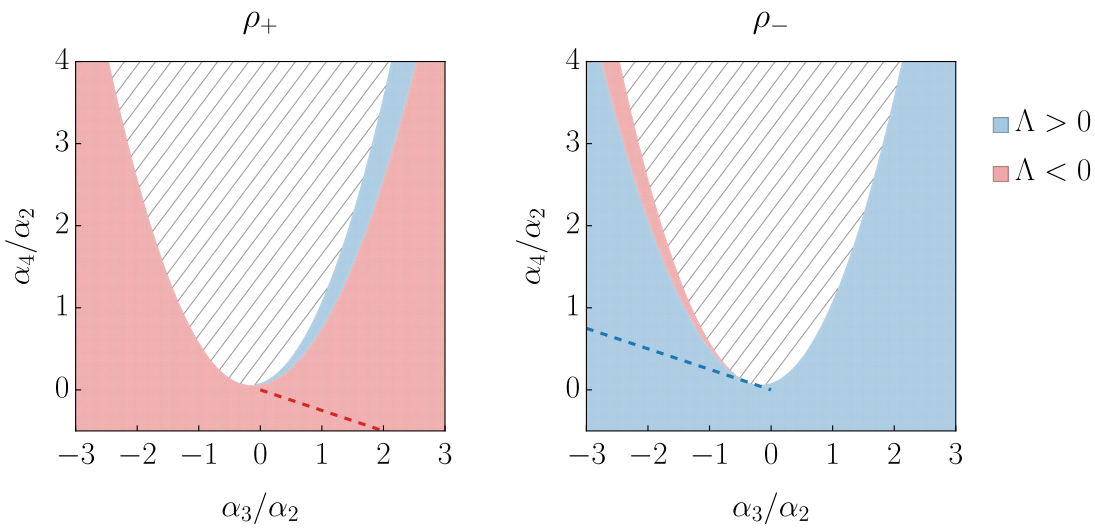

Figure 5.1 Regions of parameter space for which the Stueckelberg sector behaves as a positive (blue) or negative (red) cosmological constant in the Λ-Branch. The dashed line corresponds to the condition $\alpha_3 + 4\alpha_4 = 0$, for which the equation that identifies branch I becomes linear in G. In this special case, the Stueckelberg sector behaves as a positive cosmological constant only when $\alpha_3 > -1/3$. The white hatched region corresponds to the values of parameters for which the discriminant Δ is negative (and thus yields complex solutions $G_\pm$). Along the dashed lines ρ_ϕ diverges, with a sign indicated by the color of the line.

It is important to point out that, in general, not every region of the parameter space of the theory will allow for the existence of such roots. Indeed the above solutions will be real only when $\Delta > 0$. Similarly to the minimal-model case of the previous Section, once the above solutions for G are plugged inside $Y_{\mu\nu}$, any F dependence in the pressure term is completely washed away, ultimately leading to the following expressions for ρ_ϕ and p_ϕ:

$$\begin{aligned} \rho_\phi &= \frac{(\alpha_2 + 3\alpha_3 \pm \Delta)\left(\mp 3\alpha_3\Delta - \alpha_2\left(3\alpha_3 - 36\alpha_4 \pm \Delta\right) - 2\alpha_2^2 - 18\alpha_3^2 + \Delta^2\right)}{9\left(\alpha_3 + 4\alpha_4\right)^2} \,, \\ p_\phi &= -\rho_\phi \,. \end{aligned} \tag{5.2.28}$$

As explicitly shown by the above expression, the value of the cosmological constant now depends on the parameters of the theory. In particular, we can write $\Lambda = \rho_\phi/M_{\rm Pl}^2$, and explore the parameter space region for which $\Lambda > 0$ (see Fig. 5.1).

As before, the cosmology of the Λ-Branch is fully determined by the Stueckelberg

equation of motion. On the same lines as the discussion of the minimal model, therefore, this branch needs no extra relation between F and G to obtain the evolution of the scale factor. In particular, neither f_{ab} nor ϕ^a need to be specified. Compatibility with the symmetry conditions of Eq. (5.2.5) will however provide a relation between F and G once the reference metric is specified.

Mixed Branch

Also in the full theory, this second branch is identified by the condition $\dot{G}+H(G-F)=0$. As already discussed in the context of the minimal model, an extra relation between F and G is required to express both the functions in terms of the scale factor (or, equivalently, in terms of t) and to fully determine the cosmological history of spacetime. Again, we fix the reference metric to be Minkowski spacetime. As a consequence, the extra relation between F and G takes the form Eq. (5.2.18) and it can be combined with the continuity equation for the Stueckelberg stress-energy tensor to determine the time evolution of the functions F and G.

Following the steps of Sec. 5.2.2 we obtain a very similar set of possible cosmological scenarios. Among them, the class of solutions identified by $F \neq 0$ yields a cosmology in which the Hubble parameter is constrained to be $H \propto 1/a$. As a consequence, the Stueckelberg sector imposes a vanishing condition on the second derivative of the scale factor, giving rise to a linear expansion expansion/contraction. Solving the Friedmann equations enables to obtain the explicit expression of F and G in terms of the scale factor and of the energy density and pressure of matter (if present). As already pointed out, in this peculiar scenario, the Stueckelberg fluid counterbalances the effect of the other perfect fluids to impose the $\ddot{a}=0$ constraint.

The other, more interesting, cosmological scenario corresponds to the situation

$$F=0\ , \quad G=\frac{g}{a}\ , \tag{5.2.29}$$

where the constant $g \equiv \pm|\sigma|\sqrt{\lambda_1}$ can take either sign. As before, for this class of solutions, the Stueckelberg sector consists of a mixture of perfect fluids with different equations of state. Using the above expression for G inside Eq. (5.2.24), it is straightforward to see that

the energy density and pressure of the Stueckelberg fluid are given by

$$\rho_\phi = \frac{3m^2 M_{\rm Pl}^2}{2}\Big[-2(\alpha_2+2\alpha_3+2\alpha_4)+\frac{3g}{a}(\alpha_2+3\alpha_3+4\alpha_4)-\frac{g^2}{a^2}(\alpha_2+6\alpha_3+12\alpha_4)+ \\ +\frac{g^3}{a^3}(\alpha_3+4\alpha_4)\Big]\,,$$
$$p_\phi = \frac{m^2 M_{\rm Pl}^2}{2}\Big[6(\alpha_2+2\alpha_3+2\alpha_4)-\frac{6g}{a}(\alpha_2+3\alpha_3+4\alpha_4)+\frac{g^2}{a^2}(\alpha_2+6\alpha_3+12\alpha_4)\Big]\,. \tag{5.2.30}$$

It is evident that the rich mixture of fluids in the Stueckelberg sector consists of four components, with equations of state $w = -1$, $-2/3$, $-1/3$ and 0. The presence of non-relativistic matter in the Stueckelberg fluid is a novelty of the full model. Indeed, the energy density of this component crucially depends on α_3 and α_4, and therefore it did not appear in the minimal model. This peculiar scenario thus sees the Stueckelberg fluid behaving at early times mainly as dust, making it possible (in principle) to ascribe to the new polarizations of the massive graviton a partial contribution to the Dark Matter content. At very late times, on the other hand, the Stueckelberg fluid eventually dominates the energy budget of the universe in the form of a cosmological constant with value

$$\Lambda = -3m^2(\alpha_2+2\alpha_3+2\alpha_4)\,. \tag{5.2.31}$$

Contrary to what happened in the minimal model, there exists now a choice of parameters for which Λ is positive. It is indeed sufficient to choose

$$\alpha_3 < \alpha_4 + \frac{\alpha_2}{2}. \tag{5.2.32}$$

Notice that demanding the cosmological constant to be due entirely by the Stueckelbergs fixes m to be proportional to $H_0 \sim 10^{-33}$ eV. Moreover, in the presence of dust and radiation, additional bounds on g can be imposed by requiring the other components of ρ_ϕ not to contribute too much to curvature and to avoid a large $1/a$ density.

As mentioned in the introduction, this class of background solutions was obtained in [58] under the assumption of a spherically symmetric profile for the Stueckelberg fields and the choice of a diagonal reference metric.

Up to now, we have explored the features of viable dynamical dRGT cosmologies at the background level. The next section will address the stability of these solutions against linear perturbations in the absence of extra matter fields[10].

[10]The inclusion of a generic fluid into the description has no impact on the qualitative behaviour of the metric perturbations, as discussed in App. C.2.

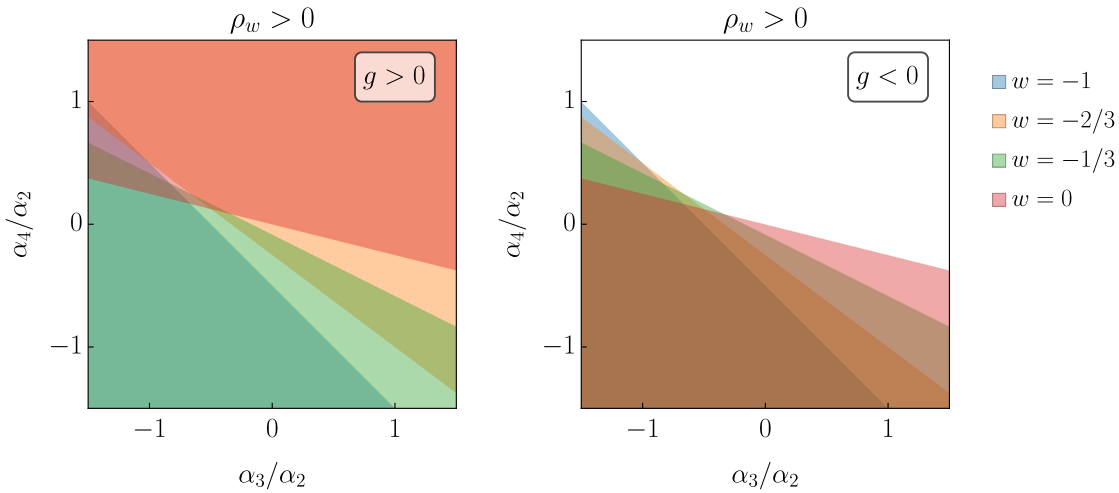

Figure 5.2 Region of parameter space for which each individual ρ_w is positive. For $g > 0$ (left), no combination of parameters ensures the positivity of all the fluid components. On the contrary, when $g < 0$ (right panel), there is a region of parameter space for which positivity of all the energy density components is fulfilled (the trapezoid resulting from the intersection of all the colored regions).

5.3 Perturbations in the Unitary Gauge

We will tackle the perturbative analysis in the unitary gauge, where the Stueckelberg perturbations are set to zero and all the degrees of freedom live inside the metric. To do so we identify the tensor $\Sigma_{\mu\nu} \equiv \partial_\mu \phi^a \partial_\nu \phi^b f_{ab}$ with its background counterpart $\bar{\Sigma}_{\mu\nu}$ and split the physical metric as $g_{\mu\nu} = \bar{g}_{\mu\nu} + h_{\mu\nu}$, where the perturbations $h_{\mu\nu}$ are SVT decomposed and parametrized by

$$h_{00} = A \ , \quad h_{0i} = \hat{B}_i + \partial_i B \ , \quad h_{ij} = C\,\delta_{ij} + \partial_{\langle i}\partial_{j\rangle} E + \partial_{(i}\hat{E}_{j)} + \hat{h}_{ij} \ , \tag{5.3.1}$$

where $\hat{B}_i$ and $\hat{E}_i$ are transverse 3-vectors and $\hat{h}_{ij}$ is a transverse and traceless 3-tensor. Notice that Eq. (5.2.3) translates into the requirements

$$\bar{\Sigma}_{00} = -F^2 \ , \quad \bar{\Sigma}_{0i} = 0 \ , \quad \delta^{ik}\bar{\Sigma}_{kj} = a^2 G^2 \delta^i_j \ . \tag{5.3.2}$$

Writing the inverse metric as $g^{\mu\nu} = \bar{g}^{\mu\nu} + H^{\mu\nu}$, where $H^{\mu\nu} = -\bar{g}^{\mu\alpha} h_{\alpha\beta} \bar{g}^{\beta\nu} + \bar{g}^{\mu\alpha} h_{\alpha\beta} \bar{g}^{\beta\gamma} h_{\gamma\delta} \bar{g}^{\delta\nu} + O(h^3)$, the explicit expression of X^2 is given by

$$
\begin{aligned}
&(X^2)^0_0 = F^2 - F^2 H^{00} \ , \\
&(X^2)^0_i = G^2 a^2 H^{0j} \delta_{ij} = G^2 h_{0i} \ , \\
&(X^2)^i_0 = -F^2 H^{i0} \ , \\
&(X^2)^i_j = G^2 \delta^i_j + G^2 a^2 H^{ik} \delta_{kj} = G^2 \delta^i_j - \frac{G^2}{a^2} \delta^{ik} h_{kj} \ .
\end{aligned}
$$

To construct the square root tensor we parametrize its components as

$$
X^\mu_\nu = \begin{bmatrix} \Omega & G_j \\ H^i & K^i_j \end{bmatrix} \ .
$$

Taking the square, we arrive at the system of equations

$$
\begin{cases}
\Omega^2 + G_j H^j = (X^2)^0_0 \\
G_j (\delta^j_i \Omega + K^j_i) = (X^2)^0_i \\
(\delta^i_j \Omega + K^i_j) H^j = (X^2)^i_0 \\
H^i G_j + K^i_k K^k_j = (X^2)^i_j
\end{cases} \ , \tag{5.3.3}
$$

whose solution is

$$
\begin{aligned}
&\Omega = F \left[1 + \frac{h_{00}}{2} + \frac{3}{8} h_{00}^2 - \frac{F(F+2G)}{2(F+G)^2} \bar{g}^{ij} h_{0i} h_{0j} \right] \ , \\
&G_i = \frac{G^2}{F+G} h_{0i} \ , \quad H^i = -\frac{F^2}{F+G} \bar{g}^{ij} h_{j0} \ , \\
&K^i_j = G \left[\delta^i_j - \frac{1}{2} \bar{g}^{ik} h_{kj} + \frac{3}{8} \bar{g}^{ik} \bar{g}^{mn} h_{km} h_{nj} - \frac{G(G+2F)}{2(F+G)^2} \bar{g}^{ik} h_{k0} h_{0j} \right] \ .
\end{aligned} \tag{5.3.4}
$$

Plugging the above expression inside (5.2.1) yields the quadratic Lagrangian for the perturbations

$$
\mathcal{L}^{(2)} = \mathcal{L}^{(2)}_{\rm S} + \mathcal{L}^{(2)}_{\rm V} + \mathcal{L}^{(2)}_{\rm T} \ , \tag{5.3.5}
$$

where we have distinguished the quadratic Lagrangians of the scalar (S), vector (V) and tensor (T) degrees of freedom. We now focus on each individual Lagrangian and study the stability of the perturbations on the Λ and Mixed branches. Notice that one might be tempted to argue that X^μ_ν depends non-analytically on the metric perturbations on the

Mixed-Branch, since the pull-back of the field-space metric f_{ab} is degenerate on that background, and hence that perturbations are strongly-coupled on that background. However, Eq. (5.3.4) shows that the components of X^μ_ν are analytic functions of the metric perturbations even on the Mixed Branch. As a consequence, a perturbative analysis is necessary in order to unveil potential pathologies of this background solution.

5.3.1 Tensors

The tensor Lagrangian is

$$\mathcal{L}^{(2)}_{\rm T} = \frac{1}{4a}\left[\dot{\hat{h}}^2_{ij} - \frac{1}{a^2}(\partial_k \hat{h}_{ij})^2 - 2(2H^2+\dot{H})\hat{h}^2_{ij} - 2m^2_{\hat{h}}\hat{h}^2_{ij}\right] \ , \tag{5.3.6}$$

where we have defined the background-dependent mass

$$\begin{aligned} m^2_{\hat{h}} = \frac{m^2}{4}\Big\{&\alpha_2\left[3F(G-2)+G^2-9G+12\right] - 3\alpha_3\left[F\left(G^2-6G+6\right)-2G^2+9G-8\right] - \\ &- 12\alpha_4(F-1)\left(G^2-3G+2\right)\Big\} \ , \end{aligned} \tag{5.3.7}$$

and contractions of spatial indexes are done with the Kronecker delta. To make sure the backgrounds are healthy we shall ask the perturbations to be free from ghost and gradient instabilities. The absence of such pathologies is evident from the kinetic term in Eq. (5.3.6). Therefore, we do not obtain any constraint on the background quantities from tensor perturbations.

5.3.2 Vectors

In the case of vector modes, the requirement of having healthy perturbations puts strong constraints on the background as we are going to show. The vector Lagrangian is given by

$$\begin{aligned} \mathcal{L}^{(2)}_{\rm V} = &\frac{1}{8a}\left[(\partial_k\dot{\hat{E}}_j)^2 - 2(2H^2+\dot{H})(\partial_k\hat{E}_j)^2 - 4m^2_{\hat{E}_i}(\partial_k\hat{E}_i)^2\right] + \\ &+\frac{1}{2a}(\partial_k\hat{B}_i)^2 + 3aH^2\hat{B}^2_i - \frac{1}{2}am^2_{\hat{B}_i}\hat{B}^2_i + \frac{1}{2a}\left(2H\partial_k\hat{B}_j\partial_k\hat{E}_j - \partial_k\hat{B}_j\partial_k\dot{\hat{E}}_j\right) \ , \end{aligned} \tag{5.3.8}$$

with

$$
\begin{aligned}
m^2_{\hat{B}_i} &= -\frac{m^2}{F+G}\Big\{\alpha_2\left[3F\left(G^2-3G+2\right)+G\left(G^2-6G+6\right)\right]-3\alpha_3(G-1)\big[F\left(G^2-5G+4\right)\\
&\quad -2(G-2)G\big]-12\alpha_4(G-1)^2[F(G-1)-G]\Big\}\ ,\\
m^2_{\hat{E}_i} &= \frac{m^2_{\hat{h}}}{2}\ .
\end{aligned}
\tag{5.3.9}
$$

Notice that $\hat{B}_i$ has no time kinetic term and therefore represents a constrained variable, that can be integrated out in terms of $\hat{E}_i$. Going to Fourier space, the equation of motion for $\hat{B}_i$ gives

$$
\hat{B}_i = -\frac{k^2/a^2\left(2\hat{E}_i H-\dot{\hat{E}}_i\right)}{2\left(6H^2-m^2_{\hat{B}_i}+k^2/a^2\right)}\ . \tag{5.3.10}
$$

By substituting this solution back into Eq. (5.3.8), we obtain the quadratic Lagrangian of the dynamical vector:

$$
\mathcal{L}^{(2)}_{\hat{E}_i} = K^2_{\hat{E}_i}\dot{\hat{E}}^2_i - Q^2_{\hat{E}_i}\hat{E}^2_i\ , \tag{5.3.11}
$$

where we have defined

$$
\begin{aligned}
K^2_{\hat{E}_i} &\equiv -\frac{k^2}{2a^2}\frac{a\dot{H}}{k^2/a^2-4\dot{H}}\ ,\\
M^2_{\hat{E}_i} &\equiv 2m^2_{E_i}a^2(k^2/a^2-4\dot{H})-4a^2\dot{H}\big(\dot{H}+2H^2\big)+k^2\big(\dot{H}+4H^2\big)\ ,\\
Q^2_{\hat{E}_i} &= \frac{k^2}{4a^3(k^2/a^2-4\dot{H})}\left[M^2_{E_i}+k^2\dot{H}-k^2H\frac{\partial_t(a^3(k^2/a^2-4\dot{H}))}{a^3(k^2/a^2-4\dot{H})}\right]\ .
\end{aligned}
\tag{5.3.12}
$$

We will now study the stability of $\hat{E}_i$ for the different backgrounds obtained in Sec. 5.2, the Λ and Mixed Branch.

$\Lambda-$Branch

On the $\Lambda-$Branch background, one has $\dot{H}=0$ and therefore the kinetic term of vectors is switched off ($K^2_{\hat{E}_i}=0$). As a consequence, the vector mode is non-dynamical and, in absence of matter perturbations, its equation of motion leads to $\hat{E}_i=0$. The absence of the vector degree of freedom at the quadratic level is a sign of strong coupling. Therefore we conclude that the Λ-Branch is not a viable background.

Mixed Branch

The Mixed Branch supports the propagation of the vector mode. Indeed, on this background $\dot{H} \neq 0$, which means that the kinetic term of $\hat{E}_i$ is non-zero.

The healthiness requirements of the vector sector are realized, first of all, by the absence of ghost instabilities in the sub-horizon limit. This is achieved if the kinetic term has a positive sign (i.e. $K^2_{E_i} > 0$) when expanded at large k/a. From Eq. (5.3.11) we then obtain $K^2_{E_i} \simeq -a\dot{H}/2$, implying that $\dot{H}$ must be negative. This is a constraint on the parameter space of the theory, and it does not depend on the wave vector k.

Additional constraints come from the absence of gradient instabilities at small scales. In the large-k limit, the vector Lagrangian acquires the form

$$\mathcal{L}^{(2)}_{\hat{E}_i} \simeq -\frac{1}{2}a\dot{H}\left[\dot{\hat{E}}_i^2 - \frac{c_s^2 k^2}{a^2}\hat{E}_i^2 - \tilde{m}^2_{\hat{E}_i}\hat{E}_i^2\right] , \tag{5.3.13}$$

where we defined the speed of sound c_s and the mass $\tilde{m}_{\hat{E}_i}$ as

$$c_s^2 \equiv -\frac{2m^2_{E_i} + 3H^2 + 2\dot{H}}{2\dot{H}} , \quad \tilde{m}^2_{\hat{E}_i} \equiv -\frac{2}{\dot{H}}(3H^2\dot{H} + \dot{H}^2 + H\ddot{H}) . \tag{5.3.14}$$

Since at small scales the k^2 will dominate over the mass, the absence of gradient instabilities implies the constraint $c_s^2 > 0$, which translates into

$$\frac{2m^2_{E_i} + 3H^2 + 2\dot{H}}{2\dot{H}} < 0 . \tag{5.3.15}$$

5.3.3 Scalars

The Lagrangian of the scalar sector is given by

$$\begin{aligned}
\mathcal{L}^{(2)}_{\mathrm{S}} = &\frac{1}{6a}\left[(\nabla^2\dot{E})^2 + \frac{1}{3a^2}(\partial_i\nabla^2 E)^2 - \left(4H^2 + 2\dot{H} + 3m_E^2\right)(\nabla^2 E)^2\right] - \\
&- \frac{a^3}{4}\left(9H^2 + 2m_A^2\right)A^2 + \frac{a}{2}\left(6H^2 - m_B^2\right)(\partial_i B)^2 - \\
&- \frac{3}{2a}\left[\dot{C}^2 - \frac{1}{3a^2}(\partial_i C)^2 + \frac{1}{2}(H^2 + 2\dot{H} + \frac{2}{3}m_C^2)C^2\right] - \\
&- 2Ha\ \partial_k A\partial_k B + \frac{1}{2a}\left[a^2(3H^2 - 2m^2_{AC})AC - 6a^2H\dot{C}A - 2\partial_k A\partial_k C\right] + \\
&- \frac{1}{3a}\nabla^2 A\nabla^2 E + \frac{2}{a}\left(\dot{C}\nabla^2 B - 2HC\nabla^2 B\right) - \frac{2}{3a}\left(B\nabla^4\dot{E} - 2HB\nabla^4 E\right) + \frac{1}{3a^3}C\nabla^4 E ,
\end{aligned} \tag{5.3.16}$$

where

$$
\begin{aligned}
m_E^2 &= \frac{2}{3} m_{\hat{h}}^2 \ , \quad m_B^2 = m_{B_i}^2 \ , \\
m_C^2 &= \frac{3m^2}{4}\Big\{\alpha_2\left(3F + G^2 - 6\right) - 3\alpha_3\left[F\left(G^2-3\right) - 2G^2 + 4\right] - 12\alpha_4(F-1)\left(G^2-1\right)\Big\} \ , \\
m_A^2 &= -\frac{3}{4}m^2(G-1)\Big[2\alpha_2 + 4\left(\alpha_3+\alpha_4\right) + \left(\alpha_3 + 4\alpha_4\right)G^2 - \left(\alpha_2 + 5\alpha_3 + 8\alpha_4\right)G\Big] = -\frac{3}{2}H^2 \ , \\
m_{AC}^2 &= \frac{3}{2}m^2\left(6\left(\alpha_2 + 2\alpha_3 + 2\alpha_4\right) + \left(\alpha_2 + 6\alpha_3 + 12\alpha_4\right)G^2 - 6\left(\alpha_2 + 3\alpha_3 + 4\alpha_4\right)G\right) \ .
\end{aligned}
\tag{5.3.17}
$$

In dRGT massive gravity, one expects only one scalar degree of freedom. Consistently, we find that the variables A, B, and C are indeed non-dynamical and can be integrated out in terms of E. Let us see this explicitly. Going to Fourier space and integrating out both B_k and A_k (they appear without time derivatives in the Lagrangian) we obtain the solutions

$$
\begin{aligned}
B_k &= \frac{k^2(3C_k + k^2E_k) + 3k^2a^2H(2E_kH - \dot{E}_k) - 9a^2\dot{H}C_k}{6a^2H(3a^2\dot{H} - k^2)} \ , \\
A_k &= \frac{H[k^4\dot{E}_k + 3\dot{C}_k(k^2 - 3a^2\dot{H})] - (2H^2 + \dot{H})[k^4E_k + 3C_k(k^2 - 3a^2\dot{H})]}{3a^2H^2(3a^2\dot{H} - k^2)} \ .
\end{aligned}
\tag{5.3.18}
$$

After replacing them inside the Lagrangian we get

$$
\mathcal{L}^{(2)}_{C,E} = K_E^2\dot{E}^2 - Q_E^2E^2 - \tilde{Q}_C^2C^2 \ . \tag{5.3.19}
$$

where

$$
\begin{aligned}
K_E^2 &\equiv -\frac{k^4\dot{H}}{2a(k^2/a^2 - 3\dot{H})} \ , \\
M_E^2 &\equiv 12a^4H^4(2k^2/a^2 - 3\dot{H}) + 3a^4H^2\left(3\dot{H}k^2/a^2 - 9m_E^2a\dot{H} - 6\dot{H}^2 + 3am_E^2k^2/a^2 + k^4/a^4\right) + k^4\dot{H} \ , \\
Q_E^2 &\equiv \frac{k^4/a^4}{18aH^2(k^2/a^2 - 3\dot{H})}\left[M_E^2 + H\partial_t(k^2(k^2 + 6a^2H^2)) - \frac{k^2\left(6a^2H^2 + k^2\right)}{a^3(k^2 - 3a^2\dot{H})}\partial_t(a^3H(k^2 - 3a^2\dot{H}))\right] \ .
\end{aligned}
\tag{5.3.20}
$$

We do not write the explicit expression for Q_C^2 since it is not needed in the following. Although not explicit initially, the Lagrangian (5.3.19) makes it clear that the variable C is also not propagating. Therefore, the only dynamical scalar is E, whilst C can be set to zero in the absence of matter sources. The absence of ghost instabilities is achieved by the positivity of the kinetic term K_E^2. Following the same reasoning as for vector modes, using Eq. (5.3.20) we obtain that for large k/a this imposes $\dot{H} < 0$.

Next, we are going to impose the absence of gradient instabilities in the two Branches.

Λ-Branch

Notice that $K_E^2 \propto \dot{H}$. This means that on the Λ-Branch, the kinetic term of the scalar mode is shut down, yielding a Lagrangian of the form

$$\mathcal{L}_{C,E}^{\Lambda-\text{Branch}} = -Q_E^2 E^2 - \tilde{Q}_C^2 C^2 \ . \tag{5.3.21}$$

As a consequence, we face the same problem that plagued the vector sector: strong coupling inhibits the propagation of the scalar mode at the linear level.

Mixed Branch

On the Mixed Branch, on the other hand, the kinetic term is nonzero and, in the large-k limit, the Lagrangian of the scalar degree of freedom becomes

$$\mathcal{L}_E^{(2)} \simeq -\frac{k^2}{2} a\dot{H} \left[\dot{E}^2 - \left(\frac{c_s^2}{a^2} k^2 + \tilde{m}_E^2 \right) E^2 \right] \ , \tag{5.3.22}$$

where we have defined

$$c_s^2 \equiv -\frac{3m_E^2 aH + 6H^3 + 7\dot{H}H + \ddot{H}}{3H\dot{H}} \ , \quad \tilde{m}_E^2 \equiv -\frac{6H^3\dot{H} + 7H\dot{H}^2 + 2H^2\ddot{H} + 2\dot{H}\ddot{H}}{H\dot{H}} \ . \tag{5.3.23}$$

Along the same lines as the previous discussion, the absence of gradient instabilities on sub-horizon scales is achieved by the requirement:

$$\frac{3m_E^2 aH + 6H^3 + 7\dot{H}H + \ddot{H}}{3H\dot{H}} < 0 \ . \tag{5.3.24}$$

Noticeably, however, on the Mixed Branch background, the above inequality is exactly saturated, with the LHS exactly zero. As a consequence, the scalar mode has zero speed of sound on sub-horizon scales. Moreover, once interactions are included, an effective speed of propagation will be generated, signalling the presence of strong coupling, as discussed in [57]. In conclusion, also the Mixed Branch becomes untenable due to the strong coupling of perturbations.

5.4 Discussion and future directions

This work extended the approach proposed in [58,65] for the classification of the admissible flat FLRW cosmologies of dRGT massive gravity. Instead of specifying a particular ansatz

for the profiles of the Stueckelberg fields and for the reference metric, FLRW symmetries are directly imposed at the level of the building block X^μ_ν of the theory. As a consequence, the Stueckelberg sector effectively behaves as a perfect fluid whose energy density and pressure only depend on two homogeneous functions F and G. The symmetry requirements imposed on X^μ_ν result in a set of consistency constraints for the Stueckelberg and the reference metric. Remarkably, the Stueckelberg fields need to be inhomogeneous and/or anisotropic to satisfy these consistency constraints and sustain a dynamical flat FLRW background.

Assuming there exists at least a choice of f_{ab} (and an associated choice of ϕ^a) which satisfies these symmetry conditions, different possible cosmological scenarios do emerge:

1. The self-accelerating background solution, in which the Stueckelberg sector behaves as a CC, and for which we did not provide a simple configuration of ϕ^a when the reference metric is chosen to be Minkowski.

2. A scenario (derived under the assumption of $f_{ab} = \eta_{ab}$) in which the Stueckelberg sector behaves as a mixture of perfect fluids, for which an example of a viable choice of ϕ^a is provided in [58].

We also studied the behaviour of linear perturbations on top of these backgrounds, both in the presence and in the absence of matter. On the self-accelerated solution, the scalar and vector modes are strongly coupled, and only the tensor degrees of freedom propagate. The other background solution can accommodate propagation of the vector modes, while the scalar modes do not propagate on small scales (their speed of sound vanishes in the large-k limit), signalling again strong coupling. Including matter into the description does not make any qualitative change, as all the metric perturbations will exhibit the very same behaviour.

Future work will address the possibility of extending the methodology presented in this paper, obtaining novel solutions by imposing the FLRW symmetries directly at the level of the Stueckelberg stress-energy tensor rather than on X^μ_ν. Unveiling novel cosmological solutions, these approaches may lead to interesting implications for dark energy, large-scale structure and cosmic tensions.

Chapter 6

Conclusions

A central aim of this work has been to explore how the logic of positivity bounds, so powerful in Lorentz-invariant quantum field theories, can be extended to regimes where Lorentz invariance is spontaneously broken. Such situations are ubiquitous: they arise in finite-density states of quantum field theory, in cosmological backgrounds, and in condensed matter systems. The breaking of boost invariance modifies the analytic structure of scattering amplitudes, challenging the direct applicability of standard dispersion-relation arguments.

The first step in this program was to examine the fate of the S-matrix in a concrete, fully UV-complete setting: the complex $\lambda|\Phi|^4$ model in a state of finite charge density. This model spontaneously breaks Lorentz invariance while retaining a well-defined S-matrix at all energies, making it an ideal theoretical laboratory for probing general principles. An explicit computation of the Goldstone scattering amplitude revealed that, unlike in the Lorentz-invariant case, the relation between the S-matrix and correlation functions acquires non-analyticities directly traceable to the breaking of boosts. These non-analytic features obstruct the straightforward derivation of positivity bounds from amplitudes in the familiar relativistic manner. An alternative approach presents itself in light of these findings: replacing amplitudes with alternative UV–IR observables, such as conserved-current correlators [66]. Such an approach may hold promise for recovering robust, model-independent constraints in Lorentz-violating effective field theories.

Motivated by the limitations of amplitude-based approaches, the focus shifts to observables whose analyticity properties remain transparent even when Lorentz symmetry is nonlinearly realized: retarded correlation functions. The central objects of interest

were the Fourier transforms of a retarded, microcausal Green function $G(\omega, k)$ and of $F(\omega, k) \equiv \omega\, G(\omega, k)$. Microcausality and retardedness identify their primitive domain of analyticity as the forward tube

$$\mathcal{T}_+ \;=\; \mathbb{R}^{d+1} + i\,\{\,|\omega_I| > |\vec{k}_I|\,\}\,.$$

Within this domain, the input of positivity (specifically, the positivity of $\operatorname{Im} G$ for positive real frequencies) combined with a mild high-energy falloff of $G(\omega, k)$, allowed us to prove that $\operatorname{Im} F$ is strictly positive throughout the primitive domain of analyticity. This was established first under rotational invariance and subsequently in the fully anisotropic case, thereby showing that F is a Herglotz–Nevanlinna function in a wide class of Lorentz-violating systems. This property guarantees the absence of zeros of F within the tube $\mathcal{T}_+$ and, consequently, that $1/F(\omega, k)$ is analytic in the same domain.

The implications of this result are broad. For example, in electromagnetism, where G is related to the photon propagator via $G_J^{\mu\nu} = ((\Pi + g^2\Delta)^{-1})^{\mu\nu}$, analyticity of F implies that the self-energy tensor $\Pi^{\mu\nu}$ itself is analytic in $\mathcal{T}_+$, even when it does not admit a local-operator representation. This analyticity could, in principle, enable the derivation of dispersion relations for the polarization functions $\pi_{L,T}(\omega, \vec{k})$ and extend the recent results of [74], where analyticity of $\Pi^{\mu\nu}$ was only established along specific slices of the tube domain.

A further nontrivial result concerns the support of the imaginary part of the Green function. By assuming that $\tilde{F}(z_1, z_2)$ vanishes at complex infinity and satisfies an unsubtracted double dispersion relation, we proved that $\operatorname{Im} G$ cannot have compact support in real frequency–momentum space. Physically, this means that dissipation in any causal, unitary, and local theory cannot be confined to a strictly finite frequency–momentum range. These results show that the core logic of dispersion relations and positivity, though traditionally tied to scattering amplitudes, can be successfully transplanted to response functions, substantially enlarging their domain of applicability to Lorentz-violating EFTs.

As a complementary line of investigation, we applied symmetry-based methods to the classification of flat FLRW cosmologies in dRGT massive gravity. Building on [58, 65], we imposed FLRW symmetries directly on the fundamental building block $X^\mu{}_\nu$, rather than on a specific ansatz for the Stueckelberg fields and reference metric. This construction leads to a Stueckelberg sector behaving as a perfect fluid, with energy density and pressure determined by two homogeneous functions. The symmetry constraints translate into nontrivial consistency conditions, typically requiring inhomogeneous and/or anisotropic Stueckelberg

configurations to sustain a dynamical flat FLRW background.

Two distinct classes of solutions were identified. The first is a self-accelerating branch in which the Stueckelberg sector mimics a cosmological constant; on this branch, scalar and vector perturbations are strongly coupled, leaving only the tensor modes as propagating degrees of freedom. The second branch, obtained for a Minkowski reference metric, supports propagating vector modes but exhibits a vanishing scalar sound speed in the high-momentum limit, again signaling strong coupling in the scalar sector. Including matter sources does not qualitatively change these conclusions. Beyond refining the classification of viable FLRW solutions in dRGT, this framework demonstrates the utility of imposing symmetry requirements directly on the building blocks of the theory. Future extensions could apply the same logic to the Stueckelberg stress-energy tensor itself, potentially uncovering new, observationally distinct cosmological backgrounds. Moreover, relaxing the exact FLRW requirement and allowing for controlled inhomogeneities could open further possibilities, particularly for exploring backreaction effects.

Looking ahead, several promising directions emerge. On the amplitude side, it would be valuable to determine whether approaches such as the weak-breaking limit or current–correlator techniques can lead to well-defined positivity constraints in a controlled manner, even in the presence of Lorentz-violations. On the correlator side, extending the present analysis beyond linear response is a natural and important goal: higher-point functions also encode rich dynamical information, and it is crucial to determine how microcausality and positivity constrain nonlinear response. In addition, the Herglotz–Nevanlinna representation in multiple variables is far more restrictive than in one dimension, as the associated measure must satisfy nontrivial integral constraints. In one dimension, essentially any suitably integrable real function (or tempered distribution) can serve as the imaginary part of a Herglotz function; in higher dimensions, this is no longer true, and the allowed imaginary parts must obey consistency conditions such as those in eq. (4.2.12). Understanding the physical implications of these multidimensional constraints may enable to identify the most general admissible structure for the imaginary part, and ultimately to formulate an analogue of the Källén–Lehmann representation for the response functions of generic media. Finally, in the massive gravity context, extending the classification framework to alternative symmetry requirements, or to mildly inhomogeneous spacetimes, may yield novel solution branches with distinctive phenomenology, further enriching the interplay between symmetry, analyticity, and ultraviolet consistency in effective field theory.

Appendix A

A.1 Second derivation of LSZ

In this appendix we derive the LSZ reduction formula starting from the expression of creation/annihilation operators. The final formula will be different from Eq. (3.2.1), before going on-shell, although it gives of course the same S-matrix. The conclusion about the lack of analyticity will remain the same.

We need to write the creation/annihilation operators in terms of the fields and their time derivative. These are given at $t = 0$ by

$$\begin{aligned} \int \mathrm{d}^3\boldsymbol{x}\, e^{-i\boldsymbol{k}\cdot\boldsymbol{x}}\phi^a(0,\boldsymbol{x}) &= \sum_{l=\pm} \frac{Z_l^a a_l + \bar{Z}_l^a a_l^\dagger}{2E_l}\,, \\ \int \mathrm{d}^3\boldsymbol{x}\, e^{-i\boldsymbol{k}\cdot\boldsymbol{x}}\dot{\phi}^a(0,\boldsymbol{x}) &= \sum_{l=\pm} -i\frac{Z_l^a a_l - \bar{Z}_l^a a_l^\dagger}{2}\,, \end{aligned} \tag{A.1.1}$$

where $a \in \{h, \pi\}$. We define

$$Y_l^a \equiv \frac{Z_l^a}{2E_l}\,, \quad X_l^a \equiv -\frac{i}{2}Z_l^a\,. \tag{A.1.2}$$

Multiplying the first and second expression of (A.1.1) respectively by $\bar{Y}^{-1}$ and $\bar{X}^{-1}$ we get

$$\begin{aligned} \int \mathrm{d}^3\boldsymbol{x}\; e^{-i\boldsymbol{k}\cdot\boldsymbol{x}}(\bar{Y}^{-1})_a^m\phi^a(0,\boldsymbol{x}) &= a_m^\dagger + \sum_{l=\pm}(\bar{Y}^{-1})_a^m Y_l^a a_l\,, \\ \int \mathrm{d}^3\boldsymbol{x}\; e^{-i\boldsymbol{k}\cdot\boldsymbol{x}}(\bar{X}^{-1})_a^m\dot{\phi}^a(0,\boldsymbol{x}) &= a_m^\dagger + \sum_{l=\pm}(\bar{X}^{-1})_a^m X_l^a a_l\,. \end{aligned} \tag{A.1.3}$$

Subtracting the two expressions we arrive at

$$\begin{aligned}\sum_{l=\pm} D_l^m a_l(\boldsymbol{k}) &= \int \mathrm{d}^3\boldsymbol{x}\; e^{-i\boldsymbol{k}\cdot\boldsymbol{x}}(\bar{Y}^{-1})_a^m \phi^a(0,\boldsymbol{x}) - \int \mathrm{d}^3\boldsymbol{x}\; e^{-i\boldsymbol{k}\cdot\boldsymbol{x}}(\bar{X}^{-1})_a^m \dot{\phi}^a(0,\boldsymbol{x})\,,\\ \sum_{l=\pm} \bar{D}_l^m a_l^\dagger(\boldsymbol{k}) &= \int \mathrm{d}^3\boldsymbol{x}\; e^{i\boldsymbol{k}\cdot\boldsymbol{x}}(Y^{-1})_a^m \phi^a(0,\boldsymbol{x}) - \int \mathrm{d}^3\boldsymbol{x}\; e^{i\boldsymbol{k}\cdot\boldsymbol{x}}(X^{-1})_a^m \dot{\phi}^a(0,\boldsymbol{x})\,,\end{aligned} \tag{A.1.4}$$

where

$$D_l^m = (\bar{Y}^{-1})_a^m Y_l^a - (\bar{X}^{-1})_a^m X_l^a\,. \tag{A.1.5}$$

Finally we have the expression of creation/annihilation operators we were after (reintroducing the time dependence):

$$\begin{aligned}a_l &= F_a^l \int \mathrm{d}^3\boldsymbol{x}\; e^{iE_l(\boldsymbol{k})t - i\boldsymbol{k}\cdot\boldsymbol{x}}\phi^a - G_a^l \int \mathrm{d}^3\boldsymbol{x}\; e^{iE_l(\boldsymbol{k})t - i\boldsymbol{k}\cdot\boldsymbol{x}}\dot{\phi}^a\,,\\ a_l^\dagger &= \bar{F}_a^l \int \mathrm{d}^3\boldsymbol{x}\; e^{-iE_l(\boldsymbol{k})t + i\boldsymbol{k}\cdot\boldsymbol{x}}\phi^a - \bar{G}_a^l \int \mathrm{d}^3\boldsymbol{x}\; e^{-iE_l(\boldsymbol{k})t + i\boldsymbol{k}\cdot\boldsymbol{x}}\dot{\phi}^a\,,\end{aligned} \tag{A.1.6}$$

with

$$F_a^l = (D^{-1})_m^l (\bar{Y}^{-1})_a^m\,, \quad G_a^l = (D^{-1})_m^l (\bar{X}^{-1})_a^m\,. \tag{A.1.7}$$

Notice that creation/annihilation operators are written as a linear combination of the two fields (and their derivative), while in the discussion in the main text we were using a single field to interpolate the asymptotic states.

We can now perform the LSZ reduction:

$$\begin{aligned}&\langle q_2, p_2|p_1, q_1\rangle = \langle q_2, p_2|a_{-,\mathrm{in}}^\dagger(\boldsymbol{q}_1)|p_1\rangle = \langle q_2, p_2|(a_{-,\mathrm{in}}^\dagger(\boldsymbol{q}_1) - a_{-,\mathrm{out}}^\dagger(\boldsymbol{q}_1))|p_1\rangle\\ &= -\left(\lim_{x^0\to+\infty} - \lim_{x^0\to-\infty}\right)\int \mathrm{d}^3\boldsymbol{x}\; e^{-iE_-(\boldsymbol{q}_1)t + i\boldsymbol{q}_1\cdot\boldsymbol{x}}\langle \bar{F}_a^- \phi^a - \bar{G}_a^- \dot{\phi}^a\rangle\\ &= -\int \mathrm{d}x^0\; \partial_0 \int \mathrm{d}^3\boldsymbol{x}\; e^{-iE_-(\boldsymbol{q}_1)t + i\boldsymbol{q}_1\cdot\boldsymbol{x}}\langle \bar{F}_a^- \phi^a - \bar{G}_a^- \dot{\phi}^a\rangle\\ &= -\int \mathrm{d}^4x\; e^{-iE_-(\boldsymbol{q}_1)t + i\boldsymbol{q}_1\cdot\boldsymbol{x}}(-iE_-(\boldsymbol{q}_1)\bar{F}_a^- + iE_-(\boldsymbol{q}_1)\bar{G}_a^-\partial_0 + \bar{F}_a^-\partial_0 - \bar{G}_a^-\partial_0^2)\langle\phi^a\rangle\\ &= \int \mathrm{d}^4x\; e^{-iq_{1,-}\cdot x}\mathcal{D}_a^-\langle q_2, p_2|\phi^a|p_1\rangle\,.\end{aligned} \tag{A.1.8}$$

The differential operator $\mathcal{D}_a^-$ achieves the LSZ reduction on each leg. Let us look at its expression in Fourier space:

$$\mathcal{D}_a^- = \frac{(\omega - E_-)(E_-^2 - \boldsymbol{k}^2 - M^2)}{(\boldsymbol{k}^2 + M^2)(E_+^2 - E_-^2)\bar{Z}_-^\pi}\left[i(\boldsymbol{k}^2\omega + M^2\omega + E_-E_+^2)\,,\quad (v/\mu^2)(E_+^2 - \boldsymbol{k}^2 - M^2)(\boldsymbol{k}^2 + M^2 + \omega E_-)\right]_a\,. \tag{A.1.9}$$

First of all let us see that this expression reduces to the usual one in the Lorentz invariant limit, $\mu = 0$. In this case,

$$Y_l^a \to \frac{\delta_l^a}{2E_l}\,,\ X_l^a \to \frac{-i}{2}\delta_l^a\,,\ D_m^l \to 2\delta_m^l\,,\ F_a^m \to E_m\delta_a^m\,,\ G_a^m \to -i\delta_a^m \tag{A.1.10}$$

so that

$$\mathcal{D}_a^- \to i\delta_a^-(E_-^2 + \partial_0^2)\,. \tag{A.1.11}$$

This can be easily read from Eq. (A.1.9). Indeed, switching off the breaking implies the following limits on the dispersion relations:

$$E_+^2 \to \boldsymbol{k}^2 + M^2\,, \quad E_-^2 \to \boldsymbol{k}^2\,, \tag{A.1.12}$$

so that

$$\mathcal{D}_a^- \to (-\omega + E_-)\left[i(\omega + E_-)\,,\quad 0\right] = \left[i(E_-^2 - \omega^2)\,,\quad 0\right]_a \tag{A.1.13}$$

which is the same as Eq. (A.1.11).

We now wish to show that this LSZ procedure is equivalent to what was obtained in the main text, Eq. (3.2.1). In terms of the field propagator Δ_{ab} this amounts to proving that

$$\lim_{\omega\to E_-} \mathcal{D}_a^-\Delta_{ba} = \lim_{\omega\to E_-} \frac{(\omega^2 - E_-^2)}{i\bar{Z}_-^\pi}\Delta_{b\pi}\,. \tag{A.1.14}$$

Using the explicit form of the propagator,

$$\Delta_{ab} = \frac{i}{2E_l}\left(\frac{Z_l^a\bar{Z}_l^b}{\omega - E_l} - \frac{\bar{Z}_l^a Z_l^b}{\omega + E_l}\right)\,, \tag{A.1.15}$$

one sees that the RHS of Eq. (A.1.14) yields Z_-^b. It is straightforward to verify that

$$\lim_{\omega\to E_-} \mathcal{D}_a^-\Delta_{\pi a} = Z_-^\pi\,,\ \lim_{\omega\to E_-} \mathcal{D}_a^-\Delta_{ha} = Z_-^h\,. \tag{A.1.16}$$

Notice that the above equality holds only in the on-shell limit $\omega \to E_-$. The two LSZ procedures give different results off-shell and thus define different functions of the complex momenta.

A.2 Feynman rules

In this appendix we explicitly compute the scattering amplitude (3.3.1). The first step is to find the Feynman rules. Let's start with the propagators. As we have seen the quadratic Lagrangian reads

$$\tilde{\mathcal{L}}_{(2)} = \frac{1}{2}\Phi_i(-k)\Pi_{ij}^{(2)}(k)\Phi_j(k)\,, \tag{A.2.1}$$

where we have defined

$$\Phi_h(k) \equiv \tilde{h}_k\,, \quad \Phi_\pi(k) \equiv \tilde{\pi}_k \quad \text{and} \quad \Pi^{(2)}_{ij}(k) \equiv \begin{pmatrix} k^2 & i\mu^2\omega/v \\ -i\mu^2\omega/v & k^2 - M^2 \end{pmatrix}_{ij} . \tag{A.2.2}$$

The propagators then read

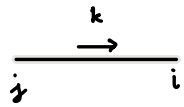

$$\begin{aligned} &= \frac{i}{(\omega^2 - E_+(\boldsymbol{k})^2)(\omega^2 - E_-(\boldsymbol{k})^2)} \begin{pmatrix} k^2 - M^2 & -i\mu^2\omega/v \\ i\mu^2\omega/v & k^2 \end{pmatrix}_{ij} \\ &\equiv \Delta_{ij}(k)\,. \end{aligned} \tag{A.2.3}$$

We can now deal with the interacting Lagrangian. The cubic Lagrangian reads

$$\begin{aligned} \tilde{\mathcal{L}}_{(3)} &= -i\frac{\mu^2}{2v^2}\omega_1\tilde{\pi}_{k_1}\tilde{h}_{k_2}\tilde{h}_{k_3} - \frac{k_1\cdot k_2}{v}\tilde{\pi}_{k_1}\tilde{\pi}_{k_2}\tilde{h}_{k_3} - \lambda v\,\tilde{h}_{k_1}\tilde{h}_{k_2}\tilde{h}_{k_3} \\ &= -i\frac{\mu^2}{6v^2}\left(\omega_1\tilde{\pi}_{k_1}\tilde{h}_{k_2}\tilde{h}_{k_3} + \omega_2\tilde{\pi}_{k_2}\tilde{h}_{k_1}\tilde{h}_{k_3} + \omega_3\tilde{\pi}_{k_3}\tilde{h}_{k_2}\tilde{h}_{k_1}\right) \\ &\quad - \frac{1}{3v}\left(k_1\cdot k_2\tilde{\pi}_{k_1}\tilde{\pi}_{k_2}\tilde{h}_{k_3} + k_1\cdot k_3\tilde{\pi}_{k_3}\tilde{\pi}_{k_1}\tilde{h}_{k_2} + k_3\cdot k_2\tilde{\pi}_{k_3}\tilde{\pi}_{k_2}\tilde{h}_{k_1}\right) \\ &\quad - \lambda v\,\tilde{h}_{k_1}\tilde{h}_{k_2}\tilde{h}_{k_3} \equiv \frac{1}{3!}\Pi^{(3)}_{i_1i_2i_3}(k_1,k_2,k_3)\Phi_{i_1}(k_1)\Phi_{i_2}(k_2)\Phi_{i_3}(k_3)\,. \end{aligned} \tag{A.2.4}$$

Written explicitly the tensor $\Pi^{(3)}_{i_1i_2i_3}(k_1,k_2,k_3)$ reads

$$\begin{aligned} &\frac{1}{3!}\Pi^{(3)}_{i_1i_2i_3}(k_1,k_2,k_3) = -\frac{i\mu^2}{v^2}\frac{\omega_1\delta_{i_1\pi}\delta_{i_2h}\delta_{i_3h} + \omega_2\delta_{i_1h}\delta_{i_2\pi}\delta_{i_3h} + \omega_3\delta_{i_1h}\delta_{i_2h}\delta_{i_3\pi}}{6} \\ &- \frac{k_1\cdot k_2\delta_{i_1\pi}\delta_{i_2\pi}\delta_{i_3h} + k_1\cdot k_3\delta_{i_1\pi}\delta_{i_2h}\delta_{i_3\pi} + k_2\cdot k_3\delta_{i_1h}\delta_{i_2\pi}\delta_{i_3\pi}}{3v} - \lambda v\,\delta_{i_1h}\delta_{i_2h}\delta_{i_3h} \\ &= -\delta_{i_3h}\begin{pmatrix} \frac{k_1\cdot k_2}{3v} & \frac{i\omega_2\mu^2}{6v^2} \\ \frac{i\omega_1\mu^2}{6v^2} & \lambda v \end{pmatrix}_{i_1i_2} - \delta_{i_3\pi}\begin{pmatrix} 0 & \frac{k_2\cdot k_3}{3v} \\ \frac{k_1\cdot k_3}{3v} & \frac{i\omega_3\mu^2}{6v^2} \end{pmatrix}_{i_1i_2} . \end{aligned} \tag{A.2.5}$$

The Feynman rule can be schematically written as

Finally we can turn to four point functions. The four-fields Lagrangian is

$$\begin{aligned} \tilde{\mathcal{L}}_{(4)} &= -\frac{k_1\cdot k_2}{2v^2}\tilde{\pi}_{k_1}\tilde{\pi}_{k_2}\tilde{h}_{k_3}\tilde{h}_{k_4} - \frac{\lambda}{4}\tilde{h}_{k_1}\tilde{h}_{k_2}\tilde{h}_{k_3}\tilde{h}_{k_4} \\ &= -\frac{1}{12v^2}\Big(k_1\cdot k_2\tilde{\pi}_{k_1}\tilde{\pi}_{k_2}\tilde{h}_{k_3}\tilde{h}_{k_4} + k_1\cdot k_3\tilde{\pi}_{k_1}\tilde{\pi}_{k_3}\tilde{h}_{k_2}\tilde{h}_{k_4} + k_1\cdot k_4\tilde{\pi}_{k_1}\tilde{\pi}_{k_4}\tilde{h}_{k_3}\tilde{h}_{k_2} \\ &\quad + k_2\cdot k_3\tilde{\pi}_{k_2}\tilde{\pi}_{k_3}\tilde{h}_{k_1}\tilde{h}_{k_4} + k_2\cdot k_4\tilde{\pi}_{k_2}\tilde{\pi}_{k_4}\tilde{h}_{k_1}\tilde{h}_{k_3} + k_3\cdot k_4\tilde{\pi}_{k_3}\tilde{\pi}_{k_4}\tilde{h}_{k_1}\tilde{h}_{k_2}\Big) \\ &\quad - \frac{\lambda}{4}\tilde{h}_{k_1}\tilde{h}_{k_2}\tilde{h}_{k_3}\tilde{h}_{k_4} \equiv \frac{1}{4!}\Pi^{(4)}_{i_1i_2i_3i_4}(k_1,k_2,k_3,k_4)\Phi_{i_1}\Phi_{i_2}\Phi_{i_3}\Phi_{i_4}\,. \end{aligned} \tag{A.2.6}$$

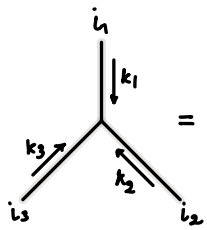

$$= i \, \Pi^{(3)}_{i_1 i_2 i_3}(k_1, k_2, k_3)$$

The Feynman rule reads

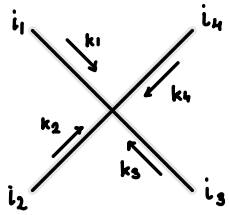

$$= i \, \Pi^{(4)}_{i_1 i_2 i_3 i_4}(k_1, k_2, k_3, k_4)$$

A.2.1 Scattering amplitudes

Four-point

$\mathcal{G}_c = \sum_j$

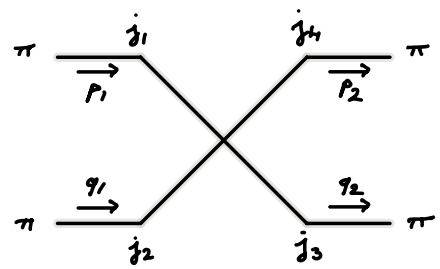

$$
\begin{aligned}
&= \sum_j \Delta_{j_1\pi}(p_1)\Delta_{j_2\pi}(q_1)\Delta_{\pi j_3}(q_2)\Delta_{\pi j_4}(p_2) i\Pi^{(4)}_{j_1,j_2,j_3,j_4}(p_1,q_1,-q_2,-p_2) \\
&= \prod_{i=1}^{2}\left(\frac{iZ^{\pi}_{-}(\boldsymbol{p}_l)}{(p_i^0)^2 - E_-(\boldsymbol{p}_l)^2}\frac{iZ^{\pi}_{-}(\boldsymbol{q}_l)}{(q_i^0)^2 - E_-(\boldsymbol{q}_l)^2}\right) i\mathcal{M}_{\mathrm{c}}\,,
\end{aligned}
\tag{A.2.7}
$$

$$
\begin{aligned}
\mathcal{M}_c = &-\frac{\mu^4}{v^4}\prod_{i=1}^{2}\left(\frac{Z^{\pi}_{-}(\boldsymbol{p}_i)^{-1}}{(p_i^0)^2 - E_+(\boldsymbol{p}_i)^2}\frac{Z^{\pi}_{-}(\boldsymbol{q}_i)^{-1}}{(q_i^0)^2 - E_+(\boldsymbol{q}_i)^2}\right)\Big[6\lambda\mu^4 p_1^0 q_1^0 q_2^0 p_2^0 \\
&- 2p_1\cdot q_1(p_1^2-M^2)(q_1^2-M^2)q_2^0p_2^0 - 2p_1\cdot p_2(p_1^2-M^2)(p_2^2-M^2)q_1^0q_2^0 \\
&- 2p_1\cdot q_2(p_1^2-M^2)(q_2^2-M^2)q_1^0p_2^0 - 2q_1\cdot p_2(q_1^2-M^2)(p_2^2-M^2)p_1^0q_2^0 \\
&- 2q_2\cdot q_1(q_2^2-M^2)(q_1^2-M^2)p_1^0p_2^0 - 2p_2\cdot q_2(q_2^2-M^2)(p_2^2-M^2)p_1^0q_1^0\Big]\,.
\end{aligned}
\tag{A.2.8}
$$

s-channel

$\mathcal{G}_s = \sum_j \sum_l$

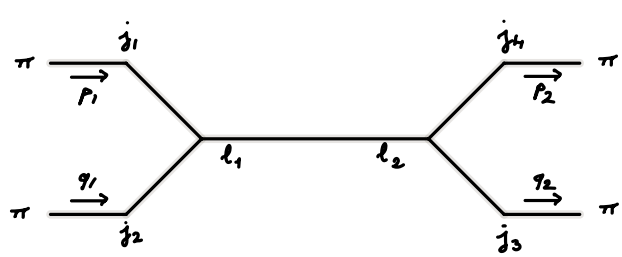

$$
\begin{aligned}
&= \sum_j \sum_l \Delta_{j_1\pi}(p_1)\Delta_{j_2\pi}(q_1) i\Pi^{(3)}_{j_1 j_2 l_1}(p_1, q_1, -p_1 - q_1)\Delta_{l_2 l_1}(p_1 + q_1) \\
&\times \Pi^{(3)}_{l_2 j_3 j_4}(p_1 + q_1, -q_2, -p_2)\Delta_{\pi j_3}(q_2)\Delta_{\pi j_4}(p_2) \\
&= \sum_l \Big[\Delta(-p_1) i\Pi^{(3)}_{l_1}(p_1, q_1, -p_1 - q_1)\Delta(q_1)\Big]_{\pi\pi} \Delta_{l_2 l_1}(p_1 + q_1) \\
&\times \Big[\Delta(p_1) i\Pi^{(3)}_{l_2}(-p_1, -p_2, q_2 + p_2)\Delta(-p_2)\Big]_{\pi\pi} .
\end{aligned}
\tag{A.2.9}
$$

So all together

$$
\begin{aligned}
\mathcal{G}_s = &\Bigg[vA(p_1, q_1)\left\{v(p_1 + q_1)^2 A(p_1, q_1) - \mu^4(p_1^0 + q_1^0)B(q_2, p_2)\right\} \\
&- \left\{v\mu^4 B(p_1, q_1)\right\} \times \left\{(p_1^0 + q_1^0)A(q_2, p_2) + v(M^2 - (p_1 + q_1)^2)B(q_2, p_2)\right\} \Bigg] \\
&\prod_{i=1}^{2} \left(\frac{1}{p_j^2(p_j^2 - M^2) - (\mu^4/v^2)(p_l^0)^2} \frac{1}{q_j^2(q_j^2 - M^2) - (\mu^4/v^2)(q_l^0)^2} \right) \\
&\times \frac{iv^{-10}}{(p_1 + q_1)^2((p_1 + q_1)^2 - M^2) - (\mu^4/v^2)(p_1^0 + q_1^0)^2} ,
\end{aligned}
\tag{A.2.10}
$$

where we have defined

$$
A(p_1, q_1) \equiv 2v^3(M^2 - p_1^2)(M^2 - q_1^2)p_1 \cdot q_1 - v\mu^4 p_1^0 q_1^0 (p_1^2 + q_1^2 + M^2) , \tag{A.2.11}
$$

and

$$
B(p_1, q_1) \equiv \mu^4 (p_1^0)^2 q_1^0 + 2v^2 q_1^0 (M^2 - p_1^2)(p_1^2 + p_1 \cdot q_1) + (p_1 \leftrightarrow q_1) . \tag{A.2.12}
$$

Finally we obtain

$$
\begin{aligned}
\mathcal{M}_s = &\prod_{i=1}^{2} \left(\frac{Z_-^\pi(\boldsymbol{p}_i)^{-1}}{(p_i^0)^2 - E_+(\boldsymbol{p}_i)^2} \frac{Z_-^\pi(\boldsymbol{q}_i)^{-1}}{(q_i^0)^2 - E_+(\boldsymbol{q}_i)^2} \right) \\
&\times \frac{v^{-9}}{(p_1 + q_1)^2((p_1 + q_1)^2 - M^2) - (\mu^4/v^2)(p_1^0 + q_1^0)^2} \\
&\Big[2\lambda v^3 \mu^4 B(p_1, q_1)B(q_2, p_2) + [B(p_1, q_1)A(q_2, p_2) \\
&+ B(q_2, p_2)A(p_1, q_1)]\mu^4(p_1^0 + q_1^0) - v[A(p_1, q_1)A(q_2, p_2) \\
&+ \mu^4 B(p_1, q_1)B(q_2, p_2)](p_1 + q_1)^2 \Big] .
\end{aligned}
\tag{A.2.13}
$$

$\mathcal{G}_t = \sum_j \sum_l$

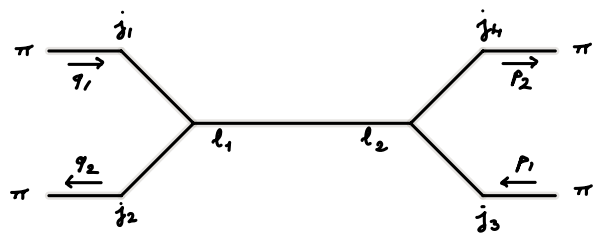

t-channel

$$= \sum_j \sum_l \Delta_{j_1\pi}(q_1)\Delta_{j_2\pi}(-q_2) i\Pi^{(3)}_{j_1 j_2 l_1}(q_1, -q_2, -q_1+q_2)\Delta_{l_2 l_1}(q_1-q_2) \times \Pi^{(3)}_{l_2 j_3 j_4}(q_1-q_2, p_1, -p_2)\Delta_{\pi j_3}(-p_1)\Delta_{\pi j_4}(p_2)\,. \tag{A.2.14}$$

$$\begin{aligned}\mathcal{M}_t = \prod_{i=1}^{2}\left(\frac{Z^{\pi}_{-}(\boldsymbol{p}_i)^{-1}}{(p_i^0)^2 - E_+(\boldsymbol{p}_i)^2}\frac{Z^{\pi}_{-}(\boldsymbol{q}_i)^{-1}}{(q_i^0)^2 - E_+(\boldsymbol{q}_i)^2}\right)\times \\ \frac{v^{-9}}{(q_1-q_2)^2((q_1-q_2)^2 - M^2) - (\mu^4/v^2)(q_1^0-q_2^0)^2} \\ \Big[2\lambda v^3\mu^4 B(q_1,-q_2)B(-p_1,p_2) + [B(q_1,-q_2)A(-p_1,p_2) \\ + B(-p_1,p_2)A(q_1,-q_2)]\mu^4(q_1^0-q_2^0) - v[A(q_1,-q_2)A(-p_1,p_2) \\ + \mu^4 B(q_1,-q_2)B(-p_1,p_2)](q_1-q_2)^2\Big]\,.\end{aligned} \tag{A.2.15}$$

u-channel

$\mathcal{G}_u = \sum_j \sum_l$

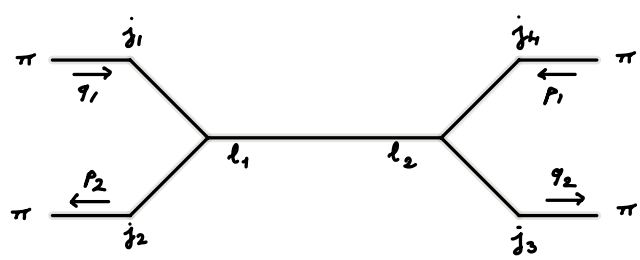

$$= \sum_j \sum_l \Delta_{j_1\pi}(q_1)\Delta_{j_2\pi}(-p_2) i\Pi^{(3)}_{j_1 j_2 l_1}(q_1, -p_2, -q_1+p_2)\Delta_{l_2 l_1}(q_1-p_2) \times \Pi^{(3)}_{l_2 j_3 j_4}(q_1-p_2, -q_2, p_1)\Delta_{\pi j_3}(q_2)\Delta_{\pi j_4}(-p_1)\,. \tag{A.2.16}$$

Thus

$$\begin{aligned}\mathcal{M}_u = \prod_{i=1}^{2}\left(\frac{Z_-^\pi(\boldsymbol{p}_i)^{-1}}{(p_i^0)^2 - E_+(\boldsymbol{p}_i)^2}\frac{Z_-^\pi(\boldsymbol{q}_i)^{-1}}{(q_i^0)^2 - E_+(\boldsymbol{q}_i)^2}\right)\times \\ \frac{v^{-9}}{(q_1-p_2)^2((q_1-p_2)^2 - M^2) - (\mu^4/v^2)(q_1^0 - p_2^0)^2} \\ \Big[2\lambda v^3\mu^4 B(q_1,-p_2)B(q_2,-p_1) + [B(q_1,-p_2)A(q_2,-p_1) \\ + B(q_2,-p_1)A(q_1,-p_2)]\mu^4(q_1^0 - p_2^0) - v[A(q_1,-p_2)A(q_2,-p_1) \\ + \mu^4 B(q_1,-p_2)B(q_2,-p_1)](q_1-p_2)^2\Big]\,.\end{aligned} \tag{A.2.17}$$

A.3 S-matrix in the low-energy EFT

In this appendix, the EFT amplitude for the $\pi\pi \to \pi\pi$ process is reported. Making use of the Feynman rules coming from Lagrangian (3.3.23), the different contributions to the full amplitude can be evaluated:

$$\begin{aligned}\mathcal{M}_c &= \frac{2c_s^4}{\lambda v^4}(p_1\cdot q_1\, p_2\cdot q_2 + q_1\cdot q_2\, p_2\cdot p_1 + p_2\cdot q_1\, p_1\cdot q_2)\,, \\ \mathcal{M}_s &= -\left(\frac{c_s^3\mu^2}{\lambda v^4}\right)^2 \frac{(2(q_1^0+p_1^0)p_1\cdot q_1 + p_1^0 q_1^2 + q_1^0 p_1^2)(2(q_2^0+p_2^0)p_2\cdot q_2 + p_2^0 q_2^2 + q_2^0 p_2^2)}{(q_1^0+p_1^0)^2 - c_s^2(\boldsymbol{q}_1+\boldsymbol{p}_1)^2}\,, \\ \mathcal{M}_t &= -\left(\frac{c_s^3\mu^2}{\lambda v^4}\right)^2 \frac{(-2(q_1^0-q_2^0)q_2\cdot q_1 - q_2^0 q_1^2 + q_1^0 q_2^2)(-2(-p_1+p_2^0)p_2\cdot p_1 + p_2^0 q_2^2 - p_1^0 p_2^2)}{(q_1^0-q_2^0)^2 - c_s^2(\boldsymbol{q}_1-\boldsymbol{q}_2)^2}\,, \\ \mathcal{M}_u &= -\left(\frac{c_s^3\mu^2}{\lambda v^4}\right)^2 \frac{(-2(q_1^0-p_2^0)p_2\cdot q_1 - p_2^0 q_1^2 + q_1^0 p_2^2)(-2(q_2^0-p_1^0)p_1\cdot q_2 - p_1^0 q_2^2 + q_2^0 p_1^2)}{(q_1^0-p_2^0)^2 - c_s^2(\boldsymbol{q}_1-\boldsymbol{p}_2)^2}\,.\end{aligned}$$

Specializing to equal energies $p_1^0 = q_1^0 = p_2^0 = q_2^0 = \omega$ yields a simpler expression for the S-matrix:

$$\begin{aligned}\mathcal{M}_c &= \frac{2c_s^4}{\lambda v^4}(3\alpha^2\omega^4 + \frac{s^2+u^2+t^2}{4} + \alpha\omega^2(s+u+t)) = \frac{c_s^4\alpha}{\mu^4}(-4\alpha^2\omega^4 + s^2+u^2+t^2)\,, \\ \mathcal{M}_s &= -\frac{16c_s^4\alpha^2\omega^2}{\mu^4}\frac{(s+\alpha\omega^2)^2}{s+4\alpha\omega^2}\,,\ \mathcal{M}_u = 0\,,\ \mathcal{M}_t = 0\,.\end{aligned} \tag{A.3.1}$$

A.4 Estimate of the decay width

In this appendix we wish to refine the estimate the decay width $\Gamma(\omega)$ for $\omega \gg M$. To this end, we work directly in the diagonal field basis $\varphi_\pm$ introduced in section 3.2. As we already pointed out there,

$$\varphi_\pm(t,\boldsymbol{x}) \equiv \int \frac{\mathrm{d}^3\boldsymbol{k}}{(2\pi)^3 2E_\pm(\boldsymbol{k})}\left(a_\pm(\boldsymbol{k})e^{-i(E_\pm(\boldsymbol{k})t-\boldsymbol{k}\cdot\boldsymbol{x})}+\text{h.c.}\right) \tag{A.4.1}$$

are the field operators that interpolate only the two states $+$ and $-$ respectively. Recalling Eq. (3.1.15) it is evident that π and h are linear combinations of the $\varphi_\pm$ fields. In particular, the (h,π)-basis is linked to the $\pm$ basis via the following transformation

$$\begin{pmatrix}\tilde{\pi}(k)\\ \tilde{h}(k)\end{pmatrix} = \begin{pmatrix} Z^\pi_-(\boldsymbol{k}) & Z^\pi_+(\boldsymbol{k}) \\ Z^h_-(\boldsymbol{k}) & Z^h_+(\boldsymbol{k})\end{pmatrix}\begin{pmatrix}\tilde{\varphi}_-(k)\\ \tilde{\varphi}_+(k)\end{pmatrix} \equiv \mathcal{U}(\boldsymbol{k})\begin{pmatrix}\tilde{\varphi}_-(k)\\ \tilde{\varphi}_+(k)\end{pmatrix}. \tag{A.4.2}$$

The transformation $\mathcal{U}(\boldsymbol{k})$ that realizes the change of basis is a unitary matrix that diagonalizes the quadratic Lagrangian (3.1.8):

$$\mathcal{L}_{(2)} = \begin{pmatrix}\tilde{\varphi}_-(-k) & \tilde{\varphi}_+(-k)\end{pmatrix}\begin{pmatrix} k^2-\frac{M^2}{2}+\frac{M^2}{2}\sqrt{1+\frac{4\omega^2}{\omega_c^2}} & 0 \\ 0 & k^2-\frac{M^2}{2}-\frac{M^2}{2}\sqrt{1+\frac{4\omega^2}{\omega_c^2}}\end{pmatrix}\begin{pmatrix}\tilde{\varphi}_-(k)\\ \tilde{\varphi}_+(k)\end{pmatrix}. \tag{A.4.3}$$

Making use of the dispersion relations (3.1.12) we can trade the $\boldsymbol{k}^2$-dependence for ω-dependence. For the interpolation functions we obtain

$$Z^\pi_-(\omega) = Z^h_+(\omega) = \frac{\frac{1}{2}+\frac{1}{2}\sqrt{1+4\frac{\omega^2}{\omega_c^2}}}{\sqrt{2\frac{\omega^2}{\omega_c^2}+\frac{1}{2}+\frac{1}{2}\sqrt{1+4\frac{\omega^2}{\omega_c^2}}}}, Z^\pi_+(\omega) = Z^h_-(\omega) = -i\frac{\omega/\omega_c}{\sqrt{2\frac{\omega^2}{\omega_c^2}+\frac{1}{2}+\frac{1}{2}\sqrt{1+4\frac{\omega^2}{\omega_c^2}}}}. \tag{A.4.4}$$

Making use of this change of basis we can now rewrite the full Lagrangian in terms of the diagonal fields $\varphi_\pm$. Thus, if we are interested in the $- \to --$ decay process we can simply focus on the trilinear vertices involving the φ_- fields only. It is important to notice that, in general, the full Lagrangian will be non-local. The energy scale at which this non-locality will become important is $\omega_c \sim \lambda v^3/\mu^2$, introduced in Eq. (3.1.33). If we are interested in a given process at energies $\omega \ll \omega_c$, we can expand the interpolating functions

$$Z^\pi_-(\omega) = Z^h_+(\omega) \sim 1 + \mathcal{O}\left(\frac{\omega^2}{\omega_c^2}\right),\ Z^\pi_+(\omega) = Z^h_-(\omega) \sim -i\frac{\omega}{\omega_c} + \mathcal{O}\left(\frac{\omega^3}{\omega_c^3}\right), \tag{A.4.5}$$

thus obtaining a local Lagrangian. Equivalently, to leading order in derivatives, we can write

$$\pi \sim \varphi_- - i\frac{\dot{\varphi}_+}{\omega_c}\,,\; h \sim \varphi_+ - i\frac{\dot{\varphi}_-}{\omega_c}\,. \tag{A.4.6}$$

Plugging these expressions back into the cubic part of the Lagrangian and focusing on the trilinear vertices involving φ_- only we obtain

$$\frac{(\partial\varphi_-)^2\dot{\varphi}_-}{v\omega_c}\,. \tag{A.4.7}$$

By dimensional analysis we thus obtain

$$\frac{\Gamma}{\omega}(M \ll \omega \ll \omega_c) \sim (1-c_s^{-2})^2\frac{\omega^4}{v^2\omega_c^2} \sim \lambda\left(\frac{\omega}{\omega_c}\right)^4\frac{\lambda\mu^4}{M^4} \ll \lambda\,. \tag{A.4.8}$$

Again we have the same kinematical suppression factor discussed in section 3.4. This is a refinement of the previous overestimate (3.4.9) and has the same functional form as the EFT decay width. We can now turn to the only missing case, namely $\omega \gg \omega_c$. The first idea that comes to mind is to expand the Z's in ω_c/ω,

$$Z_-^\pi(\omega) = Z_+^h(\omega) \sim \frac{1}{\sqrt{2}} + \mathcal{O}\left(\frac{\omega_c}{\omega}\right)\,,\; Z_+^\pi(\omega) = Z_-^h(\omega) \sim -\frac{i}{\sqrt{2}} + \mathcal{O}\left(\frac{\omega_c}{\omega}\right)\,, \tag{A.4.9}$$

to obtain a simplified Lagrangian suitable to compute processes in this regime. Although this looks technically very similar to what has been done just above, in essence it is rather different. In fact the ω_c/ω expansion brings powers of energy to the denominator and as such yields non-local vertices, which are somewhat cumbersome to deal with. For these reasons we choose to work with the unexpanded Lagrangian instead:

$$\begin{aligned}\mathcal{L}_{(3)} \supset \Bigg(&-\frac{i\omega_1\mu^2}{2v^2}Z_-^\pi(\omega_1)Z_-^h(\omega_2)Z_-^h(\omega_3) - \frac{k_1\cdot k_2}{v}Z_-^\pi(\omega_1)Z_-^\pi(\omega_2)Z_-^h(\omega_3)\\ &-\lambda v Z_-^h(\omega_1)Z_-^h(\omega_2)Z_-^h(\omega_3)\Bigg)\tilde{\varphi}_-(k_1)\tilde{\varphi}_-(k_2)\tilde{\varphi}_-(k_3)\,,\end{aligned} \tag{A.4.10}$$

and perform the expansion only at the end. The associated matrix element reads

$$\begin{aligned}\mathcal{M} = -\frac{i\mu^2}{v^2}\Bigg(&\omega_1 Z_-^\pi(\omega_1)Z_-^h(\omega_2)Z_-^h(\omega_3) + \omega_2 Z_-^\pi(\omega_2)Z_-^h(\omega_1)Z_-^h(\omega_3) + \omega_3 Z_-^\pi(\omega_3)Z_-^h(\omega_2)Z_-^h(\omega_1)\Bigg)\\ &-\frac{2}{v}\Bigg(p_1\cdot p_2 Z_-^\pi(\omega_1)Z_-^\pi(\omega_2)Z_-^h(\omega_3) + p_1\cdot p_3 Z_-^\pi(\omega_1)Z_-^\pi(\omega_3)Z_-^h(\omega_2)\\ &+p_3\cdot p_2 Z_-^\pi(\omega_3)Z_-^\pi(\omega_2)Z_-^h(\omega_1)\Bigg) - 6\lambda v\, Z_-^h(\omega_1)Z_-^h(\omega_2)Z_-^h(\omega_3)\,.\end{aligned} \tag{A.4.11}$$

In the high energy limit, using conservation of energy and momentum we find

$$\mathcal{M} = -i\frac{\mu^2}{\sqrt{2}v^2}(\omega_1-\omega_2)+i\frac{\mu^2}{\sqrt{2}v^2}(\omega_1-\omega_2)-i\frac{v\lambda}{\sqrt{2}}-i\frac{3v\lambda}{\sqrt{2}}+\mathcal{O}\left(\frac{\omega_c}{\omega}\right) = -i2\sqrt{2}\lambda v+\mathcal{O}\left(\frac{\omega_c}{\omega}\right) . \tag{A.4.12}$$

By dimensional analysis we thus conclude that the ratio between the interaction time and the decay time for the $- \to --$ process can be estimated to be

$$\frac{\Gamma}{\omega}(\omega \gg \omega_c) \sim \frac{\lambda^2 v^2}{\omega^2} \sim \lambda\frac{M^2}{\omega^2} \ll \lambda\,, \tag{A.4.13}$$

in agreement with the result obtained in the ϕ_1, ϕ_2 field basis, Eq. (3.4.9). This is a further confirmation that the ratio between interaction time and the decay time is always suppressed by λ.

Appendix B

B.1 A crash course on Tempered Distributions

In this appendix, we present a concise overview of the main properties of tempered distributions in both $0+1$ and $d+1$ dimensions, together with a proof of the main theorems discussed in Section 4.1. The treatment will be brief but pedagogical, aimed at equipping the reader with the essential tools needed in the main text. For a more complete and rigorous exposition, we refer to [70, 83].

As mentioned in Section 4.1, tempered distributions are elements of the dual space of Schwarz functions. We therefore begin by briefly recalling the definition and key properties of Schwarz functions.

B.1.1 $S(\mathbb{R}^d)$

The space of Schwarz functions $S(\mathbb{R}^d)$ consists of C^∞ functions that, together with all their derivatives, decay faster than any polynomial at infinity. Explicitly:

$$\phi(x) \in S(\mathbb{R}^d) \text{ if } \phi(x) \in C^\infty \text{ and } \sup_{x\in\mathbb{R}^d} \left| x^\alpha \partial^\beta \phi \right| \equiv C_{\alpha,\beta}(\phi) < \infty \,,\ \forall \alpha, \beta \in \mathbb{N}^d \tag{B.1.1}$$

Here, α and β are multi-indices with non-negative integer entries.

Although we are currently working in Euclidean signature, the discussion can be extended to more general metric signatures. In particular, we will specialize to the $d+1$-dimensional Lorentzian case when discussing distributions in the next subsection. A similar set we will use later is the space of compactly supported C^∞, denoted by $\mathcal{D}(\mathbb{R}^d)$.

It is straightforward to verify that this definition captures the property of rapid decrease

at infinity:

$$\begin{aligned}\lim_{x^k\to\infty}|x^\alpha\partial^\beta\phi| &= \lim_{x^k\to\infty}\frac{|x^\alpha x^k\partial^\beta\phi|}{|x^k|} < \lim_{x^k\to\infty}\frac{\sup_{x\in\mathbb{R}^d}|x^\alpha x^k\partial^\beta\phi|}{|x^k|} = \\ &= \lim_{x^k\to\infty}\frac{C_{\alpha',\beta}(\phi)}{|x^k|} = 0,\ \forall k = 1,\dots,d\end{aligned} \tag{B.1.2}$$

Here k denotes the index of a specific component of $x \in \mathbb{R}^d$, and is not itself a multi-index.

The rapid decay property makes $S(\mathbb{R}^d)$ especially useful: not only is the Fourier transform of any Schwarz function well-defined, but it is again a Schwarz function. This follows from the estimate:

$$\begin{aligned}|F[\phi]| &= \left|\int_{\mathbb{R}^d}\phi(x)e^{ikx}d^dx\right| \le \int_{\mathbb{R}^d}|\phi(x)|d^dx = \int_{\mathbb{R}^d}\frac{|(1+|x|^2)^n\phi(x)|}{(1+|x|^2)^n}d^dx \le \\ &\le \sup_{x\in\mathbb{R}^d}|(1+|x|^2)^n\phi(x)|\int_{\mathbb{R}^d}\frac{1}{(1+|x|^2)^n}d^dx < \infty\end{aligned} \tag{B.1.3}$$

together with:

$$|k^\alpha\partial^\beta F[\phi]| = \left|\int_{\mathbb{R}^d}d^dk e^{ikx}i^{|\alpha|+|\beta|}\partial^\alpha\left(x^\beta\phi\right)\right| = \left|i^{|\alpha|+|\beta|}F\left[\partial^\alpha(x^\beta\phi)\right]\right| < \infty \tag{B.1.4}$$

which implies:

$$\sup_{k\in\mathbb{R}^d}|k^\alpha\partial^\beta F[\phi]| < \infty\,,\quad \forall\alpha,\beta\in\mathbb{N}^d \tag{B.1.5}$$

Hence, $F : S(\mathbb{R}^d) \to S(\mathbb{R}^d)$. We will see later that the Fourier transform also maps the dual space $S'(\mathbb{R}^d)$, the tempered distributions, into itself.

B.1.2 Distributions in $1+d$ Dimensions

Tempered distributions are the elements of the dual space $S'(\mathbb{R}^d)$, i.e., continuous linear functionals on $S(\mathbb{R}^d)$. A functional T is tempered if and only if there exist $K > 0$ and integers $m, n \in \mathbb{N}$ such that:

$$|T[\phi]| \le K||\phi||_{m,n}\,,\ \forall\phi\in S(\mathbb{R}^d) \tag{B.1.6}$$

where $||\phi||_{m,n} \equiv \max_{|\alpha|\le m,|\beta|\le n} C_{\alpha,\beta}(\phi)$ is the norm of ϕ.

Tempered distributions are sometimes called *slowly increasing* distributions, meaning they grow at most polynomially[1].. This can be seen by considering translations. The

[1]Distributions which grow faster than polynomial are elements of $\mathcal{D}'(\mathbb{R}^d)$. They naturally act on the space of smooth compactly supported functions.

translation operator τ_x is defined by:

$$\tau_x T[\phi] \equiv T[\tau_{-x}\phi] \tag{B.1.7}$$

and one finds, as $x \to \infty$,

$$\begin{aligned}
|\tau_x T[\phi]| = |T[\tau_{-x}\phi]| \leq K||\tau_{-x}\phi||_{m,n} = K \max_{|\alpha|\leq m,|\beta|\leq n} \sup_{y\in\mathbb{R}^d} |y^\alpha \partial^\beta \phi(y-x)| = \\
= K \max_{|\alpha|\leq m,|\beta|\leq n} \sup_{y\in\mathbb{R}^d} |(y+x)^\alpha \partial^\beta \phi(y)| = K \max_{|\alpha|\leq m,|\beta|\leq n} \sup_{y\in\mathbb{R}^d} \left| \sum_{k=0}^{\alpha} \binom{\alpha}{k} y^k x^{\alpha-k} \partial^\beta \phi(y) \right| \leq \\
\leq K|x|^m \max_{|\alpha|\leq m,|\beta|\leq n} \sum_{k=0}^{\alpha} \binom{\alpha}{k} C_{k,\beta}(\phi) \leq K'|x|^m
\end{aligned} \tag{B.1.8}$$

showing polynomial boundedness. The same property holds for derivatives of tempered distributions, since:

$$\partial^\beta T[\phi] = (-)^{|\beta|} T[\partial^\beta \phi] \tag{B.1.9}$$

and $\partial^\beta \phi \in S(\mathbb{R}^d)$ for all β.

Similarly to $S(\mathbb{R}^d)$, the space $S'(\mathbb{R}^d)$ is also preserved under the Fourier transform. Explicitly:

$$F[T][\phi] \equiv \int d^d k\, F[T](k)\phi(k) = \int d^d k \int d^d x\, e^{ikx} T(x)\phi(k) = \int d^d x\, T(x) F[\phi](x) = T[F[\phi]] \tag{B.1.10}$$

Since $F[\phi] \in S(\mathbb{R}^d)$, it follows that $F[T] \in S'(\mathbb{R}^d)$. This property is fundamental: it ensures that the Fourier transform of a tempered distribution, and all its derivatives, are polynomially bounded for real arguments.

Whether polynomial boundedness continues to hold under analytic continuation away from $\mathbb{R}^d$ is a subtler question. The results presented in the main text show that, for micro-causal and retarded tempered distributions, the Fourier transform remains polynomially bounded within its primitive domain of analyticity.

A key object in our analysis is the set:

$$D[T] \equiv \{q \in \mathbb{R}^d \mid e^{-q\cdot x} T \in S'(\mathbb{R}^d)\} \tag{B.1.11}$$

That is, $D[T]$ consists of all vectors q such that $e^{-q\cdot x}T$ is a tempered distribution. If T is tempered, then $\{0\} \in D[T]$. However, not all tempered distributions admit a nontrivial $D[T]$.

The issue is that the factor $e^{-q\cdot x}$ can spoil polynomial boundedness if T has support over all of $\mathbb{R}^d$. In that case, the action of $e^{-q\cdot x}T$ on $S(\mathbb{R}^d)$ becomes ill-defined. In contrast, if $\mathrm{supp}(T)$ is such that there exists at least one $q \neq 0$ with $q \cdot x \geq 0$ for all $x \in \mathrm{supp}(T)$, then $D[T]$ is nontrivial.

In what follows, we focus on a class of tempered distributions with a particularly simple and important $D[T]$: the *microcausal and retarded* tempered distributions,

$$T \in S'(\mathbb{R}^{d,1}) \text{ is microcausal and retarded iff } \mathrm{supp}[T] = \mathrm{FLC}_x \equiv \{x \in \mathbb{R}^{d,1} \mid x^2 \geq 0,\ x^0 \geq 0\} \tag{B.1.12}$$

For such T, one finds $D[T] = V_+ \equiv \{q \in \mathbb{R}^{d,1} \mid q^2 \geq 0,\ q^0 \geq 0\}$.

The identification of $D[T]$ with the forward lightcone is closely related to the analyticity properties of the Fourier transform of T when the imaginary part of its argument is timelike. To see this more clearly, consider the Laplace transform of a tempered distribution:

$$\begin{aligned} L_{p+iq}T \equiv F[e^{-q\cdot x}T] \quad \to \quad L_{p+iq}T[\phi] &= \int d^{d+1}p \int d^{d+1}x\, T(x) e^{ip\cdot x - q\cdot x} = \\ &= T\big[e^{-q\cdot x}F[\phi]\big], \quad q \in D[T] \end{aligned} \tag{B.1.13}$$

If T is retarded and microcausal, this Laplace transform is well-defined on $S(\mathbb{R}^{d,1})$. Moreover, the analytic continuation of the Fourier transform to $p \to p + iq$ coincides with the Laplace transform of $e^{-q\cdot x}T$ evaluated at $p + iq$.

Therefore, if $D[T] = \mathrm{FLC}_q$, then $F[T]$ can be analytically continued to complex arguments $p + iq$ whenever q lies in the interior $\mathring{D}[T]$.

We can now state the main result.

Theorem B.1.1. *A tempered distribution $g \in S'(\mathbb{R}^{d,1})$ is* retarded *and* microcausal *if and only if its Laplace transform Lg is analytic in the tube*

$$\mathcal{T} = \mathbb{R}^{d+1} + i\,\mathring{D}[g]$$

and satisfies the estimate

$$|L_{p+iq}g| \leq A\,\frac{(1 + |p + iq|)^n}{\left(\sqrt{q^2}\right)^m}, \qquad \forall\, p \in \mathbb{R}^{d+1}, \quad q \in \mathring{D}[g], \tag{B.1.14}$$

where $A > 0$ and $m, n \in \mathbb{N}$ are constants that depend on g.

Proof. To prove the $\implies$ direction, we consider a retarded and microcausal tempered distribution g and study the properties of its Laplace transform on the tube $\mathcal{T} = \mathbb{R}^{d+1} + i\mathring{D}[g]$. The causality condition ensures that $D[g] = V_+$. Consequently, the interior of $D[g]$ coincides with the interior of the forward light cone, which consists exclusively of future-directed timelike vectors:

$$\mathring{D}[g] = \{q \in \mathbb{R}^{d,1} \,|\, q^0 > 0,\, q^2 > 0\}.$$

We establish the analyticity of the Laplace transform by evaluating the action of its partial derivatives on a test function and showing that the Cauchy–Riemann equations are satisfied:

$$\begin{aligned}
\partial_{q^\mu} L_{p+iq} g[\phi] &= -g\big[x_\mu e^{-q\cdot x} F[\phi]\big] = -\int d^{d+1}x\, g(x)\, x_\mu e^{-q\cdot x} \int d^{d+1}p\, e^{ip\cdot x}\phi(p) \\
&= i\int d^{d+1}x\, g(x)\, e^{-q\cdot x} \int d^{d+1}p\, (\partial_{p^\mu} e^{ip\cdot x})\, \phi(p) \\
&= -i\int d^{d+1}x\, g(x)\, e^{-q\cdot x} \int d^{d+1}p\, e^{ip\cdot x} (\partial_{p^\mu}\phi(p)) \\
&= -iF[\, g e^{-q\cdot x}\,][\partial_{p^\mu}\phi] = i(\partial_{p^\mu} F[\, g e^{-q\cdot x}\,])[\phi] = i\,\partial_{p^\mu} L_{p+iq} g[\phi].
\end{aligned} \tag{B.1.15}$$

Thus, Lg is analytic in $\mathcal{T}$.

Next, we must verify that the stated estimate holds on $\mathcal{T}$. By definition, the Laplace transform of g coincides with the action of g on the test function $e^{i(p+iq)\cdot x}$:

$$L_{p+iq} g = F[\, g e^{-q\cdot x}\,] = g\big[e^{i(p+iq)\cdot x}\big]. \tag{B.1.16}$$

Fixing $z \in T$, we compute the modulus of Lg:

$$
\begin{aligned}
|L_z g| &= \left|g\left[e^{i(p+iq)\cdot x}\right]\right| \leq K \, \|e^{i(p+iq)\cdot x}\|_{m,n} \\
&= K \max_{|\alpha|\leq m,\, |\beta|\leq n} \sup_{x\in\mathbb{R}^{1,d}} \left|x^\alpha \partial^\beta e^{i(p+iq)\cdot x}\right| \\
&= K \max_{|\alpha|\leq m,\, |\beta|\leq n} \sup_{x\in\mathbb{R}^{1,d}} |p+iq|^\beta \, |x^\alpha e^{-q\cdot x}| \\
&= K \max_{|\alpha|\leq m,\, |\beta|\leq n} \sup_{x\in\mathbb{R}^{1,d}} |p+iq|^\beta \, |(x^0)^{\alpha_0} e^{-q^0 x^0} (x^1)^{\alpha_1} e^{q^1 x^1} \cdots (x^d)^{\alpha_d} e^{q^d x^d}| \\
&\leq K \max_{|\alpha|\leq m,\, |\beta|\leq n} |p+iq|^\beta \left|\frac{\alpha_0}{q^0}\right|^{\alpha_0} e^{-\alpha_0} \sup_{|\vec{x}|<x_*^0} \left||\vec{x}|^{\alpha_1+\cdots+\alpha_d} e^{|\vec{q}||\vec{x}|}\right| \\
&= K \max_{|\alpha|\leq m,\, |\beta|\leq n} |p+iq|^\beta \left|\frac{\alpha_0}{q^0}\right|^{|\alpha|} e^{-\alpha_0} e^{|\vec{q}|\alpha_0/q^0} \\
&\leq K \max_{|\alpha|\leq m,\, |\beta|\leq n} |p+iq|^\beta \left|\frac{2\alpha_0}{\sqrt{q^2}}\right|^{|\alpha|} e^{-\alpha_0} e^{\alpha_0} = K' \frac{|p+iq|^n}{(\sqrt{q^2})^m} \leq K' \frac{(1+|p+iq|)^n}{(\sqrt{q^2})^m}
\end{aligned}
\tag{B.1.17}
$$

For the $\Longleftarrow$ direction, assume $L(z)$ is holomorphic in the tube $\mathcal{T} = \mathbb{R}^{d+1} + iS$, and satisfies the given estimate. Since the estimate guarantees polynomial boundedness in p for fixed $q \in S$, we can regard $L(p+iq)$ as a distribution in p. Analyticity implies:

$$
(\partial_{p^\mu} - i\partial_{q^\mu})\, L(p+iq) = 0. \tag{B.1.18}
$$

Applying the inverse Fourier transform (with respect to p) yields:

$$
(x_\mu + \partial_{q^\mu})\, F^{-1}[\, L(p+iq)\,] = 0. \tag{B.1.19}
$$

Define the distribution:

$$
g(x,q) \equiv e^{q\cdot x}\, F^{-1}[\, L(p+iq)\,] \in \mathcal{D}'(\mathbb{R}^{1,d}), \tag{B.1.20}
$$

which satisfies:

$$
\partial_{q^\mu} g(x,q) = 0 \quad \Rightarrow \quad g(x,q) = g(x), \quad q \in S. \tag{B.1.21}
$$

Thus, $L(z)$ is the Laplace transform of a distribution $g \in \mathcal{D}'(\mathbb{R}^{d,1})$ with $S \subset D[g]$.

We now show that g is tempered. Take $\phi \in \mathcal{D}(\mathbb{R}^{d,1})$:

$$\begin{aligned} g[\phi] &= \int d^{d+1}x\, g(x)\phi(x) \\ &= \int d^{d+1}x\, e^{q\cdot x} F^{-1}[L(p+iq)]\, \phi(x) \\ &= \int d^{d+1}x \int d^{d+1}p\, e^{q\cdot x - ip\cdot x} L(p+iq)\, \phi(x) \\ &= \int d^{d+1}p\, L(p+iq)\, F^{-1}[\, e^{q\cdot x}\phi\,] \\ &= L(p+iq)\big[\, F^{-1}[e^{q\cdot x}\phi]\,\big], \end{aligned} \tag{B.1.22}$$

with $q \in S$. Taking the modulus and using the temperedness of $L(p+iq)$:

$$|g[\phi]| \leq K\, \|F^{-1}[e^{q\cdot x}\phi]\|_{m,n} = K \max_{|\alpha|\leq m,\, \beta\leq n} \sup_{p\in\mathbb{R}^{d+1}} |p^\alpha \partial^\beta F^{-1}[e^{q\cdot x}\phi]|. \tag{B.1.23}$$

The estimate can be carried out explicitly

$$\begin{aligned} &|g[\phi]| \leq K \max_{|\alpha|\leq m,\beta\leq n} \sup_{p\in\mathbb{R}^{d+1}} |p^\alpha \partial^\beta F^{-1}[e^{q\cdot x}\phi]| = K \max_{|\alpha|\leq m,\beta\leq n} \sup_{p\in\mathbb{R}^{d+1}} |p^\alpha F^{-1}[x^\beta e^{q\cdot x}\phi]| = \\ &\quad K \max_{|\alpha|\leq m,\beta\leq n} \sup_{p\in\mathbb{R}^{d+1}} |F^{-1}[\partial^\alpha(x^\beta e^{q\cdot x}\phi)]| = K \max_{|\alpha|\leq m,\beta\leq n} \sup_{p\in\mathbb{R}^{d+1}} \left| \int d^{d+1}x e^{-ip\cdot x} \partial^\alpha(x^\beta e^{q\cdot x}\phi) \right| \leq \\ &\quad \leq K \max_{|\alpha|\leq m,\beta\leq n} \int d^{d+1}x |\partial^\alpha(x^\beta e^{q\cdot x}\phi)| \leq KA \max_{|\alpha|\leq m,\beta\leq n} \sup_{x\in\mathrm{supp}[\phi]} |\partial^\alpha(x^\beta e^{q\cdot x}\phi)| = \\ &\quad = KA \max_{|\alpha|\leq m,\beta\leq n} \sup_{x\in\mathrm{supp}[\phi]} \left| \sum_{j_0=0}^{\alpha_0} \dots \sum_{j_d=0}^{\alpha_d} \binom{\alpha_0}{j_0} \dots \binom{\alpha_d}{j_d} \frac{\beta_0!}{(\beta_0-j_0)!} \dots \frac{\beta_d!}{(\beta_d-j_d)!} x^{\beta-j} \partial^{\alpha-j}(e^{q\cdot x}\phi) \right| \leq \\ &\quad \leq KA \max_{|\alpha|\leq m,\beta\leq n} \sum_{j_0=0}^{\alpha_0} \dots \sum_{j_d=0}^{\alpha_d} \binom{\alpha_0}{j_0} \dots \binom{\alpha_d}{j_d} \frac{\beta_0!}{(\beta_0-j_0)!} \dots \frac{\beta_d!}{(\beta_d-j_d)!} \sup_{x\in\mathrm{supp}[\phi]} |x^{\beta-j}\partial^{\alpha-j}(e^{q\cdot x}\phi)| = \\ &\quad = KA \max_{|\alpha|\leq m,\beta\leq n} \sum_{j_0=0}^{\alpha_0} \dots \sum_{j_d=0}^{\alpha_d} \binom{\alpha_0}{j_0} \dots \binom{\alpha_d}{j_d} \frac{\beta_0!}{(\beta_0-j_0)!} \dots \frac{\beta_d!}{(\beta_d-j_d)!} C_{\beta-j,\alpha-j}(e^{q\cdot x}\phi) \leq \\ &\quad \leq KA \max_{|\alpha|\leq m,\beta\leq n} \sum_{j_0=0}^{\alpha_0} \sum_{l_0=0}^{\alpha_0-j_0} \dots \sum_{j_d=0}^{\alpha_d} \sum_{l_d=0}^{\alpha_d-j_d} \binom{\alpha_0}{j_0} \binom{\alpha_0-j_0}{l_0} \dots \binom{\alpha_d}{j_d} \binom{\alpha_d-j_d}{l_d} \times \\ &\quad \times \frac{\beta_0!}{(\beta_0-j_0)!} \dots \frac{\beta_d!}{(\beta_d-j_d)!} \sup_{x\in\mathrm{supp}[\phi]} |x^{\beta-j} q^j e^{q\cdot x} \partial^{\alpha-j-l}\phi| \end{aligned} \tag{B.1.24}$$

Where A is the size of $\mathrm{supp}[\phi]$. Let us restrict our attention to test functions ϕ such that $\mathrm{supp}[\phi] = \{x \in \mathbb{R}^{1,d} | k^\mu - 2 \leq |x^\mu| \leq k^\mu\, , \forall \mu\}$ for some $k^\mu \in \mathbb{Z}_0 \times \mathbb{Z}_0 \times \dots \times \mathbb{Z}_0$. Thus, we

can set $q^0 = 1/(k^0 + |\vec{k}|), |\vec{q}| = 1/(2k^0 + 2|\vec{k}|)\ , \forall\mu$ and use the previous estimate to argue that

$$|g[\phi]| \leq K^{'}||\phi||_{m,n} \tag{B.1.25}$$

where K', m, n do not depend on k^μ and we used the fact that

$$\begin{aligned} |q^j e^{q\cdot x}| &\leq |(q^0)^{j_0}|\vec{q}|^{j_1+\ldots+j_d} e^{q^0x^0+|\vec{q}||\vec{x}|}| \leq |(q^0)^{j_0+\ldots+j_d} e^{q^0(x^0+|\vec{x}|)}| = \\ &= \left|\frac{1}{(k^0+|\vec{k}|)^{j_0+\ldots+j_d}} e^{(x^0+|\vec{x}|)/(k^0+|\vec{k}|)}\right| \leq e \end{aligned} \tag{B.1.26}$$

We can then extend the extimate to any compactly supported test function. To do this we consider the partition of unity $\{e_{i_0\ldots i_d}\}$ subordinated to a covering of $\mathbb{R}^{d,1}$ by sets of the kind $\{x \in \mathbb{R}^{1,d} | k^\mu - 2 < |x^\mu| < k^\mu\ , \forall\mu\}$ and decompose any test function $\phi \in \mathcal{D}(\mathbb{R}^{1,d})$ wrt $\{e_{i_0\ldots i_d}\}$. In particular, for any compactly supported test function, only a finite number of elements of $\{e_{i_0\ldots i_d}\}$ will be nonzero on supp$[\phi]$, let's call this number N_ϕ. We can find the largest N_ϕ scanning over all the set $\mathcal{D}(\mathbb{R}^{1,d})$ of compactly supported test functions and replace A in the previous estimate with $A' \equiv 2 * \sup_{\phi\in\mathcal{D}(\mathbb{R}^{1,d})} N_\phi$, generalizing the estimate to any test function $\phi \in \mathcal{D}(\mathbb{R}^{1,d})$:

$$|g[\phi]| \leq K^{''}||\phi||_{m,n} \tag{B.1.27}$$

But since this holds for any test function $\phi \in \mathcal{D}(\mathbb{R}^{1,d})$, we can extend g to a distribution in $S'(\mathbb{R}^{1,d})$. Hence, g is tempered. It only remains to show that g is retarded. In order to do this we pick an arbitrary reference point $\bar{x} \notin$ FLC and show that there exist a neighborhood N of x_0 such that $g[\phi] = 0$ for any $\phi \in D(\mathbb{R})$ supported on N. This can be done just by using the previous estimate

$$|g[\phi]| \leq KA' \max_{\alpha\leq m,\beta\leq n} \sum_{l=0}^{\alpha} \binom{\alpha}{l} \frac{\beta!}{(\beta-\alpha)!} C_{\beta-l,\alpha-l}(e^{q\cdot x}\phi) \tag{B.1.28}$$

and considering the following three possiblities:

- sup attained for x timelike and past directed
- sup attained for x spacelike
- sup attained for x null and past directed

The first case is the most immediate one, since $q \cdot x < 0$ when x lies in the backward light-cone. As a consequence, we can send $q^0, |\vec{q}| \to +\infty$ keeping the ratio $q^0/|\vec{q}| > 1$ fixed.

In this limit, $e^{q\cdot x}$ provides an exponential suppression which will eventually kill the RHS, yielding $g[\phi] = 0$. In the second situation, we have to show that it is always possible to pick q s.t. $q \cdot x < 0$ and for which the previous limit can be performed. Indeed, we can see that

$$q \cdot x = q^0 x^0 - \vec{q} \cdot \vec{x} = q^0 |x^0| \left(\frac{x^0}{|x^0|} - \frac{\beta}{\alpha} \cos\theta \right) \tag{B.1.29}$$

where $\alpha, \beta > 1$ are defined by $|\vec{x}| \equiv |x^0|\beta, |\vec{q}| = q^0/\alpha$. Thus, if $x^0 > 0$, we can pick $|\theta| < \arccos(1/\beta)$ together with $\alpha < \beta\cos\theta$, and perform the limit $q^0, |\vec{q}| \to +\infty$. If, on the other hand, $x^0 \leq 0$, it is sufficient to pick $|\theta| < \pi/2$. This last choice applies also to the third scenario, which is just the specialization to $\beta = 1$ of the second situation with $x^0 < 0$. Hence, we have proven that $g[\phi] = 0$ for any compactly supported test function with $\text{supp}[\phi] \cap FLC = \emptyset$. Thus, we conclude that g is a retarded and microcausal tempered distribution. □

B.2 Double dispersion relations with subtractions

In this section we derive the double dispersion relation eq. (4.4.3). As stated in the main body of the discussion, we assume, without loss of generality, that each polynomial $P(z_i)$ is real on the real line and of even degree n_i. Start by performing Cauchy theorem for $\tilde{F}(z_1, t_2)/P_1(z_1)$ in the first variable, keeping the second argument real and fixed. As argued in the main text, the single variable dispersion relation will acquire the form

$$\begin{aligned} \tilde{F}(z_1, t_2) = P_1(z_1) \sum_{a_1} \left(\frac{\tilde{F}(z_{a_1}, t_2)}{P_1'(z_{a_1})(z_1 - z_{a_1})} + \frac{\tilde{F}^*(z_{a_1}, t_2)}{(P_1'(z_{a_1}))^*(z_1 - z_{a_1}^*)} \right) + \\ + \frac{P_1(z_1)}{\pi} \int dt_1 \frac{\text{Im}F(t_1, t_2)}{P_1(t_1)(t_1 - z_1 - i\epsilon)} \end{aligned} \tag{B.2.1}$$

where the sum a_1 runs over the zeros of $P_1(z_1)$ located in the UHP_{z_1}. Let us now consider $\tilde{F}(z_1, z_2)/P_2(z_2)$ and perform Cauchy theorem wrt z_2, keeping z_1 fixed and complex:

$$\tilde{F}(z_1, z_2) = P_2(z_2) \sum_{a_2} \frac{\tilde{F}(z_1, z_{a_2})}{P_2'(z_{a_2})(z_2 - z_{a_2})} + \frac{P_2(z_2)}{2\pi i} \int dt_2 \frac{\tilde{F}(z_1, t_2)}{P_2(t_2)(t_2 - z_2)} \tag{B.2.2}$$

where the sum over a_2, similarly to the previous expression, runs over the zeros of $P_2(z_2)$ which are located in the UHP_{z_2}. To arrive at the desired dispersion relation, plug eq. (B.2.1)

inside eq. (B.2.2) and use

$$\frac{P_2(z_2)}{2\pi i}\int \frac{dt_2}{P_2(t_2)(t_2-z_2)}P_1(z_1)\sum_{a_1}\frac{\tilde{F}(z_{a_1},t_2)}{P_1'(z_{a_1})(z_1-z_{a_1})} = P_1(z_1)\sum_{a_1}\frac{\tilde{F}(z_{a_1},z_2)}{P_1'(z_{a_1})(z_1-z_{a_1})}+ \\ - P_1(z_1)P_2(z_2)\sum_{a_1,a_2}\frac{\tilde{F}(z_{a_1},z_{a_2})}{P_1'(z_{a_1})P_2'(z_{a_2})(z_1-z_{a_1})(z_2-z_{a_2})} \tag{B.2.3}$$

together with

$$\frac{P_2(z_2)}{2\pi i}\int \frac{dt_2}{P_2(t_2)(t_2-z_2)}P_1(z_1)\sum_{a_1}\frac{\tilde{F}^*(z_{a_1},t_2)}{(P_1'(z_{a_1}))^*(z_1-z_{a_1}^*)} = \\ = P_1(z_1)P_2(z_2)\sum_{a_1,a_2}\frac{\tilde{F}^*(z_{a_1},z_{a_2})}{(P_1'(z_{a_1}))^*(P_2'(z_{a_2}))^*(z_1-z_{a_1}^*)(z_2-z_{a_2}^*)} \tag{B.2.4}$$

to finally argue that $\tilde{F}$ obeys the dispersion relation eq. (4.4.3) with

$$Q_{12}(z_1,z_2) \equiv -P_1(z_1)P_2(z_2)\sum_{a_1,a_2}\left(\frac{\tilde{F}(z_{a_1},z_{a_2})}{P_1'(z_{a_1})P_2'(z_{a_2})(z_1-z_{a_1})(z_2-z_{a_2})}+ \\ - \frac{\tilde{F}^*(z_{a_1},z_{a_2})}{(P_1'(z_{a_1}))^*(P_2'(z_{a_2}))^*(z_1-z_{a_1}^*)(z_2-z_{a_2}^*)}\right) \tag{B.2.5}$$

and

$$Q_1(z_1,z_2) \equiv P_1(z_1)\sum_{a_1}\frac{\tilde{F}(z_{a_1},z_2)}{P_1'(z_{a_1})(z_1-z_{a_1})}\ ,\ Q_2(z_1,z_2) \equiv P_2(z_2)\sum_{a_2}\frac{\tilde{F}(z_1,z_{a_2})}{P_2'(z_{a_2})(z_2-z_{a_2})}. \tag{B.2.6}$$

B.3 Explicit Construction Without Rotations

In this section, we provide an explicit construction of the linear maps between the orthant GUHP $= \{\mathrm{Im} z_i > 0\ ,\ \forall i\}$ and the convex cones $D_{\gamma,\vec{\theta}}$. Before presenting the general d-dimensional case, it is useful to build up the construction step by step, starting from the simpler $d=2$ and $d=3$ examples.

Explicit construction in $2+1$ dimensions

We begin by considering the unit circle S^1 in $\vec{k}$-space and choose three normalized vectors that equally split the circle into three parts, for instance:

$$n_1 = \begin{bmatrix} 1 \\ 0 \end{bmatrix}, \quad n_2 = \begin{bmatrix} -\frac{1}{2} \\ \frac{\sqrt{3}}{2} \end{bmatrix}, \quad n_3 = \begin{bmatrix} -\frac{1}{2} \\ -\frac{\sqrt{3}}{2} \end{bmatrix}. \tag{B.3.1}$$

These vectors satisfy $|n_i| = 1$ and have pairwise scalar products $n_i \cdot n_j = -1/2$ for $i \neq j$.

We now embed these vectors into $2+1$ Minkowski space, defining

$$v_1 = \begin{bmatrix} \alpha \\ \beta n_1 \end{bmatrix}, \quad v_2 = \begin{bmatrix} \alpha \\ \beta n_2 \end{bmatrix}, \quad v_3 = \begin{bmatrix} \alpha \\ \beta n_3 \end{bmatrix}. \tag{B.3.2}$$

The $\{v_i\}$ form the new basis vectors. Denoting by z_i the coordinates with respect to this basis, the transformation to $(\omega, \vec{k})$ is

$$\omega = \alpha \sum_i z_i, \quad \vec{k} = \beta \sum_i z_i \, n_i. \tag{B.3.3}$$

As stated earlier, this transformation maps the octant $\{\mathrm{Im}[z_i] > 0, \, \forall i\}$ into a "pyramid" contained inside the forward light cone, provided

$$\alpha > 0, \quad |\beta| < \alpha. \tag{B.3.4}$$

Indeed, the timelike condition reads

$$\sum_{i,j} \mathrm{Im}[z_i] \, \mathrm{Im}[z_j] \, (\alpha^2 - \beta^2 \, n_i \cdot n_j) > 0. \tag{B.3.5}$$

Thus, all v_i are future-directed timelike vectors if $\alpha > 0$ and $|\beta| < \alpha$.

It is convenient to factor out β and introduce $\gamma \equiv \alpha/\beta$, so that the condition becomes

$$\sum_{i,j} \mathrm{Im}[z_i] \, \mathrm{Im}[z_j] \, (\gamma^2 - n_i \cdot n_j) > 0. \tag{B.3.6}$$

This constraint is invariant under $SO(2)$ rotations, which act on the spatial components. Hence, we have identified a two-parameter family of linear transformations between $\mathbb{R}^3 + i\,\mathrm{GUHP}$ and $\mathbb{R}^3 + i\, D_{\gamma,\theta}$, where $D_{\gamma,\theta} \subset V_+$.

Varying θ corresponds to rotating the pyramid around the ω-axis, while γ controls the pyramid's opening angle within the forward light cone. In particular, $\gamma \in (1, \infty)$ and in the limit $\gamma \to 1^+$ the pyramid's edges approach null directions.

Explicit construction in $3+1$ dimensions

We now extend the previous construction to 3+1 dimensions. Consider the unit sphere S^2 in $\vec{k}$-space and choose four unit vectors corresponding to the vertices of a regular tetrahedron inscribed in S^2.

As an example:

$$n_1 = \begin{bmatrix} 0 \\ 0 \\ 1 \end{bmatrix}. \tag{B.3.7}$$

The second vector is taken in the (x, z) plane:

$$n_2 = \begin{bmatrix} a_2 \\ 0 \\ b \end{bmatrix}, \quad |n_2| = 1 \;\Rightarrow\; a_2 = \sqrt{1-b^2}. \tag{B.3.8}$$

We take $a_2 > 0$ without loss of generality. The third vector must have all components nonzero:

$$n_3 = \begin{bmatrix} a_3 \\ c_3 \\ b \end{bmatrix}, \tag{B.3.9}$$

where the z-component equals b to ensure all scalar products are equal, as required for a regular tetrahedron. From $n_2 \cdot n_3 = b$, we obtain

$$a_3\sqrt{1-b^2} + b^2 = b \quad \Rightarrow \quad a_3 = \frac{b(1-b)}{\sqrt{1-b^2}}. \tag{B.3.10}$$

The normalization of n_3 fixes

$$c_3 = \sigma_3\sqrt{\frac{1+b-2b^2}{1+b}}. \tag{B.3.11}$$

Thus:

$$n_3 = \begin{bmatrix} \frac{b(1-b)}{\sqrt{1-b^2}} \\ \sigma_3\sqrt{\frac{1+b-2b^2}{1+b}} \\ b \end{bmatrix}. \tag{B.3.12}$$

Similarly, n_4 is constructed imposing $|n_4| = 1$ and $n_4 \cdot n_1 = n_4 \cdot n_2 = b$:

$$n_4 = \begin{bmatrix} \frac{b(1-b)}{\sqrt{1-b^2}} \\ \sigma_4\sqrt{\frac{1+b-2b^2}{1+b}} \\ b \end{bmatrix}. \tag{B.3.13}$$

The final condition $n_4 \cdot n_3 = b$ yields two solutions: $b = 1$ or $b = -1/3$, with $\sigma_3\sigma_4 = -1$. We discard $b = 1$ since it would collapse all vectors to the same point. Choosing $b = -1/3$ gives:

$$n_1 = \begin{bmatrix} 0 \\ 0 \\ -\frac{1}{3} \end{bmatrix}, \quad n_2 = \begin{bmatrix} \frac{2\sqrt{2}}{3} \\ 0 \\ -\frac{1}{3} \end{bmatrix}, \quad n_3 = \begin{bmatrix} -\frac{\sqrt{2}}{3} \\ \sqrt{\frac{2}{3}} \\ -\frac{1}{3} \end{bmatrix}, \quad n_4 = \begin{bmatrix} -\frac{\sqrt{2}}{3} \\ -\sqrt{\frac{2}{3}} \\ -\frac{1}{3} \end{bmatrix}. \tag{B.3.14}$$

These four vectors are normalized and share the same pairwise inner product, equally partitioning S^2.

Embedding them in $3+1$ Minkowski space:

$$v_i = \begin{bmatrix} \gamma \\ n_i \end{bmatrix}, \tag{B.3.15}$$

we obtain the transformation

$$\omega = \gamma \sum_i z_i, \quad \vec{k} = \sum_i z_i \, (R_i{}^j n_j), \tag{B.3.16}$$

where $R \in SO(3)$. This yields a 4-parameter family of regular hyperpyramids covering the analyticity region: γ controls the spread within the forward light cone, and the three $SO(3)$ parameters determine the spatial orientation.

Explicit construction in higher dimensions

The same procedure extends naturally to $d+1$ dimensions. We begin by considering the $(d-1)$-dimensional unit sphere S^{d-1} in $\vec{k}$-space and choosing $d+1$ unit vectors $\{n_i\}$ corresponding to the vertices of a regular d-simplex inscribed in S^{d-1}. This choice ensures that all edges of the simplex have equal length, and its vertices partition the sphere into $d+1$ congruent spherical regions. The defining property of such a set is:

$$n_i \cdot n_j = \begin{cases} 1 & \text{if } i = j, \\ -1/d & \text{if } i \neq j, \end{cases} \tag{B.3.17}$$

which guarantees maximal symmetry and uniform angular separation between all vectors.

We then extend $\{n_i\}$ to a set of $d+1$ Minkowski vectors:

$$v_i = \begin{bmatrix} \gamma \\ n_i \end{bmatrix}. \tag{B.3.18}$$

As before, $\gamma > 1$ controls the timelike separation between the edges of the hyperpyramid and the ω-axis: the closer γ is to 1, the more the edges approach null directions; increasing γ makes the hyperpyramid narrower within the forward light cone.

The linear transformation from coordinates z_i in the $\{v_i\}$ basis to $(\omega, \vec{k})$ is:

$$\omega = \gamma \sum_{i=1}^{d+1} z_i, \quad \vec{k} = \sum_{i=1}^{d+1} R_i{}^j \, n_j \, z_i, \quad R \in SO(d). \tag{B.3.19}$$

Here R parametrizes an arbitrary rotation in the spatial subspace, allowing the hyperpyramid to be oriented freely within the forward light cone.

This construction defines a family of maps between:

$$\mathbb{R}^{d+1} + i\,\mathrm{GUHP} \quad \longleftrightarrow \quad \mathbb{R}^{d+1} + i\, D_{\gamma,\vec{\theta}}, \quad D_{\gamma,\vec{\theta}} \subset V_+,$$

where $\vec{\theta}$ denotes the set of $SO(d)$ rotation parameters. The total parameter space of the family consists of:

- One real parameter $\gamma > 1$ controlling the opening angle of the hyperpyramid.
- $\frac{d(d-1)}{2}$ parameters describing the spatial rotation $R \in SO(d)$.

By varying these $1 + \frac{d(d-1)}{2}$ parameters, one can cover the entire interior of the analyticity region. In this sense, the d-dimensional construction is the most general form of the geometric mapping between the imaginary orthant in z-space and a convex cone of timelike future-directed vectors in $(\omega, \vec{k})$-space.

Appendix C

C.1 Viable Configurations

The goal of this appendix is to show how to characterize the families of configurations of Stueckelberg fields that yield an X^μ_ν tensor which satisfies the FLRW symmetries. We will focus on the choice $f_{ab} = \eta_{ab}$, but a similar construction can be carried out for any choice of the reference metric. As a starting point, we write (5.2.3) more explicitly in terms of the Stueckelberg fields ϕ^a

$$\begin{cases} F^2 = (\dot{\phi}^0)^2 - \dot{\phi}^n \dot{\phi}^n \ , \\ \dot{\phi}^0 \partial_i \phi^0 = \dot{\phi}^n \partial_i \phi^n \ , \\ a^2 G^2 \delta_{ij} = -\partial_i \phi^0 \partial_j \phi^0 + \partial_i \phi^n \partial_j \phi^n \ . \end{cases} \tag{C.1.1}$$

Repeated spatial indices indicate contractions with the Kronecker delta. Taking the time derivative of the second equation and the spatial derivative of the first one, we arrive at

$$(\ddot{\phi}^n \dot{\phi}^0 - \ddot{\phi}^0 \dot{\phi}^n) \frac{\partial_i \phi^n}{(\dot{\phi}^0)^2} = 0 \ . \tag{C.1.2}$$

Assuming that $\mathrm{Det}[\partial_i \phi^n] \neq 0$ enables us to simplify the above equation down to

$$\ddot{\phi}^n = \dot{\phi}^n \frac{\ddot{\phi}^0}{\dot{\phi}^0} \quad \Longrightarrow \quad \dot{\phi}^n = A^n(\boldsymbol{x}) \dot{\phi}^0 \ . \tag{C.1.3}$$

Consequently, the time derivative of the spatial Stueckelbergs is proportional to the time derivative of the zeroth Stueckelberg via three functions of the spatial coordinates only, $A^n(\boldsymbol{x})$. Plugging this information back into the above system and suppressing the explicit

x-dependence, we get

$$\begin{cases} F^2 = (\dot{\phi}^0)^2(1-\boldsymbol{A}^2) \ , \\ \dot{\phi}^0(\partial_i\phi^0 - A^n\partial_i\phi^n) = 0 \ , \\ a^2G^2\delta_{ij} = -\partial_i\phi^0\partial_j\phi^0 + \partial_i\phi^n\partial_j\phi^n \ . \end{cases} \tag{C.1.4}$$

Here and in the following $\boldsymbol{A}^2 \equiv A^nA^n$. We will now investigate which families of profiles can give rise to the Mixed-Branch cosmology.

C.1.1 Λ-Branch

As a first step, one can integrate Eqs. (C.1.3) and (C.1.4) in time to fully express ϕ^n in terms of ϕ^0:

$$\phi^0 = \frac{\sigma_u}{\sqrt{1-\boldsymbol{A}^2}}\int_{t_0}^{t} \mathrm{d}t'\, F(t') + C(\boldsymbol{x}) \quad \Longrightarrow \quad \phi^n = \sigma_u\frac{A^n(\boldsymbol{x})}{\sqrt{1-\boldsymbol{A}^2}}\int_{t_0}^{t} \mathrm{d}t'\, F(t') + B^n(\boldsymbol{x}) \ , \tag{C.1.5}$$

where $B^n(\boldsymbol{x})$ and $C(\boldsymbol{x})$ are functions to be determined and σ_u is a sign. Notice that the second equation of the set (C.1.4) imposes a relation between A^n, B^n and C:

$$\partial_i C = \boldsymbol{A}\cdot\partial_i\boldsymbol{B} \ , \tag{C.1.6}$$

where the scalar product is defined with respect to the Kronecker delta δ_{ij}. Plugging the previous expressions inside the last equation of the symmetry constraints yields

$$\begin{aligned} a^2G^2\delta_{ij} = \partial_i\boldsymbol{B}\cdot\partial_j\boldsymbol{B} - (\boldsymbol{A}\cdot\partial_i\boldsymbol{B})(\boldsymbol{A}\cdot\partial_j\boldsymbol{B}) + \left[\frac{\partial_i\boldsymbol{A}\cdot\partial_j\boldsymbol{B} + \partial_j\boldsymbol{A}\cdot\partial_i\boldsymbol{B}}{\sqrt{1-\boldsymbol{A}^2}}\right]\sigma_u\int_{t_0}^{t}\mathrm{d}t'\ F(t') + \\ + \left[\frac{\partial_i\boldsymbol{A}\cdot\partial_j\boldsymbol{A}}{1-\boldsymbol{A}^2} + \frac{\partial_i\boldsymbol{A}^2\partial_j\boldsymbol{A}^2}{4(1-\boldsymbol{A}^2)^2}\right]\left(\int_{t_0}^{t}\mathrm{d}t'\ F(t')\right)^2 \ . \end{aligned} \tag{C.1.7}$$

At this stage, we shall notice that the LHS is a homogeneous function of time, while the RHS is a sum of three factorizable contributions, with the time dependence completely stored inside the factors $(\int \mathrm{d}t'\ F(t'))^n$. As a consequence, the only possible way in which the above equation can be satisfied is to impose the following conditions, for some constants

λ_1, λ_2 and λ_3:

$$\begin{aligned}
&\frac{\partial_i \boldsymbol{A}\cdot\partial_j \boldsymbol{A}}{1-\boldsymbol{A}^2}+\frac{\partial_i \boldsymbol{A}^2\partial_j \boldsymbol{A}^2}{4(1-\boldsymbol{A}^2)^2}=\lambda_1\delta_{ij}\ ,\\
&\frac{\partial_i \boldsymbol{A}\cdot\partial_j \boldsymbol{B}+\partial_j \boldsymbol{A}\cdot\partial_i \boldsymbol{B}}{\sqrt{1-\boldsymbol{A}^2}}=\lambda_2\delta_{ij}\ ,\\
&\partial_i \boldsymbol{B}\cdot\partial_j \boldsymbol{B}-(\boldsymbol{A}\cdot\partial_i \boldsymbol{B})(\boldsymbol{A}\cdot\partial_j \boldsymbol{B})=\lambda_3\delta_{ij}\ .
\end{aligned} \tag{C.1.8}$$

Each of the above equations is a nonlinear system of PDEs for the vectors A^n and B^n. A way to simplify the situation is to assume the following dependence for B^n:

$$\boldsymbol{B}=k\boldsymbol{A}\ f(\boldsymbol{A}^2)\ , \tag{C.1.9}$$

where k is a constant and f a function to be determined. Plugging this relation back inside the second and third equations of the previous system we obtain

$$\begin{aligned}
&\frac{2kf\,\partial_i \boldsymbol{A}\cdot\partial_j \boldsymbol{A}}{\sqrt{1-\boldsymbol{A}^2}}+\frac{kf'\partial_i \boldsymbol{A}^2\partial_j \boldsymbol{A}^2}{\sqrt{1-\boldsymbol{A}^2}}=\lambda_2\delta_{ij}\ ,\\
&k^2f^2\partial_i \boldsymbol{A}\partial_j \boldsymbol{A}+k^2\partial_i \boldsymbol{A}^2\partial_j \boldsymbol{A}^2\left[ff'+f'^2\boldsymbol{A}^2-\left(\frac{f}{2}+f'\boldsymbol{A}^2\right)^2\right]=\lambda_3\delta_{ij}\ .
\end{aligned} \tag{C.1.10}$$

We can notice that all these equations contain two contraction structures, $\partial_i \boldsymbol{A}\cdot\partial_j \boldsymbol{A}$ and $\partial_i \boldsymbol{A}^2\partial_j \boldsymbol{A}^2$. Therefore, we can impose the coefficients of these structures to match the ones appearing in the first equation of (C.1.8). These conditions yield the following solutions

$$f(\boldsymbol{A}^2)=\frac{1}{2\sqrt{1-\boldsymbol{A}^2}}\ ,\quad \lambda_2=k\lambda_1\ ,\quad \lambda_3=\frac{k^2}{4}\lambda_1\ . \tag{C.1.11}$$

As a consequence, the system of nonlinear PDEs reduces to a single nonlinear PDE for the vector $\boldsymbol{A}$ alone,

$$\frac{\partial_i \boldsymbol{A}\cdot\partial_j \boldsymbol{A}}{1-\boldsymbol{A}^2}+\frac{\partial_i \boldsymbol{A}^2\partial_j \boldsymbol{A}^2}{4(1-\boldsymbol{A}^2)^2}=\lambda_1\delta_{ij}\ , \tag{C.1.12}$$

enabling to write $(X^2)^i_j$ as (see last line of Eq. (C.1.4))

$$a^2G^2\delta_{ij}=\lambda_1\left(\frac{k}{2}+\sigma_u\int_{t_0}^{t}\mathrm{d}t'\ F(t')\right)^2\delta_{ij}\ , \tag{C.1.13}$$

which is the relation[1] we used in Sec. 5.2 to fully solve the background cosmology and find the time dependence of F and G. Notice that, given the knowledge of $\boldsymbol{B}$ from Eq. (C.1.9),

[1] To be precise, the relation used in the main text is obtained identifying σ with $\frac{k}{2}\sigma_u$.

one can also determine C as

$$\partial_i C = \frac{k\partial_i \boldsymbol{A}^2}{4(1-\boldsymbol{A}^2)^{3/2}} \quad \Longrightarrow \quad C = kf(\boldsymbol{A}^2) + k_0 \ . \tag{C.1.14}$$

As a consequence, the family of viable Stueckelberg configurations is now parametrized by a vector A^n and some real parameters:

$$\phi^0 = \sigma_u \frac{\int_{t_0}^t \mathrm{d}t'\, F(t')}{\sqrt{1-\boldsymbol{A}^2}} + kf(\boldsymbol{A}^2) + k_0 \quad \Longrightarrow \quad \phi^n = A^n \left[\sigma_u \frac{\int_{t_0}^t \mathrm{d}t'\, F(t')}{\sqrt{1-\boldsymbol{A}^2}} + kf(\boldsymbol{A}^2)\right] \ . \tag{C.1.15}$$

C.1.2 Mixed Branch

The Mixed Branch cosmology is characterized by $F = 0$ and $G = g/a$ (with g constant). As a consequence, the system in Eq. (C.1.4) reduces to

$$\begin{cases} 0 = (\dot{\phi}^0)^2(1-\boldsymbol{A}^2) \ , \\ \dot{\phi}^0(\partial_i\phi^0 - A^n\partial_i\phi^n) = 0 \ , \\ g^2\delta_{ij} = -\partial_i\phi^0\partial_j\phi^0 + \partial_i\phi^n\partial_j\phi^n \ , \end{cases} \tag{C.1.16}$$

with g a constant. As a consequence, the admitted profiles are either static configurations or configurations for which A^n has unit norm. Let us study these two cases separately.

$\dot{\phi}^0 = 0$

When $\dot{\phi}^0 = 0$ the first two equations of (C.1.16) are automatically satisfied. Moreover, the condition that characterizes this branch (i.e. $F = 0$) implies that the Stueckelberg fields must be time-independent. Notice that, when $F = 0$, the EOM[2] of the Stueckelberg fields imply that each ϕ^a must be a harmonic function:

$$\nabla^2\phi^a = 0 \ . \tag{C.1.17}$$

It can be easily verified that a simple solution of the system above is given by

$$\phi^a = C^a + B^a_i x^i \ , \tag{C.1.18}$$

[2]This can be verified by varying the dRGT Action wrt ϕ^a keeping in mind that the dRGT potentials now only depend on G.

for any constant matrix B^a_i which satisfies

$$B^a_i B^b_j \eta_{ab} = g^2 \delta_{ij} \ . \tag{C.1.19}$$

A family of viable profiles is given by the equivalence class of profiles $\{\Lambda^a_b \bar{\phi}^b\}$; with $\bar{\phi}^0 = 0$, $\bar{\phi}^i \propto x^i$ being the configuration found in [58].

$\boldsymbol{A}^2 = 1$

In this last case, it is still possible to relate ϕ^n to ϕ^0. Indeed, using the second equation of (C.1.16) we obtain

$$\phi^n = A^n \phi^0 + B^n \ , \ \boldsymbol{A} \cdot \partial_i \boldsymbol{B} = 0 \ . \tag{C.1.20}$$

Moreover, from the third equation of Eq. (C.1.16) $(X^2)^i_j$ becomes

$$g^2 \delta_{ij} = \partial_i \boldsymbol{B} \cdot \partial_j \boldsymbol{B} + (\partial_i \boldsymbol{A} \cdot \partial_j \boldsymbol{B} + \partial_j \boldsymbol{A} \cdot \partial_i \boldsymbol{B}) \, \phi^0 + \partial_i \boldsymbol{A} \cdot \partial_j \boldsymbol{A} (\phi^0)^2 \ . \tag{C.1.21}$$

Similarly to what happened for the Λ-Branch, we must look for diagonal solutions of the kind

$$\partial_i \boldsymbol{B} \cdot \partial_j \boldsymbol{B} = h_i(\boldsymbol{x}) \delta_{ij} \, , \quad \partial_i \boldsymbol{A} \cdot \partial_j \boldsymbol{B} + \partial_j \boldsymbol{A} \cdot \partial_i \boldsymbol{B} = l_i(\boldsymbol{x}) \delta_{ij} \, , \quad \partial_i \boldsymbol{A} \cdot \partial_j \boldsymbol{A} = m_i(\boldsymbol{x}) \delta_{ij} \ , \tag{C.1.22}$$

where, with abuse of notation, we are indicating that each of the above matrices must be diagonal but their entries $h_i(\boldsymbol{x})$, $l_i(\boldsymbol{x})$, $m_i(\boldsymbol{x})$ can be different functions of the spatial coordinates. This freedom comes from the fact that each of these matrices is multiplied by a different power of $\phi^0(t, \boldsymbol{x})$.

C.2 Perturbations with Matter

To study the stability of metric perturbations in the presence of a generic fluid it is convenient to study the linearized Einstein equations. Similarly to Sec. 5.3, we work in unitary gauge and split the metric tensor as $g_{\mu\nu} = \bar{g}_{\mu\nu} + h_{\mu\nu}$, where the components of the perturbations are given by Eq. (5.3.1), while the stress-energy tensor of the matter sector is given by

$$\begin{aligned} &T_{00} = \bar{\rho} + \delta\rho - A\bar{\rho} \, , \quad T_{i0} = -\bar{\rho}(\hat{B}_i + \partial_i B) - a^2(\bar{\rho} + \bar{p})(\hat{v}_i + \partial_i v) \, , \\ &T_{ij} = a^2 \delta_{ij}(\bar{p} + \delta p) + \partial_{\langle i} \partial_{j \rangle} \Pi + \partial_{(i} \hat{\Pi}_{j)} + \hat{\Pi}_{ij} \ . \end{aligned} \tag{C.2.1}$$

We will also need to consider the linearized conservation equations for both the Stueckelberg and Matter Stress-Energy tensors:

$$\nabla_\mu Y^\mu_\nu = 0 \, , \quad \nabla_\mu T^\mu_\nu = 0 \ . \tag{C.2.2}$$

C.2.1 Λ-Branch

On the Λ-branch, the conservation equation of Y^μ_ν acquires the following form

$$\nabla_\mu Y^\mu_0 = \mathcal{F}_C C = 0\,, \quad \nabla_\mu Y^\mu_i = \mathcal{F}_E \partial_i \nabla^2 E = 0\,, \quad \nabla_\mu Y^\mu_i = \mathcal{F}_{\hat{E}_i} \hat{E}_i = 0\,, \tag{C.2.3}$$

where $\mathcal{F}_\mathcal{O}$ are functions of time, for $\mathcal{O} = \{C, E, \hat{E}_i\}$. As a consequence, the two scalars C, E and the vector $\hat{E}_i$ are forced to vanish. Let us now explore the behaviour of each perturbative sector.

Scalars

The scalar content of the Einstein equations consists of

$$\begin{aligned}
&-2\frac{H}{a^2}\nabla^2 B + \frac{3H^2}{M_{\rm Pl}^2} A = \frac{\delta\rho}{M_{\rm Pl}^2}\,,\\
&\partial_i\left[-2\dot{H}B - HA + a^2\frac{\bar{\rho}_m + \bar{p}_m}{M_{\rm Pl}^2} v\right] = 0\,,\\
&\partial_{\langle i}\partial_{j\rangle}\left[\frac{1}{2}A - HB - \dot{B} - a^2\frac{\Pi}{M_{\rm Pl}^2}\right] = 0\,,\\
&-\nabla^2 A - 3a^2(3H^2 + 2\dot{H})A - 3a^2 H\dot{A} + 2\nabla^2(HB + \dot{B}) = 3a^2\frac{\delta p}{M_{\rm Pl}^2}\,.
\end{aligned} \tag{C.2.4}$$

It is evident that neither A nor B are dynamical metric perturbations. Indeed, the first two equations of (C.2.4) (respectively, the 00 and $0i$ components of the Einstein equations) can be used to fully determine the remaining metric perturbations in terms of $\delta\rho$ and v. It can be concluded that the scalar sector is plagued by strong coupling, as no degree of freedom is able to propagate at the linear level.

Vectors

The vector part of the $0i$ and ij components of the Einstein equations is given by

$$\begin{aligned}
&-\frac{m^2 f_B}{2}\hat{B}_i - \left(3H^2 + 2\dot{H}\right)\hat{B}_i - \frac{1}{2a^2}\nabla^2\hat{B}_i = -a^2\frac{\bar{\rho}_m + \bar{p}_m}{M_{\rm Pl}^2}\hat{v}_i - \frac{\bar{\rho}_m}{M_{\rm Pl}^2}\hat{B}_i\,,\\
&-H\partial_{(i}\hat{B}_{j)} - \partial_{(i}\dot{\hat{B}}_{j)} = \frac{\partial_{(i}\hat{\Pi}_{j)}}{M_{\rm Pl}^2}\,,
\end{aligned} \tag{C.2.5}$$

where f_B is a function of $F(t)$ and of the parameters α_i. Since $\hat{B}_i$ can be algebraically determined in terms of the matter perturbations we can see that also the vector sector is strongly coupled, as no metric degree of freedom propagates on the Λ-Branch.

Tensors

The evolution of the tensor modes[3] is governed by

$$\ddot{\hat{h}}_{ij} + 3H\dot{\hat{h}}_{ij} - \frac{1}{a^2}\nabla^2\hat{h}_{ij} + \left(2\frac{\bar{p}_\phi}{M_{\rm Pl}^2} - m^2 f_h\right)\hat{h}_{ij} = 2\frac{\hat{\Pi}_{ij}}{M_{\rm Pl}^2} \ , \tag{C.2.6}$$

where f_h depends on $F(t)$ and on the dRGT parameters. Similarly to the discussion of Sec. 5.3, the tensor modes are the only dynamical degrees of freedom on the Λ-Branch. Their evolution equation differs from its GR form by the addition of a mass term (remember that $\bar{p}_\phi \propto m^2 M_{\rm Pl}^2$), as expected for a massive degree of freedom.

C.2.2 Mixed Branch

On the Mixed Branch, the conservation equation of Y^μ_ν acquires the form

$$\begin{aligned}
&\nabla_\mu Y^\mu_0 = 0 \ , \\
&\nabla_\mu Y^\mu_i = 3\beta_0 A - 6(2\tilde{y}HB + \beta_0\dot{B}) + 2\tilde{y}(\nabla^2\tilde{E} - 3\tilde{C}) = 0 \ , \\
&\nabla_\mu Y^\mu_i = \tilde{y}\frac{\nabla^2\hat{E}_i}{a^2} - 4(\beta_0\dot{\hat{B}}_i + 2\tilde{y}H\hat{B}_i) = 0 \ ,
\end{aligned} \tag{C.2.7}$$

where $\tilde{y}$ and β_0 are functions of the scale factor and the dRGT parameters and obey

$$\dot{\beta}_0 + 2H(\beta_0 - \tilde{y}) = 0 \ . \tag{C.2.8}$$

Notice that the first equation is identically satisfied.

[3]Notice that $\hat{h}_{ij}$ differs from its main text counterpart by a factor a^2.

Scalars

The full set of Einstein equations for the scalar sector is given by

$$
\begin{aligned}
&-2\frac{H}{a^2}\nabla^2 B + 3H\dot{\tilde{C}} - \frac{\nabla^2\tilde{C}}{a^2} + \frac{1}{3a^2}\nabla^4\tilde{E} + 3\frac{m^2 G\beta_0}{4}\tilde{C} + 3H^2 A = \frac{\delta\rho}{M_{\rm Pl}^2}\ ,\\
&\partial_i\left[-2\dot{H}B - HA - \dot{\tilde{C}} + \frac{1}{3}\nabla^2\dot{\tilde{E}}\right] = -a^2\frac{\bar{\rho}_m + \bar{p}_m}{M_{\rm Pl}^2}\partial_i v\ ,\\
&\partial_{\langle i}\partial_{j\rangle}\left[\frac{1}{2}A - HB - \dot{B} - \frac{1}{2}\tilde{C} + \frac{a^2}{2}\left(\ddot{\tilde{E}} + 3H\dot{\tilde{E}} + \left(\frac{\bar{p}_\phi}{M_{\rm Pl}^2} - m^2\tilde{f}_h\right)\tilde{E}\right) + \frac{1}{6}\nabla^2\tilde{E}\right] = a^2\frac{\partial_{\langle ij\rangle}\Pi}{M_{\rm Pl}^2}\ ,\\
&-\nabla^2 A - 3a^2(3H^2 + 2\dot{H})A - 3a^2 H\dot{A} + 2\nabla^2(HB + \dot{B}) - 3a^2\left[\ddot{\tilde{C}} + 3H\dot{\tilde{C}} - \left(\frac{\bar{p}_\phi}{M_{\rm Pl}^2} - \frac{m^2\tilde{f}_C}{2}\right)\tilde{C}\right] +\\
&+\nabla^2\tilde{C} - \frac{1}{3}\nabla^4\tilde{E} = \frac{3a^2\delta p}{M_{\rm Pl}^2}\ ,
\end{aligned}
\tag{C.2.9}
$$

where $\tilde{f}_h$ and $\tilde{f}_C$ depend on the scale factor as well as on the dRGT parameters. On the other hand, the conservation of the matter stress-energy tensor yields

$$
\begin{aligned}
\nabla_\mu T_0^\mu \ &: \quad -\frac{3}{2}(\bar{\rho}_m + \bar{p}_m)\dot{\tilde{C}} - 2a^2\left[3H(\delta p + \delta\rho) + \delta\dot{\rho} + (\bar{\rho}_m + \bar{p}_m)\nabla^2 v\right] = 0\ ,\\
\nabla_\mu T_i^\mu \ &: \quad -\frac{1}{2}(\bar{\rho}_m + \bar{\rho}_m)A + \frac{1}{a^3}\partial_t\left[a^3(\bar{\rho}_m + \bar{\rho}_m)(B + a^2 v)\right] + \delta p + \frac{2}{3}\nabla^2\Pi = 0\ .
\end{aligned}
\tag{C.2.10}
$$

First of all, the continuity equation can be integrated to fully express $\tilde{C}$ in terms of the matter perturbations. Moreover, the 00 and $0i$ components of the Einstein equations can be solved to yield $A[\tilde{E}, \dot{\tilde{E}}; \delta_{\rm matter}]$ and $B[\tilde{E}, \dot{\tilde{E}}; \delta_{\rm matter}]$. Thus, we can combine the trace-free and trace parts of Einstein equations to extract an evolution equation for the scalar $\tilde{E}$. The detailed expression is complicated and not very illuminating, but we can schematically write it, in Fourier space, as

$$
\ddot{\tilde{E}}_k + \mathcal{G}_1(k,t)\dot{\tilde{E}}_k + \mathcal{G}_2(k,t)\tilde{E}_k = \mathcal{S}_{\rm S}[\delta_{{\rm matter},k}]\ . \tag{C.2.11}
$$

The source term on the RHS is built out of matter perturbations, while the LHS is the differential operator which captures the time evolution of the scalar modes $\tilde{E}_k$. To verify whether the addition of matter succeeds in curing the pathologies encountered in Sec. 5.3, we take the $k \to \infty$ limit of the above equation. In this limit, the LHS simplifies to

$$
\ddot{\tilde{E}}_k + \mathcal{G}_0\tilde{E}_k + \mathcal{O}\left(\frac{H}{k}\right)\ . \tag{C.2.12}
$$

Thus, in the sub-horizon limit, we end up with a zero speed of sound for the scalar mode. We can therefore conclude that the presence of ordinary matter does not affect the qualitative behaviour of the scalar sector, which is still plagued by strong coupling. However, the presence of scalar anisotropic stress would bring contributions proportional to $\tilde{E}_k$ in the RHS of eq. (C.2.11).

Vectors

The vector content of the Einstein equations is given by

$$\begin{aligned} &-2\dot{H}\hat{B}_i - \frac{1}{2a^2}\nabla^2\hat{B}_i - \frac{H}{2}\nabla^2\hat{E}_i = -a^2\frac{\bar{\rho}_m + \bar{p}_m}{M_{\rm Pl}^2}\hat{v}_i \ , \\ &-H\partial_{(i}\hat{B}_{j)} - \partial_{(i}\dot{\hat{B}}_{j)} + \frac{a^2}{2}\partial_{(i}\left[\left(\frac{\bar{\rho}_\phi}{M_{\rm Pl}^2} - m^2\tilde{f}_h\right)\hat{E}_{j)} + 3H\dot{\hat{E}}_{j)} + \ddot{\hat{E}}_{j)}\right] = a^2\frac{\partial_{(i}\hat{\Pi}_{j)}}{M_{\rm Pl}^2} \ . \end{aligned} \tag{C.2.13}$$

Differently from the Λ-Branch, the vector $\hat{E}_i$ is now able (in principle) to propagate. Combining the two equations (expressing, first of all, $\hat{B}_i$ in terms of $\hat{E}_i$ and the matter perturbations) enables us to find an evolution equation for the vector d.o.f. $\hat{E}_i$:

$$\ddot{\hat{E}}_{i,k} + \mathcal{V}_1(k,t)\dot{\hat{E}}_{i,k} + \mathcal{V}_2(k,t)\hat{E}_{i,k} = \mathcal{S}_{\rm V}[\delta_{{\rm matter},k}] \ . \tag{C.2.14}$$

Along the lines of the previous subsection, we are not interested in the details of the form of the matter source or the differential operator on the LHS. Rather, we will simply extract the shape of the LHS in the subhorizon limit, which happens to be

$$\ddot{\hat{E}}_i + \frac{k^2\tilde{y}}{2a^2\beta_0}\hat{E}_i + \mathcal{O}\left(\frac{H}{k}\right) . \tag{C.2.15}$$

Thus, contrary to the scalar sector, the vector mode keeps propagating on sub-horizon scales, with a speed of sound

$$c_s^2 = \frac{\tilde{y}}{2\beta_0}. \tag{C.2.16}$$

A similar conclusion was obtained in Sec. 5.3.

Tensors

On the Mixed Branch, the tensor modes evolve according to

$$\ddot{\hat{h}}_{ij} + 3H\dot{\hat{h}}_{ij} - \frac{1}{a^2}\nabla^2\hat{h}_{ij} + \left(2\frac{\bar{p}_\phi}{M_{\rm Pl}^2} - m^2\tilde{f}_h\right)\hat{h}_{ij} = 2\frac{\hat{\Pi}_{ij}}{M_{\rm Pl}^2} \ . \tag{C.2.17}$$

Once again, the tensor modes are free to propagate on the background, with an evolution equation which deviates from its standard GR form by the addition of the matter term. In the large-k limit, the tensor modes propagate with a speed of sound $c_s^2 = 1$.

Bibliography

[1] Enrico Fermi. Tentativo di una Teoria Dei Raggi β. *Il Nuovo Cimento*, 11(1):1–19, January 1934.

[2] Sheldon L. Glashow. Partial-symmetries of weak interactions. *Nuclear Physics*, 22(4):579–588, 1961.

[3] Steven Weinberg. A Model of Leptons. , 19(21):1264–1266, November 1967.

[4] Abdus Salam. Elementary particle theory. In *Prog. Of the Nobel Symposium, 1968, Stockholm, Sweden*, volume 367, 1968.

[5] H. Leutwyler. On the foundations of chiral perturbation theory. *Annals of Physics*, 235(1):165–203, October 1994.

[6] H. Leutwyler. Phonons as goldstone bosons, 1996.

[7] Christoph P. Hofmann. Spin-wave scattering in the effective lagrangian perspective. *Physical Review B*, 60(1):388–405, July 1999.

[8] John F. Donoghue. General relativity as an effective field theory: The leading quantum corrections. *Physical Review D*, 50(6):3874–3888, September 1994.

[9] J. Goldstone. Field theories with Superconductor solutions. *Il Nuovo Cimento*, 19(1):154–164, January 1961.

[10] Yoichiro Nambu. Quasi-Particles and Gauge Invariance in the Theory of Superconductivity. *Physical Review*, 117(3):648–663, February 1960.

[11] Allan Adams, Nima Arkani-Hamed, Sergei Dubovsky, Alberto Nicolis, and Riccardo Rattazzi. Causality, analyticity and an ir obstruction to uv completion. *Journal of High Energy Physics*, 2006(10):014–014, October 2006.

[12] Alberto Nicolis, Riccardo Rattazzi, and Enrico Trincherini. Energy's and amplitudes' positivity. *JHEP*, 05:095, 2010. [Erratum: JHEP 11, 128 (2011)].

[13] Brando Bellazzini, Luca Martucci, and Riccardo Torre. Symmetries, Sum Rules and Constraints on Effective Field Theories. *JHEP*, 09:100, 2014.

[14] Brando Bellazzini. Softness and amplitudes' positivity for spinning particles. *JHEP*, 02:034, 2017.

[15] Brando Bellazzini, Francesco Riva, Javi Serra, and Francesco Sgarlata. Beyond Positivity Bounds and the Fate of Massive Gravity. *Phys. Rev. Lett.*, 120(16):161101, 2018.

[16] Cen Zhang and Shuang-Yong Zhou. Positivity bounds on vector boson scattering at the LHC. *Phys. Rev. D*, 100(9):095003, 2019.

[17] Yuta Hamada, Toshifumi Noumi, and Gary Shiu. Weak Gravity Conjecture from Unitarity and Causality. *Phys. Rev. Lett.*, 123(5):051601, 2019.

[18] Nima Arkani-Hamed, Tzu-Chen Huang, and Yu-tin Huang. The EFT-Hedron. *JHEP*, 05:259, 2021.

[19] Andrew J. Tolley, Zi-Yue Wang, and Shuang-Yong Zhou. New positivity bounds from full crossing symmetry. *JHEP*, 05:255, 2021.

[20] Brando Bellazzini, Joan Elias Miró, Riccardo Rattazzi, Marc Riembau, and Francesco Riva. Positive moments for scattering amplitudes. *Phys. Rev. D*, 104(3):036006, 2021.

[21] Simon Caron-Huot and Vincent Van Duong. Extremal Effective Field Theories. *JHEP*, 05:280, 2021.

[22] Andrea Guerrieri, Joao Penedones, and Pedro Vieira. Where Is String Theory in the Space of Scattering Amplitudes? *Phys. Rev. Lett.*, 127(8):081601, 2021.

[23] Simon Caron-Huot, Dalimil Mazac, Leonardo Rastelli, and David Simmons-Duffin. Sharp boundaries for the swampland. *JHEP*, 07:110, 2021.

[24] Simon Caron-Huot, Yue-Zhou Li, Julio Parra-Martinez, and David Simmons-Duffin. Causality constraints on corrections to Einstein gravity. *JHEP*, 05:122, 2023.

[25] Brando Bellazzini, Giulia Isabella, Sergio Ricossa, and Francesco Riva. Massive gravity is not positive. *Physical Review D*, 109(2), January 2024.

[26] Carl Beadle, Giulia Isabella, Davide Perrone, Sara Ricossa, Francesco Riva, and Francesco Serra. Non-forward uv/ir relations, 2024.

[27] Aninda Sinha and Ahmadullah Zahed. Crossing symmetric dispersion relations in quantum field theories. *Phys. Rev. Lett.*, 126:181601, May 2021.

[28] Clifford Cheung, A. Liam Fitzpatrick, Jared Kaplan, Leonardo Senatore, and Paolo Creminelli. The effective field theory of inflation. *Journal of High Energy Physics*, 2008(03):014–014, March 2008.

[29] Giulia Gubitosi, Federico Piazza, and Filippo Vernizzi. The effective field theory of dark energy. *Journal of Cosmology and Astroparticle Physics*, 2013(02):032–032, February 2013.

[30] Gregory Walter Horndeski. Second-order scalar-tensor field equations in a four-dimensional space. *Int. J. Theor. Phys.*, 10:363–384, 1974.

[31] Christos Charmousis, Edmund J. Copeland, Antonio Padilla, and Paul M. Saffin. General second-order scalar-tensor theory and self-tuning. *Physical Review Letters*, 108(5), January 2012.

[32] Claudia de Rham, Gregory Gabadadze, and Andrew J. Tolley. Resummation of massive gravity. *Physical Review Letters*, 106(23), June 2011.

[33] Alberto Nicolis, Riccardo Rattazzi, and Enrico Trincherini. Galileon as a local modification of gravity. *Physical Review D*, 79(6), March 2009.

[34] Steven Weinberg. *The Quantum theory of fields. Vol. 1: Foundations.* Cambridge University Press, 6 2005.

[35] C. Itzykson and J. B. Zuber. *Quantum Field Theory.* International Series In Pure and Applied Physics. McGraw-Hill, New York, 1980.

[36] E. Wigner. On Unitary Representations of the Inhomogeneous Lorentz Group. *Annals of Mathematics*, 40(1):149–204, January 1939.

[37] G. Sommer. Present state of rigorous analytic properties of scattering amplitudes. *Fortsch. Phys.*, 18:577–688, 1970.

[38] Vasiliy Sergeyevich Vladimirov. *Methods of the theory of functions of many complex variables*. Courier Corporation, 2007.

[39] N. N. Bogolyubov, B. V. Medvedev, and M. C. Polivanov. *Problems of the theory of dispersion relations*. Inst. Adv. Stud., Princeton, NJ, 1956.

[40] J. Bros, H. Epstein, and Vladimir Jurko Glaser. Some rigorous analyticity properties of the four-point function in momentum space. *Nuovo Cim.*, 31:1265–1302, 1964.

[41] Andre Martin. Extension of the axiomatic analyticity domain of scattering amplitudes by unitarity. 1. *Nuovo Cim. A*, 42:930–953, 1965.

[42] J. Bros, H. Epstein, and V. Glaser. A proof of the crossing property for two-particle amplitudes in general quantum field theory. *Commun. Math. Phys.*, 1(3):240–264, 1965.

[43] H Lehmann. Analytic properties of scattering amplitudes in two variables in general quantum field theory. *Communications in Mathematical Physics*, 2(1):375–383, 1966.

[44] André Martin. *Scattering Theory: Unitarity, Analyticity and Crossing*, volume 3. 1969.

[45] Marcel Froissart. Asymptotic behavior and subtractions in the mandelstam representation. *Phys. Rev.*, 123:1053–1057, Aug 1961.

[46] David E. Kaplan, Surjeet Rajendran, and Francesco Serra. Wrong signs are alright, 2025.

[47] M. Fierz and W. Pauli. On relativistic wave equations for particles of arbitrary spin in an electromagnetic field. *Proc. Roy. Soc. Lond. A*, 173:211–232, 1939.

[48] H. van Dam and M. J. G. Veltman. Massive and massless Yang-Mills and gravitational fields. *Nucl. Phys. B*, 22:397–411, 1970.

[49] V. I. Zakharov. Linearized gravitation theory and the graviton mass. *JETP Lett.*, 12:312, 1970.

[50] A.I. Vainshtein. To the problem of nonvanishing gravitation mass. *Physics Letters B*, 39(3):393–394, 1972.

[51] D. G. Boulware and Stanley Deser. Can gravitation have a finite range? *Phys. Rev. D*, 6:3368–3382, 1972.

[52] Claudia de Rham. Massive gravity from dirichlet boundary conditions. *Physics Letters B*, 688(2–3):137–141, May 2010.

[53] Ian Grant Macdonald. *Symmetric functions and Hall polynomials*. Oxford university press, 1998.

[54] S. F. Hassan and Rachel A. Rosen. On non-linear actions for massive gravity. *Journal of High Energy Physics*, 2011(7), July 2011.

[55] S. F. Hassan, Rachel A. Rosen, and Angnis Schmidt-May. Ghost-free massive gravity with a general reference metric. *Journal of High Energy Physics*, 2012(2), February 2012.

[56] G. D'Amico, C. de Rham, S. Dubovsky, G. Gabadadze, D. Pirtskhalava, and A. J. Tolley. Massive Cosmologies. *Phys. Rev. D*, 84:124046, 2011.

[57] Guido D'Amico. Cosmology and perturbations in massive gravity. *Phys. Rev. D*, 86:124019, 2012.

[58] Mikhail S. Volkov. Exact self-accelerating cosmologies in the ghost-free massive gravity – the detailed derivation. *Phys. Rev. D*, 86:104022, 2012.

[59] A. Emir Gümrükçüoğlu, Chunshan Lin, and Shinji Mukohyama. Anisotropic friedmann–robertson–walker universe from nonlinear massive gravity. *Physics Letters B*, 717(4–5):295–298, October 2012.

[60] Pierre Gratia, Wayne Hu, and Mark Wyman. Self-accelerating massive gravity: Exact solutions for any isotropic matter distribution. *Physical Review D*, 86(6), September 2012.

[61] Gianmassimo Tasinato, Kazuya Koyama, and Gustavo Niz. Exact solutions in massive gravity. *Classical and Quantum Gravity*, 30(18):184002, September 2013.

[62] Nima Khosravi, Gustavo Niz, Kazuya Koyama, and Gianmassimo Tasinato. Stability of the self-accelerating universe in massive gravity. *Journal of Cosmology and Astroparticle Physics*, 2013(08):044–044, August 2013.

[63] Gianmassimo Tasinato, Kazuya Koyama, and Gustavo Niz. Vector instabilities and self-acceleration in the decoupling limit of massive gravity. *Physical Review D*, 87(6), March 2013.

[64] Antonio De Felice, A. Emir Gümrükçüoğ, Chunshan Lin, and Shinji Mukohyama. Nonlinear stability of cosmological solutions in massive gravity. *Journal of Cosmology and Astroparticle Physics*, 2013(05):035–035, May 2013.

[65] Nejat Tevfik Yılmaz. Effective matter cosmologies of massive gravity i: non-physical fluids. *Journal of Cosmology and Astroparticle Physics*, 2014(08):037–037, August 2014.

[66] Paolo Creminelli, Oliver Janssen, and Leonardo Senatore. Positivity bounds on effective field theories with spontaneously broken lorentz invariance. *Journal of High Energy Physics*, 2022(9), September 2022.

[67] Lam Hui, Ioanna Kourkoulou, Alberto Nicolis, Alessandro Podo, and Shengjia Zhou. s-matrix positivity without lorentz invariance: a case study, 2023.

[68] H. Lehmann, K. Symanzik, and W. Zimmermann. On the formulation of quantized field theories. *Nuovo Cim.*, 1:205–225, 1955.

[69] Nikolaj Nikolaevič Bogolûbov, Anatoly A Logunov, AI Oksak, and I Todorov. *General principles of quantum field theory*, volume 10. Springer Science & Business Media, 2012.

[70] H. M. Nussenzveig. *Causality and dispersion relations*, volume 95. Academic Press, New York, London, 1972.

[71] Lam Hui, Alberto Nicolis, Alessandro Podo, and Shengjia Zhou. Microcausality without Lorentz invariance. *JHEP*, 07:188, 2025.

[72] Mikhail Leontovich. Generalization of the Kramers-Kronig formulas to media with spatial dispersion. *J. Exptl. Theoret. Phys. (U.S.S.R.)*, 40:907–912, 1961.

[73] D B Melrose and R J Stoneham. Generalised kramers-kronig formula for spatially dispersive media. *Journal of Physics A: Mathematical and General*, 10(1):L17, jan 1977.

[74] Paolo Creminelli, Oliver Janssen, Borna Salehian, and Leonardo Senatore. Positivity bounds on electromagnetic properties of media. *JHEP*, 08:066, 2024.

[75] Volker Scheidemann. *Introduction to complex analysis in several variables.* Springer Nature Switzerland Birkhäuser, 2023.

[76] Sean A. Hartnoll. Lectures on holographic methods for condensed matter physics. *Class. Quant. Grav.*, 26:224002, 2009.

[77] W. Cauer. The Poisson integral for functions with positive real part. *Bulletin of the American Mathematical Society*, 38(10):713 – 717, 1932.

[78] Rolf Herman Nevanlinna. *Asymptotische Entwicklungen beschränkter Funktionen und das Stieltjess' sche Momentproblem.* Suomal. Tiedeakat., 1922.

[79] Annemarie Luger and Mitja Nedic. A characterization of herglotz–nevanlinna functions in two variables via integral representations. *Arkiv för Matematik*, 55(1):199–216, 2017.

[80] Christopher P. Herzog, William H. Pannell, Biswajit Sahoo, and Andreas Stergiou. Magnetised bounds for conformal field theories, 2025.

[81] Solomon Endlich, Alberto Nicolis, and Junpu Wang. Solid inflation. *Journal of Cosmology and Astroparticle Physics*, 2013(10):011–011, October 2013.

[82] D. Comelli, M. Crisostomi, F. Nesti, and L. Pilo. Frw cosmology in ghost free massive gravity from bigravity. *Journal of High Energy Physics*, 2012(3), March 2012.

[83] Elias M Stein and Guido Weiss. *Introduction to Fourier analysis on Euclidean spaces*, volume 1. Princeton university press, 1971.